NORTHWESTERN UNIVERSITY

Multiscale Computational Analysis of Sex Hormone Effects on Secondary Collagen Damage Following Acute Knee Injury

A DISSERTATION

SUBMITTED TO THE GRADUATE SCHOOL

IN PARTIAL FULFILLMENT OF THE REQUIREMENTS

for the degree

DOCTOR OF PHILOSOPHY

Field of Biomedical Engineering

By

Bethany Powell

EVANSTON, ILLINOIS

March 2019

Abstract

Knee injury causes a loss of stability in the joint and frequently leads to secondary degeneration of the cartilage in the months and years after injury, which can further impair joint function and cause pain and disability. Moreover, the secondary damage to the joint appears to be worse for females compared to males. One factor that has been widely proposed to affect outcomes but has been largely neglected in study designs is the influence of sex hormones. Even though sex hormones are known to regulate inflammation, which is triggered in the knee by injury, hormonal influences have not been examined in the injured knee joint. Thus, we sought to investigate the mechanisms whereby sex hormones may alter the secondary damage to the cartilage after injury, focusing on two interrelated biological processes: hormonal modulation of post-injury inflammation in the knee and degradation of collagen, a key load-bearing structure in cartilage.

First, we used a systems biology computational approach to examine the post-injury inflammatory response in the knee joint, since sex hormones have been widely documented as modulators of inflammatory processes throughout the body. Hormonal effects on inflammation in the knee may be particularly important in the context of tissue damage because inflammatory molecules regulate the production of matrix metalloproteinases (MMPs), which cleave and denature collagen fibrils. Further, sex hormones are present in the knee joint at concentrations similar to serum, which could allow them to modulate production of inflammatory factors and MMPs by the cells in the joint. To examine hormonal influences on inflammation and MMP production, we specified three hormone conditions: high estrogen with low testosterone ("Female High E"); low estrogen with low testosterone ("Female Low E"); and low estrogen with high testosterone ("Male"). The "Female High E" condition led to the highest concentrations of collagenase, a type of MMP, the "Male" condition led to the lowest collagenase production, and the "Female Low E" condition led to an intermediate concentration of collagenase. The collagenase concentrations differed significantly between each condition at nearly every day during the twenty-day

simulation period. Thus, collagenase production did not just depend on whether male or female hormone concentrations were present in the knee joint, but also depended on estrogen concentrations among the female hormonal levels.

After investigating hormonal effects on the post-injury inflammatory process, we examined the process of collagen fibril degradation using a Metropolis Monte Carlo algorithm and examined the subsequent loss of collagen mechanical integrity using a coarse-grained steered molecular dynamics approach. In the degradation simulations, we investigated the combined influences of two types of MMPs, collagenases and gelatinases, which work in tandem to degrade collagen structures; collagenases cleave intact tropocollagen molecules, while gelatinases cleave tropocollagen molecules that are partially denatured due to collagenase action. The simulated fibril was subjected degradation by both MMP types until it lost 1.1% of its mass. Subsequently, the fibril was subjected to tensile testing using steered molecular dynamics. These simulations revealed that toughness and ultimate tensile strength were lowest when the relative amount of collagenase was highest. That is, as the relative number of collagenases increased, the mechanical integrity decreased for a specified amount of lost fibril mass. However, these mechanical properties were unaffected by the total number of enzymes on the fibril when tensile testing occurred after a fixed amount of degradation.

Together, our approaches begin to uncover a mechanism whereby female concentrations of sex hormones may enhance degradation of the collagenous structures in the injured knee joint. The results of our systems biology simulations suggest that post-injury collagenase concentration is highest when estrogen concentrations are highest and lowest for male hormone concentrations. Further, the simulations of fibril degradation and mechanics revealed that mechanical integrity decreased as the relative amount of collagenase increased after the fibril had lost a specified amount of mass. Taken together, these results hint at one mechanism by which estrogen may increase collagenase production and cause a reduction of collagen mechanical integrity. This possible mechanism could begin to explain sex differences in post-injury

outcomes and may inform future observational studies. Further, the results of this work could eventually be used to develop treatment strategies that reduce or prevent the loss of cartilage mechanical integrity while accounting for the hormonal effects that may have the potential to worsen post-injury outcomes for females.

Acknowledgements

First, I would like to thank my co-advisors, Igal Szleifer, Ph.D., and Yasin Dhaher, Ph.D., for all of their guidance and support throughout my graduate studies. In particular, I want thank Dr. Szleifer for his willingness to mentor me, even though I had little experience in his field when I began my studies. Dr. Szleifer has been patient, kind, and encouraging, and has demonstrated not only how to excel scientist but also demonstrated to me the importance of pursuing a fulfilling and meaningful life outside the workplace.

I also want to thank my thesis committee members, Tom O'Halloran, Ph.D., and Ellen Casey, M.D., whose insights guided my work and improved its quality over the years.

Another pivotal person in my graduate studies was David Malaspina, Ph.D., who always took the time to answer my questions and critically assess my work. I am especially grateful for all of the time he spent to help me, even after leaving Northwestern and moving to Spain. Without his willingness to help, graduate school would have been an entirely different, and likely much more difficult, experience for me.

Finally, I want to thank Kristin Burtaine, L.C.P.C., my therapist, because I would not have finished graduate school without her. Unfortunately, graduate students are six times more likely to experience moderate-to-severe depression and anxiety compared to the general population, according to a recent study in Nature Biotechnology. Because I was among the approximately 40 percent of graduate students with moderate-to-severe anxiety and depression, I sincerely believe that my mental illness would have caused me to leave graduate school before finishing if I had not received thoughtful and expert guidance and support from Kristin. I cannot thank her enough.

Table of Contents

List of Figures

List of Tables

D.3	Contact stiffness for selected specimens.	202

Chapter 1: Introduction

1.1 Sex differences in post-injury outcomes

Following knee injury, females consistently experience poorer outcomes than males, as noted in a recent meta-analysis (Tan, Lau, Khin, & Lingaraj, 2016). Sex hormones have been widely proposed as a factor that may cause differences in post-injury outcomes, but hormonal factors are largely neglected in observational studies. So, while some studies of post-injury outcomes consider sex as a biological variable, they seldom divide women into groups according to hormonal status (c.f. (Ahlden, Sernert, Karlsson, & Kartus, 2012; Laxdal et al., 2005; Tan et al., 2016)); post-menopausal women are grouped together with pre-menopausal women, and naturally cycling women are grouped together with hormonal contraceptive users. Groups with such drastically different hormonal levels may lead to results that could obscure hormonally driven differences in outcomes between the groups.

Sex hormones seem to be one factor among many that may confound studies of sex differences after injury in human subjects. Other potential confounding influences include activity levels, perceptions of pain, body mass index, and other lifestyle differences that may differ between men and women but may also be difficult to take into account (Tan et al., 2016). To overcome these challenges, mechanistic studies may be required. However, mechanistic studies are infeasible in humans because of ethical concerns, so other approaches, such as computation, may be necessary to control the factors that continue to confound studies of human subjects.

Computational modeling may be an efficient way to probe the mechanisms of sex differences in outcomes, since computational models facilitate the study of numerous “what-if” scenarios in a relatively short amount of time and can be used to focus on smaller individual processes that may influence the larger system. To date, computational models have not been employed to study the mechanisms underlying sex

differences in outcomes after knee injury. In the present work, we leverage computational tools to begin probing possible mechanisms that could lead to sex differences in post-injury outcomes.

1.2 Targets of study

Computational models can be best utilized when the targets of study are appropriately identified and thoroughly defined. In this work, our modeling approaches target a key outcome, cartilage damage, and examine the effects of sex hormones and inflammation, potential regulators of the process that leads to damage. Cartilage damage is arguably one of the most detrimental outcomes of ACL injury, since it can lead to a self-perpetuating cycle of damage that can ultimately lead to osteoarthritis (OA), causing pain, disability, and loss of function (Lohmander, Englund, Dahl, & Roos, 2007). Sex hormones are one of many factors that have been posited to explain the potential male-female disparity in cartilage damage after an ACL injury, but no mechanistic studies have comprehensively examined sex hormone effects on the ACL-injured knee. Thus, the poorly understood processes that lead to cartilage damage and the hormonal factors that may modulate the damage seem to be appropriate targets for computational modeling.

1.3 Model of hormonal effects on inflammation

Post-injury inflammation is one potential effector of cartilage damage, and numerous reports have indicated that sex hormones, particularly estrogen, progesterone, and testosterone, can affect the production of inflammatory mediators by many different immune cells (D'Agostino et al., 1999; Kou et al., 2015; Lei et al., 2014; Straub, 2007). Sex hormone effects on inflammation appear to depend on the particular cell types involved. Broadly speaking, progesterone and testosterone tend to be anti-inflammatory (Lei et al., 2014; Menzies, Henriquez, Alexander, & Roberts, 2011; Miller, Alley, Murphy, Russell, & Hunt, 1996; Miller & Hunt, 1998; Sun et al., 2012), while the effects of estrogen are more complex. Estrogen may be

pro- or anti-inflammatory, depending on its concentration and the cell type. The most abundant immune cell type in the injured knee joint is the macrophage (Murakami et al., 1995) and the concentrations of estrogen in the synovial fluid will be in a range where the hormone has been shown to exert pro-inflammatory effects on macrophages (Rovensky et al., 2004; Straub, 2007). These effects on inflammation suggest that sex hormones may modulate the knee inflammation that occurs in the aftermath of a knee injury.

Much research has focused on how estrogen and progesterone might directly modulate cellular transcription of matrix metalloproteinases (MMPs), which eventually cause permanent structural damage to the cartilage. However, the evidence does not suggest that these hormones directly modulate MMP production in the cells of the knee joint (Powell, Dhaher, & Szleifer, 2015). Although hormones do not directly regulate MMP production by the cells in the knee synovium, a clear connection has been established between inflammation and MMP production, so hormones may indirectly regulate MMP production by influencing the inflammatory factors that can, in turn, directly modulate MMP production. Indeed, pro-inflammatory molecules like IL-1β and TNF-α are known to enhance MMP production by multiple cell types, including macrophages and synovial fibroblasts (SFs), the resident cells of the synovium (Asano et al., 2006; Kar et al., 2016; Pratta et al., 2003; Yorifuji, Sawaji, Endo, Kosaka, & Yamamoto, 2016).

While hormone effects on inflammation and effects of inflammatory mediators on MMP production have been documented, no study has comprehensively examined the interactions between hormones, inflammatory mediators, and MMPs to elucidate possible sex differences after knee injury. In this work, we will present a systems biology model that synthesizes information about components of the post-injury inflammatory response in the joint and we will use the model to examine the effects of the principal sex hormones, estrogen, progesterone, and testosterone, on inflammation and MMP production. With this approach, we will quantify how MMP production and inflammation differ when male concentrations of hormones are present compared to female hormone concentrations and examine the

potential differences in inflammation for concentrations of hormones associated with different phases of the menstrual cycle.

1.4 Models of degradation and tensile mechanics

The systems biology approach to studying the inflammatory response will provide a framework for predicting MMP production in an injured knee joint based on the concentrations of sex hormones present, though it lacks the ability to provide insights into the resulting deterioration of the cartilage. That deterioration occurs when two types of MMPs, collagenases and gelatinases, work in tandem to cleave and denature fibrillar collagen (Rosenblum et al., 2010; Saffarian, Collier, Marmer, Elson, & Goldberg, 2004; Sarkar, Marmer, Goldberg, & Neuman, 2012), which is the key load bearing structure in cartilage (Cowin & Doty, 2007). This process of degradation will ultimately reduce the mechanical integrity of the collagen and reduce the ability of the cartilage to perform its load-bearing function (Laasanen et al., 2003; Panwar et al., 2013; Panwar et al., 2015; Park, Nicoll, Mauck, & Ateshian, 2008).

Collagenase and gelatinase actions on collagen and gelatin, respectively, have been well characterized individually (Collier et al., 2011; Collier, Saffarian, Marmer, Elson, & Goldberg, 2001; Rosenblum et al., 2010; Saffarian et al., 2004; Sarkar et al., 2012; Welgus, Jeffrey, Stricklin, Roswit, & Eisen, 1980). However, their combined effects have not been examined extensively, and thus their relative contributions to the degradation of collagen fibrils have not been documented. Further, experiments have not yet examined the mechanical sequelae of MMP-induced degradation of collagen fibrils. Here, we will develop a dynamic Metropolis Monte Carlo (MC) algorithm to glean insights into the relative contributions of collagenases and gelatinases to the degradation of an isolated collagen fibril. Using the collagen fibril structures generated by the MC degradation model, we will examine the associated losses of mechanical integrity using a coarse-grained molecular dynamics approach that has been described previously (Malaspina, Szleifer, & Dhaher, 2017).

1.5 Why this is important

In this work, we present several computational approaches designed to probe the mechanisms that underlie cartilage damage after knee injury with an emphasis on sex hormone effects on the process. Because of the role that MMPs play in the initiation of damage to the cartilage, we begin with a review of the effects of female sex hormones on MMP production at different spatial scales and in systems throughout the body. This review of literature highlights the complexity and inhomogeneity of cellular responses to sex hormones throughout the body, and hints at a role for inflammation as an intermediary between hormone action and MMP production. Next, we examine sex hormone effects on inflammation and MMP production by macrophages and synovial fibroblasts using a systems biology modeling approach that aggregates and synthesizes data from a number of well-controlled cellular studies. This analysis demonstrates how sex hormones can modulate the transient inflammatory response caused by an injury and subsequently elevate or reduce MMP production by the resident cells in the synovium. Finally, we develop a model of MMP-driven collagen fibril degradation, which we couple with an existing coarse-grained molecular dynamics model to simulate the collagen fibril mechanical response after degradation. The analysis of degradation and mechanics provides a connection between hormonally modulated MMP production after injury and the resulting collagen destruction and loss of cartilage load-bearing capacity that impairs function of the knee joint after an injury.

The modeling approaches we will present here are intended to be building blocks that allow us to learn about initiation of damage and associated loss of mechanical integrity in the injured knee, and how the process may differ due to the influences of sex hormones. By clarifying a potential mechanism underlying sex differences in outcomes, this work may inform the design of future studies that investigate sex differences and may eventually inform treatment strategies for the injured knee joint.

Chapter 2: Hormonal regulation of MMPs

Abstract

Collagenases and gelatinases regulate many physiological processes and are involved in the pathogenesis and progression of various disease states, such as osteoarthritis, renal fibrosis, and atherosclerosis. These enzymes belong to the matrix metalloproteinase (MMP) family and are regulated by a number of factors, including sex hormones. Estrogen, relaxin, and progesterone can alter the balance between tissue degradation and repair by modulating MMPs, leading to sex disparities in many MMP-related disease states. In these diseases, MMPs initiate collagen degradation at the nanoscale when they cleave and denature collagen molecules. However, the net effect on the tissue is generally observed at the macroscale. To understand how the nanoscale events lead to macroscale changes, we must examine the intermediate scales. In this paper, we review the literature that examines the effects of estrogen, relaxin, and progesterone on MMP production and activity, connecting the nano-, micro-, and macroscale details to relevant disease states. From our analysis, we conclude that each of these sex hormones has inconsistent effects on MMP production, depending on which cell types are present and what hormone concentrations are studied. Thus, sex hormone effects on MMP production must be considered within specific contexts of different tissue and organ systems.

2.1 Introduction

The ovarian hormones estrogen, relaxin, and progesterone can alter the production and activity of collagenases and gelatinases in many tissues, including cartilage, (Ahmad, Wang, Nair, & Kapila, 2012; Claassen et al., 2010; Kapila, Wang, & Uston, 2009; Lee et al., 2003; Naqvi et al., 2005) ligament, (Henneman, Bildt, Degroot, Kuijpers-Jagtman, & Von den Hoff, 2008) female reproductive tissue (Imada

et al., 1997; Sato et al., 1991; Vassilev et al., 2005; Zong, Meyn, & Moalli, 2009), the cardiovascular system, and the kidneys (Chow et al., 2012; Heeg et al., 2005; Lekgabe et al., 2005; Mahmoodzadeh, Dworatzek, Fritschka, Pham, & Regitz-Zagrosek, 2010; Potier et al., 2001; Wingrove, Garr, Godsland, & Stevenson, 1998). By regulating these enzymes, which belong to the matrix metalloproteinase (MMP) family and cleave both fibrillar and non-fibrillar collagens (Fields, 2013; Lauer-Fields, Juska, & Fields, 2002; Overall, 2002; Rosenblum et al., 2010; Xu, Chen, Wang, Yamada, & Steffensen, 2005), female sex hormones may influence numerous disease states that can be caused or worsened by MMP activity. Indeed, numerous studies have demonstrated that sex hormones can increase or decrease MMP expression that may ultimately influence disease risk and outcomes (Burrage, Mix, & Brinckerhoff, 2006; Cawston & Wilson, 2006; Chen et al., 2013; Giannandrea & Parks, 2014; Gupta, Shamseddin, & Khaira, 2011; Y. Okada, 2000; Troeberg & Nagase, 2012; Walter, Kawashima, Nebelung, Neumann, & Roessner, 1998).

Hormones can alter the physiological environment by modulating MMP concentrations, potentially contributing to disease. In synovial joints, for example, hormones can disrupt the tightly regulated activity of MMPs, contributing to the development of osteoarthritis (OA) (Ahmad et al., 2012; Kapila et al., 2009; Naqvi et al., 2005). Many have suggested that hormones may contribute to the development and progression of OA in young women, since some studies seem to suggest that OA is more prevalent in young women than young men after anterior cruciate ligament (ACL) injury (Lohmander et al., 2007). However, the mechanistic details of this sex bias are not clear. Sex hormone effects on MMPs may provide one mechanistic explanation for the bias: hormones may up regulate MMP production and, consequently, increase the irreversible MMP-mediated degeneration of the cartilage. To understand the effects of hormones on MMP production in the joint and the subsequent destruction of the cartilage, it may be advantageous to examine how hormones affect MMP production throughout the body. The insights gained from the other systems in the body may help us form a global picture of the connections between hormones and MMPs and help elucidate the mechanisms that contribute to the hormone-induced degradation in osteoarthritic joints.

Joint health is regulated by biological processes at multiple spatial and temporal scales; joints are multi-scale systems. Examinations at the different scales may provide significant insights into the pathogenesis of joint diseases. At the nanoscale, hormones like estrogen, relaxin, and progesterone interact with their receptors, causing molecular events that lead to changes in collagenase and gelatinase production, activation, and activity (Ahmad et al., 2012; Chow et al., 2012; M. Fang, Wu, & Huang, 2013; Guccione, Silbiger, Lei, & Neugarten, 2002; Heeg et al., 2005; Mahmoodzadeh et al., 2010). These enzymes then act at the nanoscale, binding, cleaving, and denaturing collagen and gelatin (Fields, 2013; Manka et al., 2012; Rosenblum et al., 2010; Rosenblum et al., 2007; Sarkar et al., 2012). At the cellular level or microscale, the hormones can modulate extracellular MMP concentration (Clark, Swingler, Sampieri, & Edwards, 2008). In some cases, the hormones have differential effects at the microscale. For example, estrogen inhibits collagenase in articular chondrocytes, but induces collagenase in fibrochondrocytes (Claassen et al., 2010; Kapila et al., 2009; Lee et al., 2003). Ultimately, the varied responses at the microscale will lead to varied responses at the tissue and organ level (macroscale) where the hormonally regulated enzymes can produce beneficial changes in some circumstances (Qu, Abe, Yokoyama, & Ishikawa, 2006; Silbiger & Neugarten, 2008), while they can produce detrimental changes in others (Ahmad et al., 2012; Kapila et al., 2009; Naqvi et al., 2005).

The varied macroscale tissue responses to hormone-induced MMPs depend on the varied micro- and nanoscale changes that occur in the cells and in the extracellular space. In this review, we address three scales of hormone-MMP action: nanoscale, microscale, and macroscale. Figure 2.1 depicts examples of the nano- and microscale structures. At the nanoscale, we will briefly discuss the hormones, their receptors, and their signaling pathways, as well as the nanoscale function and non-hormonal regulation of MMPs. At the microscale, we will summarize the literature that examines the effects of estrogen, relaxin, and progesterone on cellular production of collagenases and gelatinases. And at the macroscale, we will discuss the influence of estrogen, relaxin, and progesterone at the tissue-level in processes that may depend on

MMP action. By understanding the current knowledge in this field at multiple scales, we can identify gaps in knowledge and help clarify the role of hormones in MMP-dependent disease states, including OA.

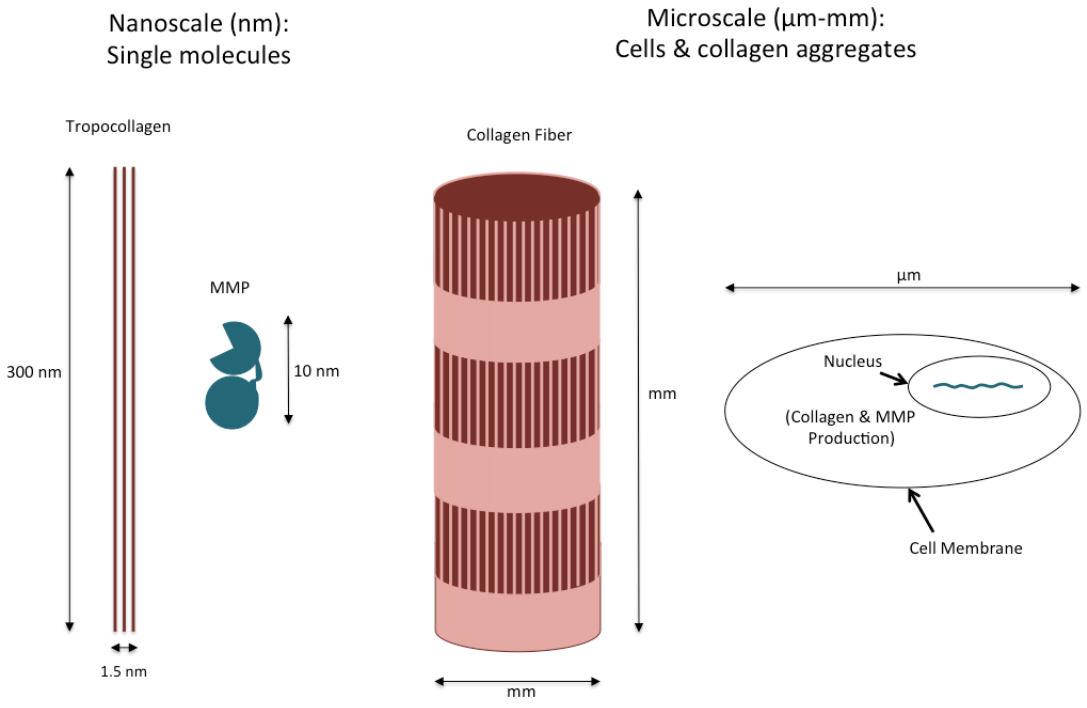

Figure 2.1: Examples of nanoscale and micro-scale structures. The nanoscale comprises single molecules, such as tropocollagen and matrix metalloproteinases (MMPs). Hormones and their receptors are also nanoscale structures, though they are not depicted here. The microscale comprises cells and collagen aggregates, such as collagen fibers. Tissues and organs (not shown) are considered macro-scale.

2.2 Nanoscale

2.2.1 Hormones, receptors, and target tissues

Three ovarian hormones can regulate collagenases and gelatinases: estradiol, H2 relaxin, and progesterone. In the following section, we briefly summarize the production of these hormones, then discuss the functions of their receptors in relation to MMP regulation. Here we note that MMPs can also be regulated by androgens (Freeman et al., 2014; Henmi et al., 2001), but few studies have addressed their influence on MMPs. Thus, we will focus here on estrogen, relaxin, and progesterone because of the limited number of available publications relating to androgens and MMP production.

Estradiol, H2 relaxin, and progesterone are all secreted by the ovaries during the menstrual cycle, though other sources of these hormones also exist. During the menstrual cycle, the primary source of estradiol is the developing follicle during the follicular phase, while the corpus luteum is the primary source of estradiol, progesterone, and relaxin during the luteal phase (Bani, 1997; Barbieri, 2014; Greenspan & Gardner, 2004; Nelson & Bulun, 2001; Simpson, 2003). The major sources of these hormones and their fluctuations through the menstrual cycle are depicted in Figure 2.2. This cycle-dependent production of the hormones suggests that their concentration during the menstrual cycle will vary. Indeed, estrogen and progesterone fluctuations have been well characterized (Greenspan & Gardner, 2004). The cyclic changes in these hormones are known to regulate MMPs and the consequent tissue remodeling in the endometrium during each cycle (Barbieri, 2014; Gaide Chevronnay et al., 2012; Greenspan & Gardner, 2004; Mihm, Gangooly, & Muttukrishna, 2011; Vassilev et al., 2005). However, the fluctuations of relaxin concentrations are not as clear. Bani reported that relaxin rises by 30 to 150 pg/mL during the luteal phase of the menstrual cycle (Bani, 1997), while others have reported no change in relaxin concentrations across the cycle (Pehrsson, Westberg, Landen, & Ekman, 2007).

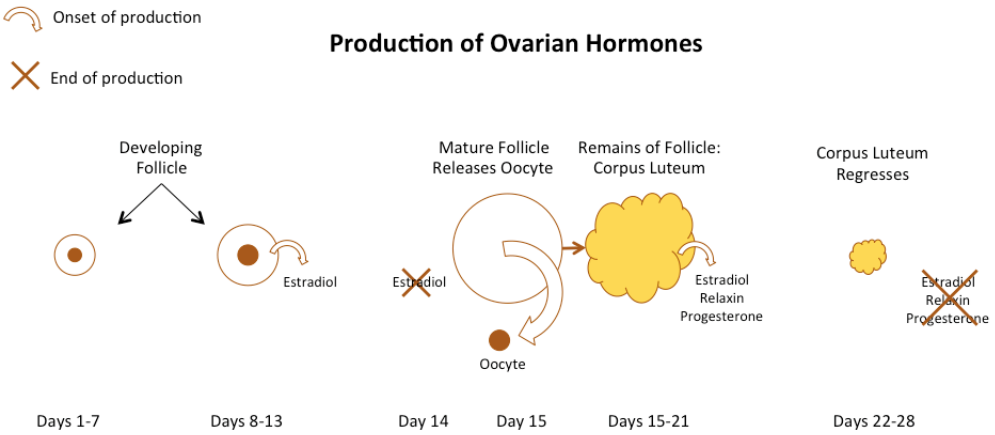

Figure 2.2: Production of ovarian hormones. The developing follicle produces estrogen until the day before ovulation. Following ovulation, the remains of the follicle become the corpus luteum, which secretes estrogen, relaxin, and progesterone. Eventually, the corpus luteum regresses and ceases hormone production, leading to menstruation. Day 1 = onset of menses.

Once the ovaries have produced these hormones, they can subsequently regulate tissue remodeling through receptor binding. There are three receptors for estrogen: estrogen receptor (ER) -α, ER-β, and the G-protein coupled estrogen receptor (GPER) (Matthews & Gustafsson, 2003; Rae & Johnson, 2005; Vrtacnik, Ostanek, Mencej-Bedrac, & Marc, 2014). ER-α and –β are nuclear receptors that can directly and indirectly regulate gene transcription, as depicted in Figure 2.3 (Bjornstrom & Sjoberg, 2005; Vrtacnik et al., 2014). The estrogen-ER complex can directly regulate genomic signaling when the target gene contains an estrogen response element (ERE). When the target gene has no ERE, estrogen can indirectly regulate genomic signaling by interacting with other proteins that can signal the target gene (Bjornstrom & Sjoberg, 2005; Vrtacnik et al., 2014). These indirect genomic signals can lead to MMP transcription when the ER binding induces transcription factors to activate genes for MMPs (Bjornstrom & Sjoberg, 2005).

Additionally, estrogen can signal through non-genomic pathways, including cascades that the GPER initiates.(Bjornstrom & Sjoberg, 2005; Rae & Johnson, 2005; Vrtacnik et al., 2014)

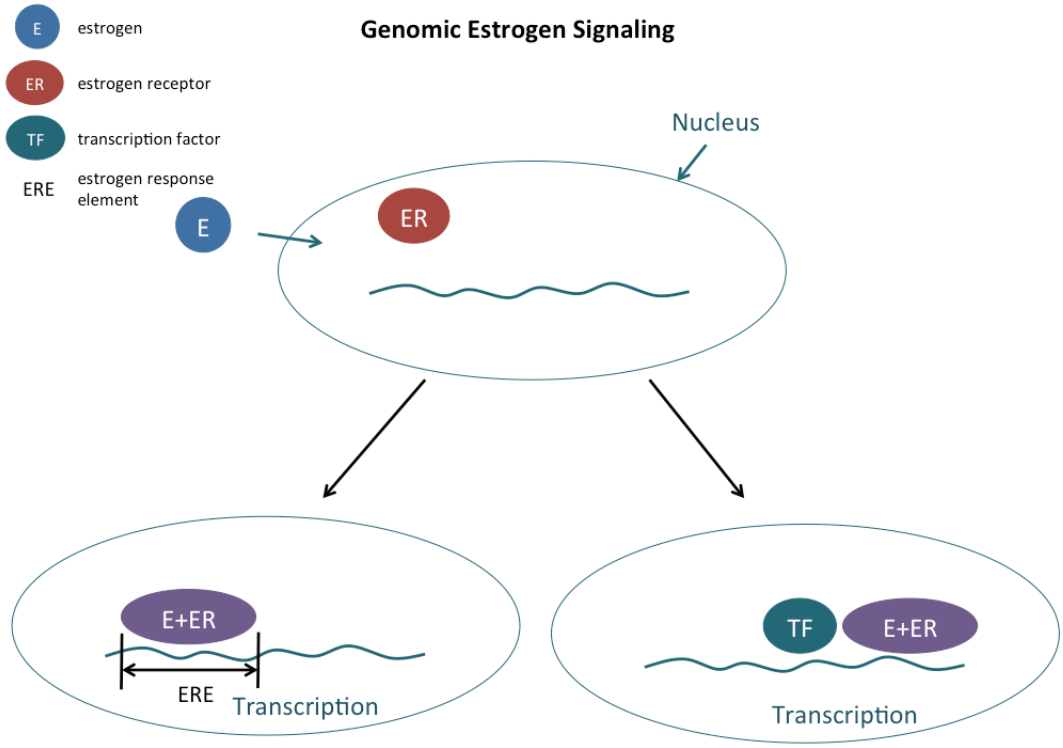

Figure 2.3: Genomic estrogen signaling. The estrogen-ER complex can initiate transcription when there is an estrogen response element (ERE) on the target gene (bottom left) or it can initiate transcription by binding other transcription factors that will lead to transcription of a gene without an ERE. E=estrogen; ER=estrogen receptor; ERE=estrogen response element; TF=transcription factor.

Estrogen receptors have been detected in tissues and organs throughout the body, including female reproductive tissue, cartilage, ligaments, cardiovascular tissue, in the kidneys, and in the nervous system (Brailoiu et al., 2007; Goldsmith & Weiss, 2005; Knowlton & Korzick, 2014; Potier et al., 2001; Sciore,

Frank, & Hart, 1998; Wang, Hayami, & Kapila, 2009). The different receptor types may mediate the varied responses to estrogen in these tissues. For example, MMP-2 is suppressed when estrogen binds ER-α in cardiac fibroblasts (Mahmoodzadeh et al., 2010), but MMP-2 is induced when estrogen binds ER-β in mesangial cells (M. Fang et al., 2013). Both receptor subtypes exist in cartilage and ligament (Faryniarz, Bhargava, Lajam, Attia, & Hannafin, 2006; Wang et al., 2009), but the effects of the different subtypes are not well understood in these two tissue types. Little is known about which estrogen receptors lead to induction and suppression of MMPs in most tissues.

In addition to estrogen and ERs, relaxin and its receptors are involved in the regulation of MMPs. The relaxin receptors are part of the insulin receptor family, and include relaxin family peptide (RXFP) 1 receptor, RXFP2, RXFP3, and RXFP4 (Bathgate et al., 2013; Bathgate, Ivell, Sanborn, Sherwood, & Summers, 2005; Kong, Shilling, Lobb, Gooley, & Bathgate, 2010). RXFP1 and RXFP2 generally initiate cAMP cascades (Figure 2.4), and can also signal through the ERK1/2 MAPK pathway (Bathgate et al., 2013; Bathgate et al., 2005; Halls, Bathgate, & Summers, 2006; Kong et al., 2010). Conversely, RXFP3 and RXFP4 generally suppress the cAMP signaling cascade (Bathgate et al., 2005; Kong et al., 2010). Of these four receptors, RFXP1 has the highest affinity for H2 relaxin, the most common type of relaxin, which is produced by the corpus luteum (Bani, 1997; Bathgate et al., 2013; Bathgate et al., 2005). H2 relaxin bound to RFXP1 initiates signaling cascades that can up-regulate MMP production throughout the body. In contrast, RFXP3 and RFXP4 cascades do not appear to affect pathways that regulate MMP transcription (Ahmad et al., 2012; Bathgate et al., 2005; Chow et al., 2012). However, these receptor types are not as relevant to connective tissue remodeling, since they are not present in most connective tissues (Kong et al., 2010). RFXP1 is the most relevant receptor type in this context.

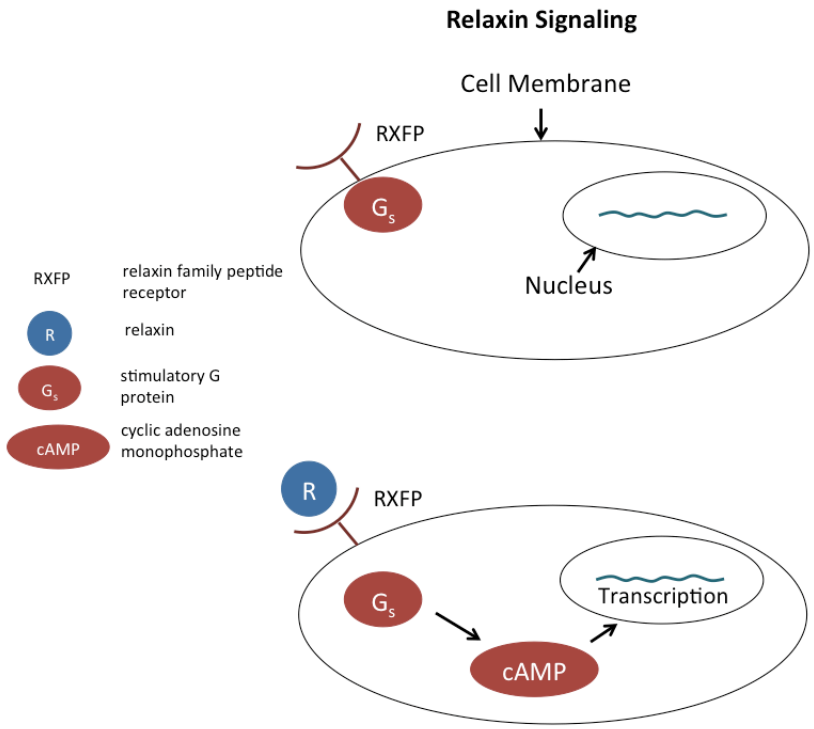

Figure 2.4: Relaxin signaling through the cAMP cascade. R=relaxin; RXFP=relaxin family peptide receptor; Gs=stimulatory G protein; cAMP=cyclic AMP.

Several researchers have examined the expression of relaxin receptors and relaxin-MMP signaling pathways (Ahmad et al., 2012; Chow et al., 2012; Kapila et al., 2009). Kapila, et al. showed that temporomandibular joint (TMJ) fibrochondrocytes express RXFP1 and RXFP2, and up regulate MMPs when they are treated with relaxin (Kapila et al., 2009). Relaxin receptors have also been isolated in ligament and tendon fibroblasts, and renal myofibroblasts, among other cell types (Chow et al., 2012; Dehghan, Muniandy, Yusof, & Salleh, 2014).

Relaxin signals MMPs through the RXFP1 receptor and an ERK- or pERK-dependent pathway. In TMJ fibrochondrocytes, Ahmad et al. showed that relaxin signals MMP-9 and MMP-13 through the RXFP1 receptor, which signals an ERK-dependent pathway (Ahmad et al., 2012). And in renal myofibroblasts, Chow et al. showed that relaxin up regulates MMP-2, MMP-9, and MMP-13 through a pERK-dependent pathway (Chow et al., 2012). However, the signaling pathways between relaxin and MMPs are not clearly defined in other tissues like cartilage and ligament.

The other relevant receptors for the hormonal regulation of MMPs are the progesterone receptors (PRs). Two nuclear PR isoforms exist, PRA and PRB (Giangrande, Kimbrel, Edwards, & McDonnell, 2000), along with several membrane PRs that play a role in fast progesterone signaling in the nervous system (Labombarda et al., 2010; Zuloaga et al., 2012), PRA inhibits transcription by recruiting co-repressors of transcription, while PRB promotes transcriptional activity by recruiting co-activators. The two isoforms have a similar sequence, but PRB contains additional amino acid residues that counteract the inhibitory domain of the receptor, which is found in both isoforms (Giangrande et al., 2000). However, progesterone likely does not modulate MMPs through PR transcriptional activity, since none of the MMP genes contains a PR recognition sequence (Gaide Chevronnay et al., 2012). Rather, progesterone bound to its nuclear receptor likely suppresses cytokines and other inflammatory factors that initiate MMP production, including IL-1, TGF-β, and TNF-α (Burrage et al., 2006; Cawston & Wilson, 2006; Chen et al., 2013; Critchley, Kelly, Brenner, & Baird, 2001; Evans & Salamonsen, 2012; Gaide Chevronnay et al., 2012; Kelly, King, & Critchley, 2001; Salamonsen, 1998; Salamonsen & Woolley, 1996). The regulation of transcription by progesterone is illustrated in Figure 2.5, and the influence of progesterone on MMPs through cytokines is illustrated in Figure 2.6.

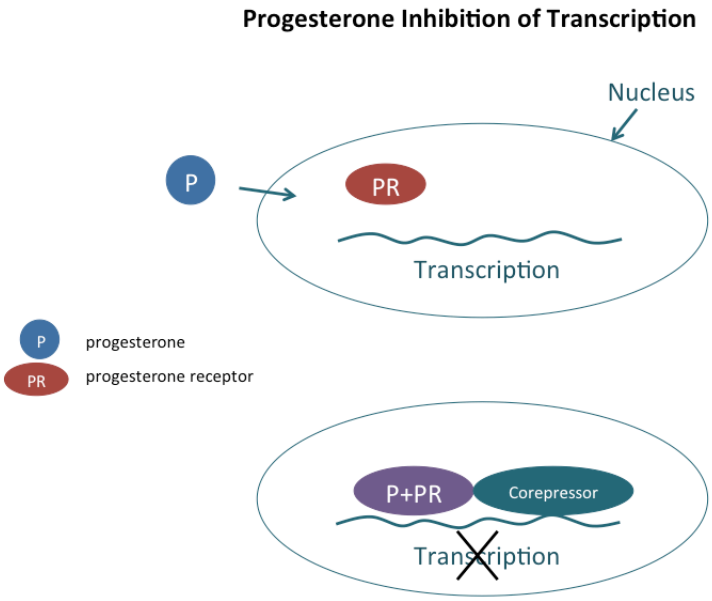

Figure 2.5: Inhibition of transcription by progesterone. The progesterone-PR complex recruits a corepressor to suppress transcription. P=progesterone; PR=progesterone receptor.

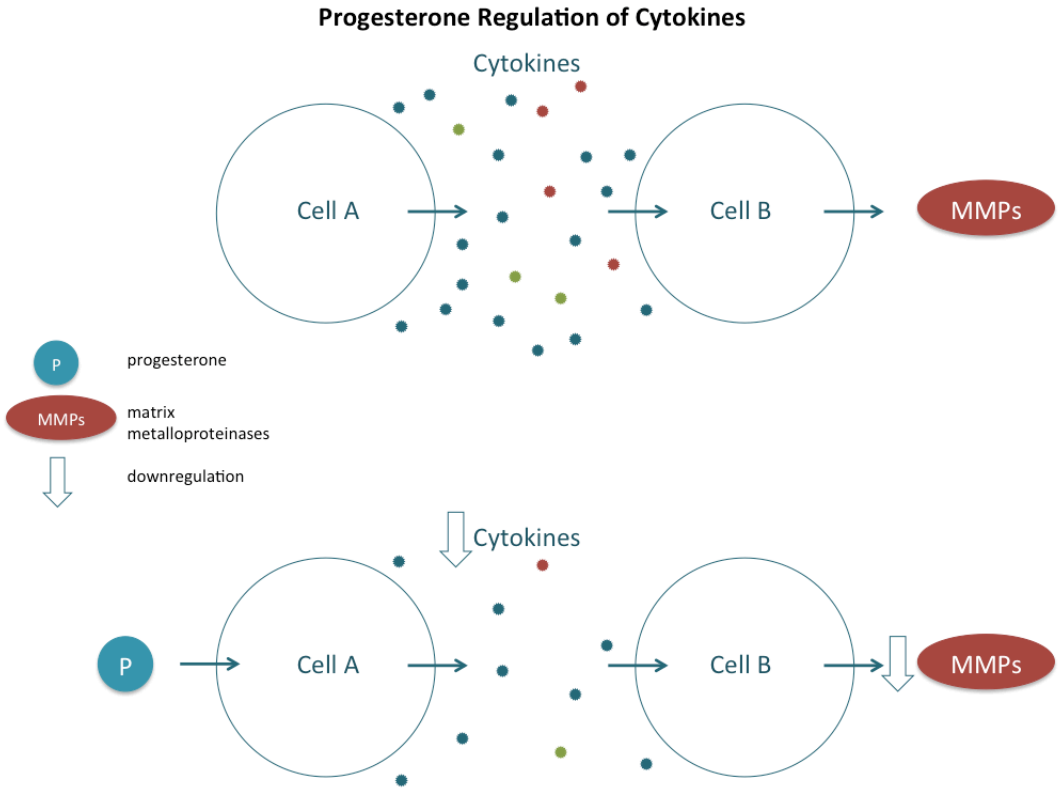

Figure 2.6: Progesterone regulation of MMPs through suppression of cytokines. Top: Cell A produces cytokines, causing cell B to produce MMPs. Bottom: Progesterone acts on cell A to reduce its production of cytokines, leading to reduced MMP production by cell B. Downward arrows indicate down-regulation of cytokines and MMPs. P=progesterone.

When these three ovarian hormones, estrogen, relaxin and progesterone, interact with their receptors, they can regulate MMPs in numerous cell types in several target tissues. Combined with their receptors, estrogen and relaxin modulate MMPs in fibroblasts of female reproductive tissues, chondrocytes, fibrochondrocytes, ligament fibroblasts, cardiac fibroblasts, vascular smooth muscle cells (VSMCs), renal fibroblasts and myofibroblasts, and mesangial cells (see Appendix Table A.1). Progesterone is known to affect female reproductive tissue fibroblasts, chondrocytes, fibrochondrocytes, and fibroblasts in ligaments

(see Appendix Table A.1). The hormone-receptor complexes alter MMP production and activity, and these changes may disrupt homeostasis in the target tissues, leading to disease or injury risk.

2.2.2 MMP function

2.2.2.1 Non-hormonal regulation

MMPs are regulated on several levels, and their activity can be altered when changes occur in signaling, transcription, activation, inhibition, or endocytosis (Amalinei, Caruntu, & Balan, 2007; Burrage et al., 2006; Cawston & Wilson, 2006; Clark et al., 2008; Emonard et al., 2005; Giannandrea & Parks, 2014; Malemud, 2006; Mancini & Di Battista, 2006; Y. Okada, 2000; Yan & Boyd, 2007). Figure 2.7 illustrates the production and regulation of MMPs. MMP signaling generally occurs through the MAPK ERK1/2 pathway in the cell (Clark et al., 2008; Mancini & Di Battista, 2006), although signaling may also occur through the nuclear factor-κB (NF-κB) pathway, which is known to lead to the production of inflammatory factors in many cell types (Clark et al., 2008; Mancini & Di Battista, 2006). Once signaling occurs, acetylation can enhance or reduce transcription, and methylation can also reduce transcription (Cawston & Wilson, 2006; Clark et al., 2008; Mancini & Di Battista, 2006; Yan & Boyd, 2007). Following transcription, the MMP mRNA can be destabilized or stabilized, preventing or enhancing translation (Burrage et al., 2006; Clark et al., 2008; Malemud, 2006; Mancini & Di Battista, 2006; Yan & Boyd, 2007). The resulting protein is an inactive zymogen that is activated by MMPs or other enzymes, such as plasmin (Amalinei et al., 2007; Malemud, 2006; Murphy et al., 1999). The activated enzyme can then be inhibited by its endogenous inhibitors, tissue inhibitors of metalloproteinases (TIMPs), or can proceed to cleave collagen (Amalinei et al., 2007; Clark et al., 2008). Additionally, MMPs and MMP-TIMP complexes can be removed from the extracellular space by endocytosis through the low-density lipoprotein receptor-related protein (LRP) (Emonard et al., 2005; Emonard, Theret, Bennasroune, & Dedieu, 2014; Etique, Verzeaux, Dedieu, & Emonard, 2013; Selvais et al., 2009).

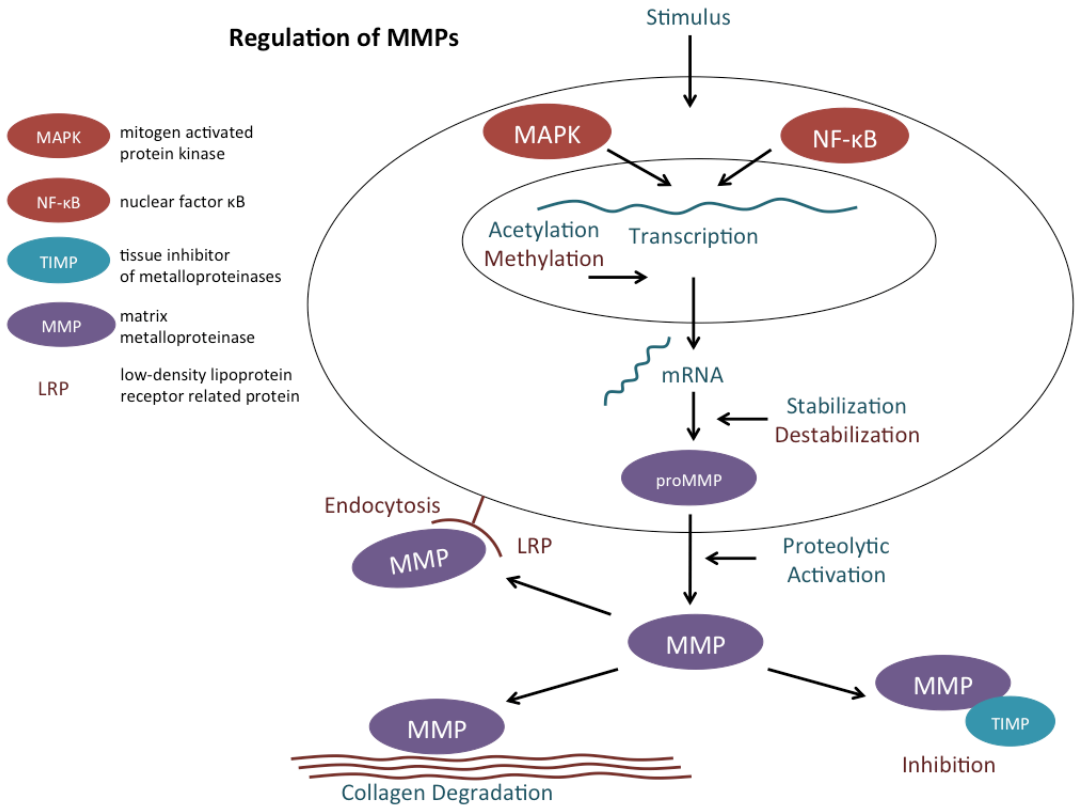

Figure 2.7: Regulation of MMPs. An extracellular stimulus initiates either the MAPK or NF-κB pathway, which leads to transcription. Translation can be prevented by acetylation or methylation and can be enhanced by acetylation. mRNA can be stabilized or destabilized in the cellular environment before the zymogen is formed. The secreted zymogen must be activated by another MMP or protease. The active enzyme can form a complex with TIMP, leading to inhibition. The active enzyme can also be endocytosed via the LRP receptor, or the enzyme may bind and degrade collagen.

2.2.2

2.2.2.2 Action

Active collagenases recognize and bind distinct sequences along tropocollagen molecules (Fields, 1991; Lauer-Fields et al., 2002; Overall, 2002). These sequences may be vulnerable to proteolytic attack

by MMPs when the collagen experiences thermal unfolding (Lu & Stultz, 2013; Overall, 2002; Perumal, Antipova, & Orgel, 2008). However, some researchers suggest that the thermal unfolding is not sufficient to allow collagen cleavage, and collagenases actively unwind the triple helix to facilitate cleavage (Bertini et al., 2012; Chung et al., 2004; Fields, 2013; Lauer-Fields et al., 2002; Overall, 2002). In either case, the triple helical collagen molecule locally unwinds prior to cleavage, since the triple helix of the tropocollagen is too large to fit into the catalytic cleft of the MMP (Fields, 2013; Lauer-Fields et al., 2002; Overall, 2002). A catalytic zinc ion resides in this cleft, and hydrolyzes a peptide bond between a glycine residue and either a leucine or isoleucine residue, leading to the characteristic ¼ and ¾ collagen fragments (Fields, 1991; Lauer-Fields et al., 2002; Overall, 2002). The collagenase then moves toward the C-terminus of the cleaved tropocollagen and to neighboring tropocollagen molecules where it continues to cleave (Saffarian et al., 2004). Once a tropocollagen has been cleaved by collagenase, it becomes susceptible to gelatinase cleavage and denaturation (Rosenblum et al., 2010). This nanoscale process is schematically shown in Figure 2.8.

Active gelatinases recognize cleaved fibrillar collagen as well as nonfibrillar collagens found in extracellular matrix (ECM) (Rosenblum et al., 2010; Van den Steen et al., 2002). These enzymes bind the tails of collagenase-cleaved tropocollagen molecules, preferring to bind the tail of the ¾ fragment (Rosenblum et al., 2010). Once they bind the cleaved tropocollagen, they begin to cleave bonds and move toward the collagenase cleavage site, eventually denaturing the entire molecule (Rosenblum et al., 2010).

Under normal physiological conditions, collagenases and gelatinases are tightly regulated to ensure normal tissue function (Cawston & Wilson, 2006). This tight regulation can be enhanced or disrupted by hormonal influences, as discussed below.

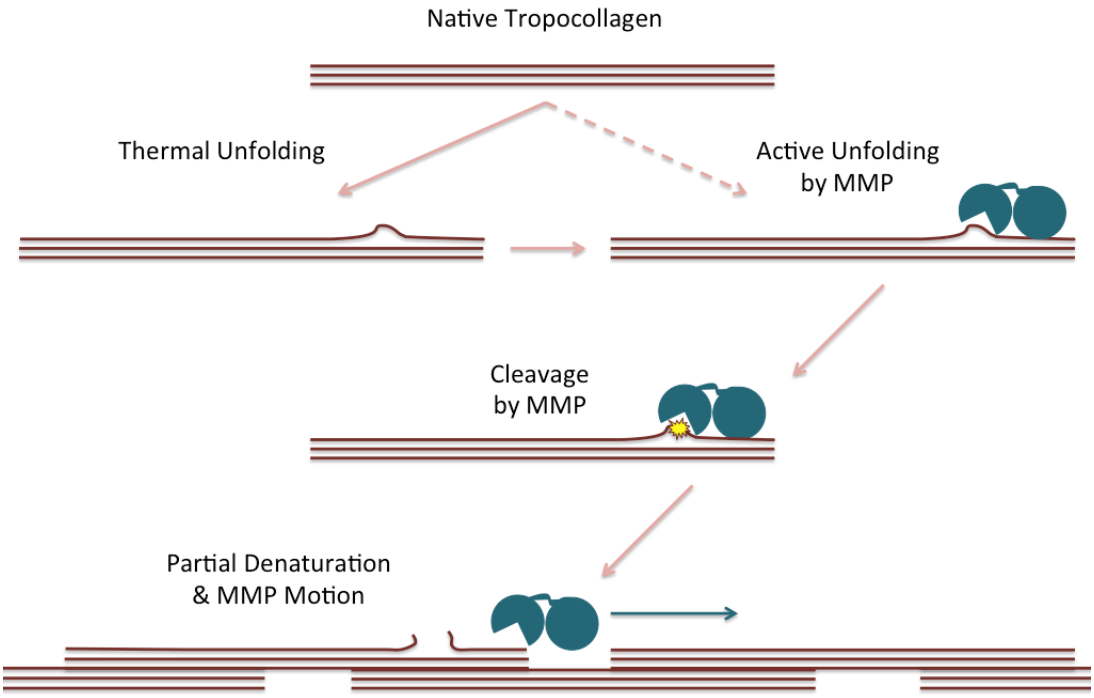

Figure 2.8: Collagenase degradation of tropocollagen. Native tropocollagen thermally unfolds, allowing collagenase to bind. Alternatively, the collagenase binds and then actively unwinds the tropocollagen. Either process allows the collagenase to fit one tropocollagen helix into its catalytic cleft, since the cleft is too narrow to accommodate the entire triple helix. The catalytic zinc ion of the collagenase hydrolyzes a peptide bond between glycine and either leucine or isoleucine, leaving the tropocollagen partially denatured and susceptible to gelatinase degradation. Following cleavage, the collagenase moves away from the cleavage site along the collagen fibril with biased motion.

2.3 Microscale: hormone regulation of MMPs at the cellular level

Appendix Table A.1 summarizes the effects of estrogen, relaxin, and progesterone on MMP production. The fractional changes in MMPs were extracted from figures and tables in the cited works. This table includes data on hormone concentration, the metric for MMP response, the cell type, the type of model

(animal or human), and the duration of treatment. In the section below, we review the influences of estrogen, relaxin, and progesterone on MMPs at the cellular or micro-scale tissue level.

We discuss multiple cell types and tissues to provide a thorough description of hormonal effects on MMPs. These tissues include female reproductive tissue, skin, cartilage, fibrocartilage, blood vessels, the heart, and the kidneys. Hormonal influences modulate remodeling in all of these tissues, even though their functions are disparate. Reproductive tissue is cyclically remodeled due to hormonal regulation of MMPs during the menstrual cycle, making it an ideal model of hormonal influences on tissue degeneration and repair. Hormones also regulate the collagen content and integrity of skin partially through their ability to regulate MMPs. In cartilage and fibrocartilage, hormones are thought to contribute to OA risk through their influences on MMPs. Hormonally modulated MMPs also regulate the structure of ECM. The structure of the ECM collagen in the blood vessels, the heart, and the kidneys may affect organ function, leading to beneficial or detrimental changes to system function. Each tissue type responds differently to hormonal treatments, some tissues increasing MMP production in response to a given hormone and others decreasing MMP production in response to the same hormone. Additionally, increased concentrations of MMPs may be beneficial in one tissue, but detrimental in another.

The descriptors beneficial and detrimental, positive and negative refer to the overall effect of MMPs on each system as discussed by the researchers who originally presented the data that we consider here. We use these terms to clarify the potential significance of changes in MMP concentrations, though we recognize that these labels are a matter of interpretation and may be subject to debate.

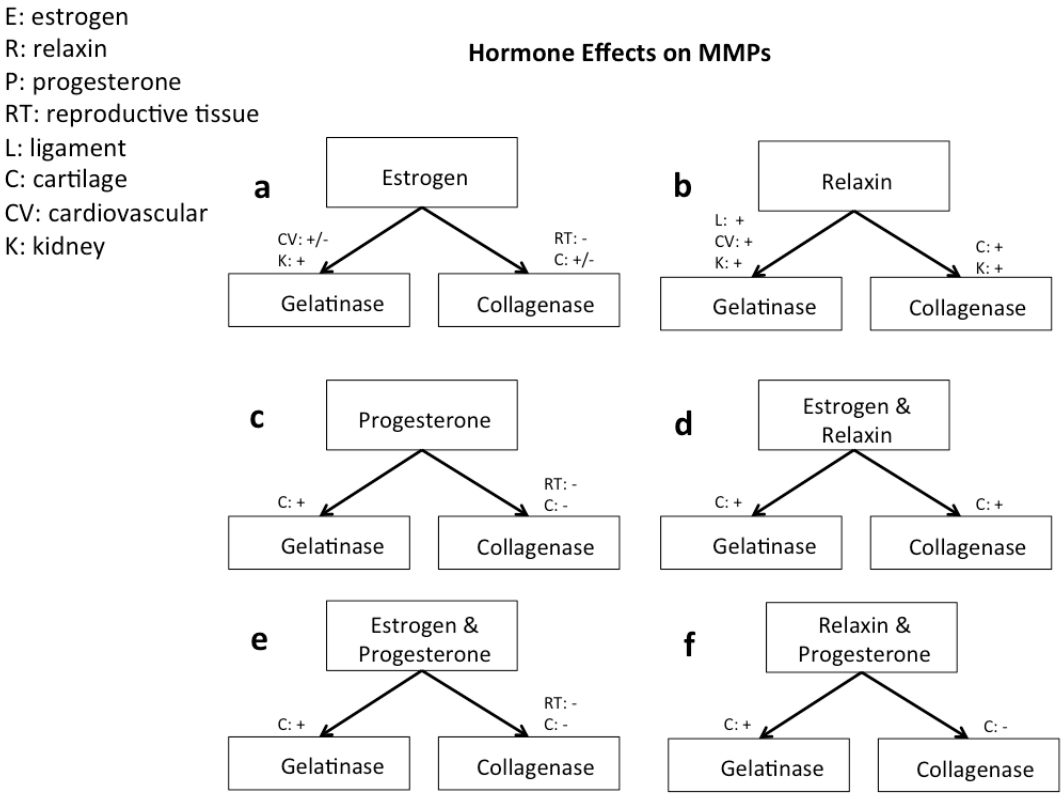

Figure 2.9: Effects of hormones and pairwise combinations of hormones on MMPs. RT: Reproductive Tissue; C: Cartilage; L: Ligament; CV: Cardiovascular system; K: Kidney; + induces MMP; - suppresses MMP.

2.3.1 Estrogen (17β-estradiol)

While many forms of estrogen exist, 17β-estradiol is the form with the highest concentration and potency in cycling women (Greenspan & Gardner, 2004). Throughout this chapter, the term estrogen refers only to 17β-estradiol. This form of estrogen regulates MMPs at the cellular level in many different tissues, including female reproductive tissue, skin, cartilage, fibrocartilage, blood vessels, and the cardiovascular system and kidneys. The effects of estrogen on collagenases and gelatinases in the cells of these tissues are listed in Appendix Table A.1 and summarized in Figure 2.9a. These tissues and their cells are functionally

diverse and respond in varied ways to estrogen. In the paragraphs below, we will address these diverse responses, describing the local consequences of estrogen treatment on MMP production in various tissues.

The female reproductive system is a good model system to illustrate the effects of local hormones on MMP production, since sex hormones are known to regulate monthly tissue remodeling through the menstrual cycle via MMPs (Gaide Chevronnay et al., 2012). Zong, et al. and Sato, et al. examined the influence of estrogen on the fibroblasts of female reproductive tissue in vivo (Sato et al., 1991; Zong et al., 2009). When the fibroblasts of the tendinous arch of the pelvic fascia are treated with estrogen, the expression and activity of MMP-13 decreases, but the expression of proMMP-13 increases (Zong et al., 2009). In this case, estrogen likely does not alter the production of new proteins, but rather prevents activation of the propeptides. Sato et al. found that active MMP-1 protein expression and mRNA decrease, but the expression of proMMP-1 is not significantly altered when cervical fibroblasts are treated with supraphysiological levels of estrogen (Sato et al., 1991). These results suggest interplay between production and activation of propeptides in response to estrogen in this system.

Similar to reproductive tissue, estrogen reduces MMP production in the skin, potentially reducing collagen degradation and preserving the integrity of the tissue. Human dermal fibroblasts down regulate proMMP-1 production in response to a physiological dose of estrogen (Qu et al., 2006). However, proMMP levels may not adequately describe the levels of active MMP, since hormone treatment can cause an increase in the propeptide and a decrease in the active enzyme, as discussed above.

Estrogen has differential effects on OA risk through MMPs in contrast to its tissue-protecting influences on the reproductive system and skin. Joint health and OA risk depend on many factors but can be partly described by the function of the cells associated with cartilage, fibrocartilage, and the synovial fluid. Articular cartilage health is related to chondrocyte function, and estrogen either reduces or does not affect MMP production in these cells (Claassen et al., 2010; Lee et al., 2003). Synoviocytes are also critical to joint health, since synovitis is a key feature of OA (Orlowsky & Kraus, 2015). Estrogen does not affect

synoviocyte production of MMPs, but these cells may indirectly regulate MMPs through inflammatory factors that act on other cell types in the joint space (Kapila & Xie, 1998). In fibrocartilaginous joints, such as the temporomandibular joint (TMJ), estrogen up-regulates the MMP production in the fibrochondrocytes but does not influence MMP levels in fibrocartilage tissue cultures (Kapila et al., 2009; Naqvi et al., 2005).

Estrogen can positively influence the cartilage by reducing MMP production in chondrocytes, the functional cells of articular cartilage (Claassen et al., 2010; Lee et al., 2003). In healthy chondrocytes from females, estrogen reduces MMP-1 and MMP-13 mRNA (Claassen et al., 2010). However, estrogen has no significant effect on MMP-1 or MMP-13 mRNA in articular chondrocytes from males (Claassen et al., 2010), a result that highlights the differences between male and female responses to hormones. However, mRNA does not necessarily provide insights to the extracellular behavior of the enzymes. Extracellular behavior is better described by protein expression and activity, which are not reported in these experiments. These two metrics are more informative than mRNA because they give a closer estimate of the amount of MMPs that will be able to act on the collagen in the extracellular space. In another set of experiments, MMP-1 protein expression in OA articular chondrocytes decreased in response to physiological doses of estrogen, but the estrogen treatments did not significantly alter MMP-1 mRNA production or activity (Lee et al., 2003). These results emphasize that MMP behavior is not always fully described by the mRNA levels, which might not provide insights into the tissue-level response of the articular cartilage.

While estrogen may have a protective effect for the collagen in articular cartilage, it may have neutral or negative effects in the cells of fibrocartilaginous joints, such as the TMJ. Kapila et al. found that estrogen significantly increases MMP-13 and MMP-9 mRNA in TMJ fibrochondrocytes (Kapila et al., 2009; Kapila & Xie, 1998; Naqvi et al., 2005). However, Kapila and Xie showed that estrogen does not affect MMP-1 protein expression in TMJ synoviocytes or fibrochondrocytes (Kapila & Xie, 1998). Additionally, MMP-1 activity is unaffected by estrogen treatment in TMJ fibrocartilaginous explants (Naqvi et al., 2005).

There may be several different reasons for the varied responses to estrogen in fibrochondrocytes and fibrocartilaginous tissue. First, estrogen simply may not affect MMP-1 expression, while it does affect MMP-13 and MMP-9 expression. Second, the choice of animal model may influence the response. A rabbit model was used in the studies that showed estrogen had no effect on MMP-1 mRNA production in fibrochondrocytes and fibrocartilaginous tissue, while a mouse model was used in the study that showed an increase in MMP-13 and MMP-9 mRNA in response to estrogen. And third, the studies used different metrics for MMPs. The mRNA levels of MMPs might not correlate to protein expression and activity, so comparison of MMP-1 expression to MMP-13 and MMP-9 mRNA may not be meaningful in the context of the larger physiological system.

In the cases discussed above, increases in MMP concentration may have detrimental effects on the tissues, leading to tissue destruction and loss of mechanical integrity. However, in other cases, increased MMP concentration may lead to beneficial remodeling in tissues with disparate functions such as cardiac tissue, arterial tissue, and the glomerulus of the kidney (Lekgabe et al., 2005; Mahmoodzadeh et al., 2010; Potier et al., 2001; Wingrove et al., 1998). Modulation of MMPs can occur in the heart after myocardial infarction, in the blood vessels during the progression of atherosclerosis, and in kidneys as fibrosis develops.

Hormones, among other factors, can modulate the protective effects of MMPs in these tissues. Estrogen increases expression of MMP-2 by mouse vascular smooth muscle cells, possibly reducing the progression of atherosclerosis (Wingrove et al., 1998). However, in cardiac fibroblasts, estrogen reduces MMP-2 mRNA and protein expression (Mahmoodzadeh et al., 2010). The authors of the study suggest that this effect may also be beneficial because MMP-2 activity in the heart may cause detrimental effects to the tissue. However, it is not entirely clear that MMP-2 is detrimental, since others argue that it may lead to beneficial remodeling (Lekgabe et al., 2005). In contrast to its effect on cardiac fibroblasts, estrogen significantly increases MMP-9 mRNA and activity in the mesangial cells of the kidney, which may reduce the effects of glomerulosclerosis (Potier et al., 2001).

2.3.2 Relaxin

Relaxin generally increases MMP production by the cells in numerous tissues, including ligaments, fibrocartilage, the synovium, the cardiovascular system, and kidneys (Heeg et al., 2005; Henneman et al., 2008; Kapila & Xie, 1998; Lekgabe et al., 2005). Although relaxin mostly increases MMP production in these cell types, its effects can be helpful or harmful, depending on the tissue and organ. The effects of relaxin on collagenases and gelatinases are summarized in Appendix Table A.1 and depicted in Figure 2.9b.

Relaxin may negatively influence ligament health. In a prospective study about ACL injury in elite female collegiate athletes, this hormone was associated with an increased risk of ACL rupture (Dragoo et al., 2011). In periodontal ligament fibroblasts, relaxin has no effect on proMMP-2 expression, and only has an effect on MMP-2 expression at one supraphysiological concentration, 250 ng/mL (Henneman et al., 2008). These results suggest that relaxin has little influence on MMPs in this ligament at physiological concentrations, but do not exclude the possibility that relaxin may affect other ligaments, such as the ACL.

Similar to estrogen, relaxin has differential effects on the cells of the cartilage, fibrocartilage, and synovium, which may relate to joint health and OA risk. In TMJ synoviocytes, relaxin does not significantly alter MMP-1 expression (Kapila & Xie, 1998). However, in TMJ fibrochondrocytes, relaxin significantly increases the expression of MMP-1, MMP-9, and MMP-13, as well as MMP-1 mRNA (Ahmad et al., 2012; Kapila et al., 2009; Kapila & Xie, 1998). Relaxin also increases MMP-1 activity in fibrocartilaginous explants (Naqvi et al., 2005). These results seem to indicate that relaxin induces collagenases and gelatinases in fibrocartilage in a dose dependent fashion, as shown in Appendix Table A.1. In this context, relaxin may lead to excessive tissue destruction, increasing the risk of joint disease.

In contrast to its effects on ligament and cartilage, relaxin leads to beneficial changes in the cardiovascular system and kidneys by increasing gelatinase concentrations, even though the cell populations and tissues are quite different between the cardiac and renal systems. In an in vivo rat model, relaxin administration increases the expression of MMP-2 by cardiac fibroblasts, which may help reduce

cardiac fibrosis caused by hypertension (Lekgabe et al., 2005). However, MMP-9 is not significantly altered by relaxin treatment. Heeg et al. and Chow et al. showed that relaxin causes MMP-2 activity to increase in renal fibroblasts and myofibroblasts, respectively (Chow et al., 2012; Heeg et al., 2005). Additionally, Chow et al. found that MMP-13 and MMP-9 activity increases when renal myofibroblasts are treated with relaxin (Chow et al., 2012). However, when renal fibroblasts are treated with relaxin, no significant change in MMP-9 activity is observed (Heeg et al., 2005). Relaxin benefits the cardiovascular system and kidneys by inducing MMP-2 in multiple cell populations, combating abnormal collagen accumulation.

2.3.3 Progesterone

The effects of progesterone on MMP expression and activity have not been studied as extensively as the effects of estrogen and relaxin, possibly because progesterone does not directly promote or inhibit MMP transcription, but instead inhibits the transcription of factors such as IL-1 and TNF-α, which can lead to MMP transcription, as depicted in Figure 2.6 (Gaide Chevronnay et al., 2012). These indirect effects on cellular production of MMPs are depicted in Figure 2.9c. The effects of progesterone have been relatively well studied in the context of the female reproductive tract where progesterone acts to reduce inflammation and tissue degradation.

Progesterone appears to suppress MMP production in the fibroblasts of the reproductive tract, preventing tissue degradation during the luteal phase of the menstrual cycle (Selvais et al., 2009). Zong et al. found that progesterone decreased MMP-13 protein expression and activity, but increased proMMP-13 expression by pelvic fibroblasts (Zong et al., 2009). In this case, progesterone may inhibit the activation of the propeptide, rather than inhibiting production, an effect similar to that of estrogen in these cells.

Imada et al. and Sato et al. examined the effects of progesterone on MMP production in cervical fibroblasts (Imada et al., 1997; Sato et al., 1991). The former found that progesterone treatment decreases MMP-9 mRNA in these cells (Imada et al., 1997), and the latter found that progesterone treatment decreases

MMP-2 mRNA, protein expression, and activity at most concentrations (Sato et al., 1991). However, progesterone has no significant effect on MMP-2 protein expression or activity at a concentration of 0.0314 ng/mL and has no significant effect on MMP-2 activity at a concentration of 3.14 ng/mL (see Appendix Table A.1).

The effects of progesterone on fibrocartilage differ from its effects on reproductive tissue, showing differential effects on collagenase and gelatinase mRNA. Progesterone reduces MMP-13 mRNA in TMJ fibrochondrocytes but significantly increases MMP-9 mRNA in these cells (Kapila et al., 2009). Again, mRNA levels do not directly relate to protein expression or activity, so the functional effects of progesterone on fibrocartilage are unclear.

2.3.4 Pairwise combinations

Hormonal effects are generally not isolated; they act in concert with each other in physiological systems, suggesting that they should be studied together rather than in isolation. In the following paragraphs, we will discuss the effects of pairwise combinations of hormones on MMP production. These studies of pairwise hormonal effects do not completely describe the physiological systems in question, but they begin to address some of the complexities of hormonal interactions that are not addressed in experiments with individual hormones. These interactions have been studied in the cells of the TMJ, as well as the female reproductive tract.

In the TMJ, estrogen and relaxin have a detrimental effect on the tissue through MMPs. This combination increases MMP mRNA, protein expression, and activity from TMJ fibrochondrocytes and fibrocartilaginous tissue explants, but has no effect on TMJ synoviocytes (Kapila & Xie, 1998; Naqvi et al., 2005). Relaxin combined with a supraphysiological dose of estrogen increases MMP-1 mRNA, protein expression, and activity, as well as MMP-9 and MMP-13 mRNA (Kapila et al., 2009; Kapila & Xie, 1998). However, estrogen combined with relaxin has no significant effect on MMP-1 protein expression in TMJ

synoviocytes (Kapila & Xie, 1998). These results agree with the results found for estrogen and relaxin individually, but their combined effect is greater than either individual effect in most cases (Kapila et al., 2009). The combined effects of estrogen and relaxin are summarized in Figure 2.9d.

In fibrocartilage, progesterone appears to partially attenuate the detrimental effects of estrogen and relaxin. When progesterone treatment accompanies estrogen treatment, fibrochondrocytes decrease MMP-13 mRNA, though they increase MMP-9 mRNA (Kapila et al., 2009). Progesterone and relaxin together reduce MMP-13 mRNA in TMJ fibrochondrocytes but increase MMP-9 mRNA in these cells (Kapila et al., 2009). The effects of these combinations are shown in Figure 2.9e and 2.9f.

While pairwise hormonal effects are not entirely clear in the fibrocartilage, they are better defined in reproductive tissues. Progesterone and estrogen prevent MMP-mediated tissue degradation in reproductive tissue. In this context, their combined effects are similar to the effects of the individual hormones and are depicted in Figure 2.9e. Together in pelvic fibroblasts, they decrease MMP-13 expression and activity, but increase proMMP-13 levels (Zong et al., 2009). These hormones appear to produce slightly different responses across the menstrual cycle, suppressing MMPs to varying degrees during different phases as demonstrated by Vassilev et al. (Vassilev et al., 2005). At all time points in the secretory phase, MMP-1 is suppressed by treatment with a combination of estrogen and progesterone (Vassilev et al., 2005). However, in the late secretory phase, the combined hormones suppress MMP-1 to a greater degree than in the early/midsecretory phase.

The microscale changes that hormones induce are summarized in Figure 2.10 and Appendix Table A.1. The changes at this scale relate to changes at the macroscopic level, and the following section describes the functional consequences of these microscale changes.

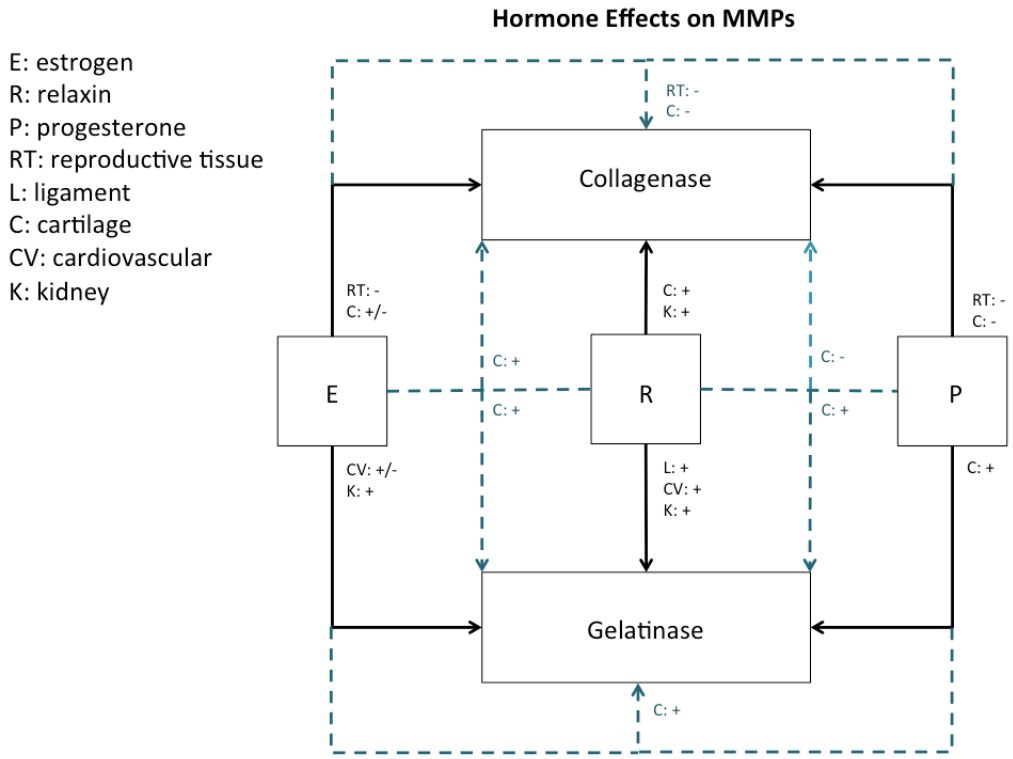

Figure 2.10: Effects of estrogen, relaxin, progesterone (solid lines), and pairwise combinations of those hormones (dashed lines) on collagenases and gelatinases. RT: Reproductive Tissue; C: Cartilage; L: Ligament; CV: Cardiovascular; K: Kidney; + induces MMP; - suppresses MMP.

2.4 Macroscale: tissue-level effects of hormones in MMP-related processes

The changes that hormones cause at the microscale, or cellular level, can alter MMP-related processes at the tissue level. The endometrium is a well-studied example of the macroscopic effects of hormones on tissue remodeling. Each month, the endometrium sheds and regenerates in response to hormonal fluctuations. The tissue regenerates during the proliferative phase until ovulation, and then

thickens and prepares for implantation of an embryo after ovulation (Greenspan & Gardner, 2004). If implantation does not occur, progesterone and estrogen levels drop, leading to menstruation, the shedding of the endometrial lining (Gaide Chevronnay et al., 2012; Greenspan & Gardner, 2004; Salamonsen, Butt, Hammond, Garcia, & Zhang, 1997).

As mentioned previously, progesterone does not directly inhibit transcription of MMPs, but rather influences other factors that do directly inhibit transcription, such as cytokines and growth factors (Figure 2.6) (Critchley et al., 2001; Evans & Salamonsen, 2012; Gaide Chevronnay et al., 2012; Kelly et al., 2001; Salamonsen, 1998; Salamonsen & Woolley, 1996). Progesterone may also prevent MMP-induced tissue breakdown by enhancing the function of LRP receptors, which endocytose the MMPs before they can degrade the tissue (Selvais et al., 2009). When serum progesterone concentration drops before menstruation, it ceases to suppress these cytokines and growth factors, and allows them to initiate MMP transcription. The drop in progesterone at menstruation also causes a decrease in the functionality of the LRP receptors, leading to higher levels of extracellular MMPs (Selvais et al., 2009). The MMPs in turn act on the endometrial lining and activate proMMP-9, which is present throughout the cycle but only becomes active during menstruation (Gaide Chevronnay et al., 2012).

MMPs are expressed variably in the human endometrium throughout the cycle, peaking at menstruation (H. F. Huang, Hong, Tan, & Sheng, 2004; Vassilev et al., 2005). But in the peritoneal fluid, serum estrogen levels are positively correlated with MMP-2 levels, while serum progesterone levels are negatively correlated with MMP-2 levels in patients with endometriosis (H. F. Huang et al., 2004). However, this finding may be specific to patients with endometriosis or the correlation may be specific to peritoneal fluid, since conflicting data exist that show estrogen and progesterone inhibit MMPs in female reproductive tissue (Sato et al., 1991; Vassilev et al., 2005; Zong et al., 2009).

Cartilage and fibrocartilage are also subject to the effects of ovarian hormones (Sniekers, Weinans, Bierma-Zeinstra, van Leeuwen, & van Osch, 2008; Warren & Fried, 2001). However, the hormonal effects

are not well understood. In some animal models, removing hormonal influences by ovariectomy worsens outcomes of OA, but does not affect outcomes in other cases (Sniekers et al., 2008). Additionally, estrogen replacement therapy in animal models improves OA outcomes in some cases but worsens them in others (Sniekers et al., 2008).

Women experience TMJ disorders much more frequently than men, and hormones are thought to play a role in the sex bias (Warren & Fried, 2001). Despite the increased incidence of TMJ disorders in women, the literature is unclear about the influence of hormones on the incidence of these disorders (Warren & Fried, 2001). However, in vitro studies of fibrocartilaginous cells have showed that estrogen, relaxin, and progesterone modulate MMP production by these cells, suggesting that the hormones may regulate TMJ disease through their influence on MMPs (Ahmad et al., 2012; Kapila et al., 2009; Kapila & Xie, 1998; Naqvi et al., 2005).

The impact of ovarian hormones on ligaments is still unclear. Dragoo et al. found that relaxin levels correlate with ACL injury risk in female collegiate athletes (Dragoo et al., 2011). Additionally, some researchers have observed a varying risk of ACL injury throughout the menstrual cycle, while others have observed no correlation between phase of the menstrual cycle and injury risk (Wojtys, Huston, Boynton, Spindler, & Lindenfeld, 2002; Zazulak, Paterno, Myer, Romani, & Hewett, 2006). One study showed that estrogen treatment in vivo had no effect on the mechanical properties of rat ACLs (Warden, Saxon, Castillo, & Turner, 2006). However, this study did not examine the effects of relaxin, which may play a crucial role in susceptibility to ACL injury (Dragoo et al., 2011). In light of these observations, further research is required to clarify the influence of hormones on ligaments, particularly the ACL.

Relaxin and estrogen appear to benefit the cardiovascular system by reducing cardiac fibrosis and remodeling atherosclerotic lesions. Estrogen protects the cardiovascular system through several mechanisms, including MMP-2 regulation (Knowlton & Korzick, 2014; Wingrove et al., 1998). High doses of estrogen induce MMP-2, which may reduce or prevent vascular disease (Wingrove et al., 1998). Relaxin

also has positive effects on the cardiovascular system when administered in high doses. The hormone reduces cardiac fibrosis in rats, likely through MMP-2 induction (Lekgabe et al., 2005).

Renal fibrosis, like cardiac fibrosis, may be attenuated by estrogen and relaxin because of their regulatory effects on MMPs. Estrogen induces MMP-2 and MMP-9 and relaxin induces MMP-2 in the kidneys, which may lead to their anti-fibrotic effects (Heeg et al., 2005; Silbiger & Neugarten, 2008). Women are at lower risk for renal disease than men, and renal disease progresses more slowly in women than in men (Silbiger & Neugarten, 2008). A number of factors influence the incidence and progression of renal disease in men and women, and hormones are among these factors (Silbiger & Neugarten, 2008), likely because of their influence on MMPs.

2.5 Discussion

Many researchers have studied the influences of estrogen, relaxin, and progesterone on collagenases and gelatinases. However, gaps in knowledge still exist. In many cases, we do not fully understand the link between the nanoscale chemical events and the microscale cell responses. We do not yet understand what nanoscale mechanisms cause some cell types to have opposite microscale responses to the same hormone. For example, it is not clear why estrogen reduces MMP-13 protein expression in pelvic fibroblasts but increases MMP-13 in fibrochondrocytes. Further research is required to clarify the mechanisms that dictate the microscale behavior.

A deeper understanding of microscale responses to hormones is required to elucidate the mechanisms of hormonally mediated gender biases in diseases such as OA. The studies presented in this review focus primarily on the functional cells for each tissue and seem to show that female sex hormones have a mostly protective role when they interact with chondrocytes, the functional cell type in hyaline cartilage. In contrast, fibrocartilage appears to be susceptible to damage due to the effects of estrogen and

relaxin, which up regulate MMP production by fibrochondrocytes and may contribute to OA. These effects may be especially important in fibrocartilaginous joints like the TMJ, but also may contribute to production of MMPs in the fibrocartilage that is present in joints that primarily contain hyaline cartilage, such as the knee joint. Additionally, hormones might exert important degenerative effects indirectly by modulating inflammatory cytokines. Recall that progesterone exerts its effects by inhibiting inflammatory molecules that lead to cellular MMP production. Under some circumstances, estrogen may also affect cytokines produced by inflammatory cells (Capellino, Straub, & Cutolo, 2014; Dimitrijevic et al., 2013; Kovats, 2015). When excess inflammatory cells are present, following ACL reconstruction surgery for example (Heard et al., 2013), their interactions with estrogen may lead to increased inflammatory cytokines and MMPs, potentially resulting in OA. This pathway of inflammation and degradation could help explain the sex bias in post-ACL reconstruction OA, despite the evidence that estrogen inhibits MMP production in chondrocytes.

By elucidating the hormonal effects on MMPs in the joint capsule, new strategies for OA treatments may be developed to target the most important hormonal influences on MMPs. For example, targeted strategies to locally inhibit estrogen and relaxin could be developed to prevent up regulation of MMPs in fibrocartilaginous tissue. Alternatively, it may be possible to target molecules in the signaling cascades that lead to MMP transcription as a result of hormone receptor activation in fibrochondrocytes. And if hormones significantly modulate inflammatory factors that eventually lead to MMP production, anti-inflammatory strategies may help reduce the sex disparity in OA initiation and progression. Before these strategies can be implemented, however, further work must be done to determine which of these mechanisms is most critical to OA initiation and progression.

The effects of estrogen, relaxin, and progesterone may partially explain sex biases in OA and other pathologies, but androgens may also contribute to the gender biases in these diseases. Henmi et al. showed that DHEA (an androgen) may suppress MMPs in rats with polycystic ovary syndrome (Henmi et al., 2001), and Bobjer et al. also showed that low levels of testosterone are correlated with higher levels of circulating

inflammatory factors (Bobjer, Katrinaki, Tsatsanis, Lundberg Giwercman, & Giwercman, 2013), indicating a possible inhibitory effect of testosterone on inflammatory factors. Direct inhibition of MMPs, or indirect inhibition of MMPs through inhibition of inflammatory factors may slow the development and progression of diseases, such as OA, where a sex bias exists. Further studies of the influences of testosterone and other androgens are necessary to give a more thorough understanding of sex biases in various disease states, including OA.

In addition to their effects on cartilage, hormones may influence the sex bias in ACL injuries through their effects on MMPs but research in this area is lacking. The ACL may experience accelerated collagen degradation due to hormone-induced MMPs. Hormones are known to affect ACL injury risk in female athletes (Dragoo et al., 2011; Zazulak et al., 2006), and this risk may be caused by hormonally modulated MMPs. However, to our knowledge, no experiments have addressed the effects of estrogen, relaxin, and progesterone on MMP production in ACL fibroblasts or resident tissue macrophages, or the effects of MMPs on ACL collagen integrity. Further work is required to clarify the influence of hormones and MMPs in this ligament and in other tissues.

Along with a deeper understanding of hormonal modulation of MMPs as it relates to ACL injury risk, a deeper understanding of other potential hormonal influences on injury risk is required. For example, hormones may modulate neural control, increasing the risk of ACL injury. Estrogen and progesterone receptors are present throughout the nervous system, including areas that play a part in motor control (Brailoiu et al., 2007; Labombarda et al., 2010; Zuloaga et al., 2012). Additionally, estrogen receptors are present in muscles (Wiik, Ekman, Johansson, Jansson, & Esbjornsson, 2009; Wiik et al., 2003), and their activity may modulate the muscular response to neural stimuli. Several experiments have demonstrated that neuromuscular control varies across the menstrual cycle (Bryant, Crossley, Bartold, Hohmann, & Clark, 2011; Casey, Hameed, & Dhaher, 2014; Dedrick et al., 2008), while others have demonstrated no difference across the cycle (Friden et al., 2003; Hertel, Williams, Olmsted-Kramer, Leidy, & Putukian, 2006). If

changes in neuromuscular control do occur, they could alter the loading on the knee joint, and lead to ACL injury risk and OA risk, independent of the hormonal regulation of MMPs.

The research reviewed here may be used not only as a tool to better understand physiology, but also as a tool in the design of biomaterials. Biomaterials can be used for a variety of purposes, including cell therapies and drug delivery (Jha et al., 2016; Van Hove, Beltejar, & Benoit, 2014). Some biomaterials incorporate MMP-degradable crosslinks, which can enhance cell function and control drug release. These adaptive materials can be used in a range of different systems throughout the body. For example, they could be used to help regenerate cartilage, repair ischemic heart tissue, and promote vascular healing after balloon angioplasty (Jha et al., 2016; Seliktar, Zisch, Lutolf, Wrana, & Hubbell, 2004; Sridhar et al., 2015). However, hormones affect MMP production in each of these tissues, potentially complicating the implementation these designs. Hormones may continue to influence the state of the native tissue once a material has been implanted and affect the degradation kinetics of the implanted material. The consequences of these effects are not entirely clear but will depend on the cell type and may lead to differential effectiveness in populations with varied sex hormone profiles.

In addition to synthetic materials with MMP-degradable crosslinks, other biomaterials are susceptible to degradation by MMPs. For example, natural materials have been considered as candidates for cartilage repair and regeneration. These materials include various types of collagen as well as fibrin, which can be digested by MMPs (Duarte Campos, Drescher, Rath, Tingart, & Fischer, 2012). Again, the efficacy of these materials may depend on the extent to which sex hormones modulate MMPs in the tissues.

Finally, we must address some of the shortcomings of the existing research that was presented in this review. These shortcomings include the issues of in vitro studies rather than in vivo studies, the choice of experimental hormone concentrations, and the effects of other cell types that may be present in the tissues of interest. Though some studies in this review used in vivo data, many used in vitro techniques to examine the influences of hormones. Often, the in vitro studies examined supraphysiological levels of hormones,

and few studies addressed the local concentrations of hormones that the cells experience in vivo, which may differ from normal serum concentrations. Additionally, few studies have addressed the effect of hormones on the local inflammatory cells that may lead to MMP production in the tissues of interest. It is possible that estrogen and relaxin also modulate inflammatory factors and MMP expression in a similar manner to progesterone, and this possibility should be explored. For the reasons listed above, it is still unclear in many cases how the experimental results apply to the physiological systems that are more complex than the simplified experimental systems.

2.6 Conclusion

Despite some gaps in knowledge, the research community has made considerable progress toward understanding the nanoscale, microscale, and macroscale effects of estrogen, relaxin, and progesterone on collagenases and gelatinases. This knowledge will help researchers understand how hormones affect the balance of degradation and repair in many tissues, will aid the development of treatment strategies for diseases, such as OA, and will inform prevention strategies for common injuries, such as ACL rupture.

Chapter 3: Study of principal sex hormone effects on post-injury synovial inflammatory response

Abstract

Following an anterior cruciate ligament injury, premenopausal females tend to experience poorer outcomes than males, and sex hormones are thought to contribute to the disparity. Evidence seems to suggest that the sex hormones estrogen, progesterone, and testosterone may regulate the inflammation caused by macrophages, which invade the knee after an injury. While the individual effects of hormones on macrophage inflammation have been studied in vitro, their combined effects on post-injury inflammation in the knee have not been examined, even though both males and females have detectable levels of both estrogen and testosterone. In the present work, we developed an *in silico* kinetic model of the post-injury inflammatory response in the human knee joint and the hormonal influences that may shape that response. Our results indicate that, post-injury, sex hormone concentrations observed in females may lead to a more pro-inflammatory, catabolic environment, while the sex hormone concentrations observed in males may lead to a more anti-inflammatory environment. These findings suggest a mechanism that may lead to increased damage to the cartilage and poorer post-injury outcomes for females. Furthermore, we observed that different concentrations of estrogen that are physiologically relevant for females led to significant differences in the post-injury inflammatory response. Thus, future studies of post-injury outcomes should not only examine potential differences between males and females, but should also examine differences among females that may arise due to different hormonal concentrations at the time of injury. The model developed herein may inform future *in vitro* and *in vivo* studies that seek to uncover the origins of sex differences in outcomes and may ultimately serve as a starting point for developing targeted therapies to prevent or reduce the cartilage damage that results from post-injury inflammation, particularly for females.

3.1 Introduction

Females tend to have poorer prognoses after anterior cruciate ligament (ACL) injury compared to males, particularly with respect to cartilage damage (R. T. Li et al., 2011; Lohmander, Ostenberg, Englund, & Roos, 2004). This difference has been widely observed, but few, if any, studies have attempted to uncover the biological link between sex and damage to the cartilage after knee injury. One potential link between sex and cartilage damage may be the inflammatory process, which is modulated by sex hormones and can modulate the production of matrix metalloproteinases (MMPs), the catabolic molecules that eventually cause permanent cartilage destruction (Troeberg & Nagase, 2012). However, while some studies have shown that hormones affect cytokine production (Calippe et al., 2010; D'Agostino et al., 1999; Lei et al., 2014; L. Liu et al., 2014; Sun et al., 2012) and other studies have shown that those cytokines affect production of MMPs (Asano et al., 2006; Saren, Welgus, & Kovanen, 1996; Yorifuji et al., 2016), no study has comprehensively examined the effects of sex hormones on MMPs via their effects on inflammation in the synovial environment after ACL injury.

The principal sex hormones – estrogen, progesterone, and testosterone – each have distinct effects on macrophages, the primary invading cell type after ACL injury (Murakami et al., 1995). Testosterone, a predominantly male hormone, and progesterone, a predominantly female hormone, tend to promote a more anti-inflammatory response from macrophages (D'Agostino et al., 1999; Lei et al., 2014), while estrogen may be pro- or anti-inflammatory, depending on its concentration and microenvironment (Guery, 2012; Straub, 2007). In the synovial environment for males and pre-menopausal females, estrogen concentrations fall into a range where it has pro-inflammatory effects on macrophages (Rovensky et al., 2004; Straub, 2007), though estrogen can have anti-inflammatory effects on macrophages at other concentrations or when acting on other cell types (Straub, 2007). Together and individually, these three hormones have the potential to alter the inflammatory environment that develops after an ACL injury.

Although hormonal regulation of inflammation has not been directly connected to subsequent MMP production in the knee synovium, a clear connection has been established between inflammation and MMP production. Pro-inflammatory molecules like IL-1β and TNF-α enhance MMP production by multiple cell types, including macrophages and synovial fibroblasts (SFs), the resident cells of the synovium (Asano et al., 2006; Saren et al., 1996; Yorifuji et al., 2016). Furthermore, anti-inflammatory molecules like IL-10 can reduce MMP production (Kothari et al., 2014), creating a complex environment with opposing effects of inflammatory mediators, along with hormonal action.

Such inflammatory environments have been examined *in silico* (Anderson et al., 2015; Cobbold & Sherratt, 2000; Nagaraja, Wallqvist, Reifman, & Mitrophanov, 2014). These models revealed insights about which cytokines exert the greatest influence on inflammation in a system of macrophages or a system with both macrophages and neutrophils, laying a methodological foundation for future *in silico* studies of inflammatory processes. However, these models could be adapted to include more thorough uncertainty analysis. One of the previous studies performed local sensitivity analysis to determine which cytokine would have the strongest effect on macrophage migration (Nagaraja et al., 2014), but the study did not report how uncertainties in the nominal parameters would influence the time course of inflammation for all cytokines. Such analysis would help account for uncertainties in the *in vitro* experiments that were used to estimate the nominal values, such as varied experimental conditions and limited numbers of samples. Furthermore, such analysis would help account for biological differences that exist between the *in vitro* experiments from which the parameters were formulated and the *in vivo* states that the model sought to predict.

Previous models could also be adapted to include analysis of hormonal effects on the process of inflammation. To date, no model has incorporated the effects of sex hormones on the inflammatory responses under investigation.

Thus, in the present work, we sought to examine the interplay between sex hormones, inflammation, and MMP production in the injured synovium using an *in silico* approach. Recognizing the limitations of *in silico* studies, we accounted for uncertainties in the nominal model parameters using a statistical sampling approach that provided upper and lower bounds for our results. We hypothesized that 1) distinct patterns of inflammation would emerge when the cells found in the injured knee were exposed to expected male and female concentrations of the principal sex hormones, with a more pro-inflammatory response and greater MMP involvement for female concentrations, 2) the anti-inflammatory influence of progesterone would partially attenuate the pro-inflammatory influence of estrogen for females, and 3) the low estrogen concentrations at levels consistent with the early follicular phase would result in an attenuated inflammatory response compared to higher estrogen concentrations. With this quantitative framework, we aimed to shed light on the underlying processes that may cause increased cartilage damage for females after knee injury (Lohmander et al., 2007), and open avenues of research directed toward prevention or reduction of post-injury damage to the cartilage, particularly for females.

3.2 Methods

Using a system of first order differential equations, we modeled two key physiological processes: 1) cellular migration of monocytes/macrophages and platelets, and 2) cellular production of inflammatory mediators by those cells and by the resident synovial fibroblasts (SFs). Figure 3.1 shows these processes in a schematic form. The procedure for formulating such a model has been reported previously (Nagaraja et al., 2014), but we also describe the procedure in detail here for completeness. To formulate the model parameters, we first performed an extensive review of literature to obtain *in vitro* studies that reported the quantitative data necessary for each parameter. This search included hundreds of search queries and resulted in over 40 useable publications from the PubMed database.

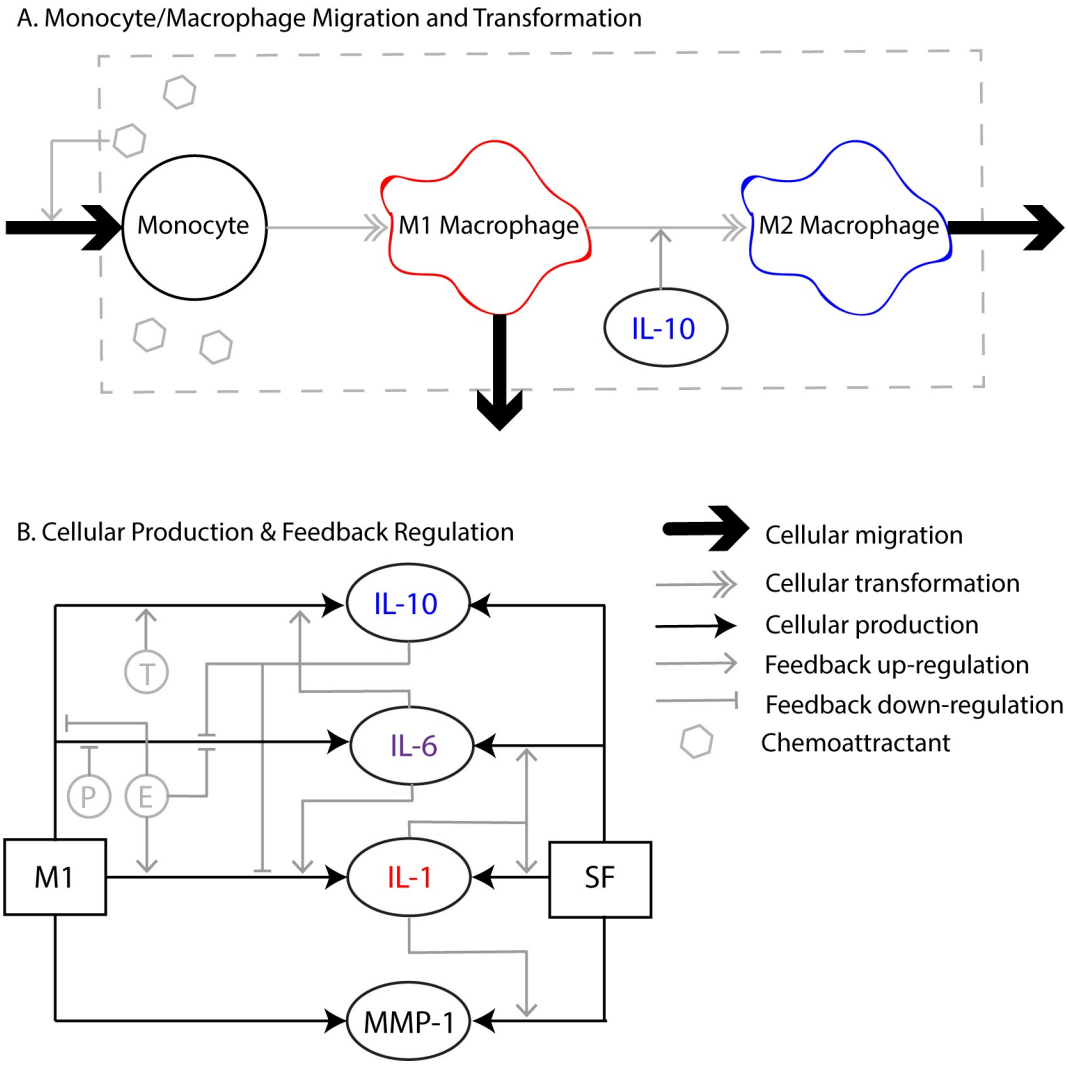

Figure 3.1: A. Depiction of monocyte and macrophage migration and transformation. Injury to the knee causes the production of chemoattractants, such as TNF-α and TGF-β, which lead to monocyte migration from the bloodstream to the synovium. The synovium is indicated by the gray dashed box. Monocytes transform into pro-inflammatory M1 macrophages. The molecular processes that drive transformation to M1 cells are not modeled. Instead, a 12-hour delay is incorporated into the model as a way to account for the time it takes for monocytes to transform, as previously described (Nagaraja et al., 2014). IL-10 drives the transformation of M1 cells to anti-inflammatory M2 macrophages (Kuwata et al.,

2003). Both M1 and M2 cells can migrate out of the synovium. **B. Cellular production and feedback regulation of a subset of the substances incorporated in the model.** M1 and SF both produce IL-10, IL-1, IL-6, and MMP-1. IL-10 down-regulates M1 production of IL-1 and IL-6, while IL-1 up-regulates SF production of IL-1, IL-6, and MMP-1. IL-6 up-regulates M1 IL-10 and up-regulates M1 IL-1. Estrogen (E) up-regulates M1 production of IL-1 and down-regulates M1 production of IL-10 and IL-6, while testosterone (T) up-regulates M1 production of IL-10. Progesterone (P) down-regulates M1 IL-6. M1: pro-inflammatory macrophage. M2: anti-inflammatory macrophage. SF: synovial fibroblast. E: estrogen. T: testosterone.

3.2.1 Production and decay

We calculated the production coefficients using the simplifying assumption that production was a linear function of time according to the expression:

$$k_{x,y} = \frac{C_x}{C_y t} \quad (1)$$

Where C_x is the concentration of the substance of interest in ng/mL, C_y is the experimentally reported concentration of cell type y in cells/mL, and t is the duration of cellular production in hours. To determine the degradation coefficients, we utilized experimentally reported half-lives for each substance:

$$k_{d,x} = \frac{0.693}{t_{1/2}} \quad (2)$$

where $t_{1/2}$ is the half-life of a substance in hours. Appendix Table B.1 shows all production coefficients and degradation coefficients, and S1 Text shows sample calculations for both quantities. In the sample

calculations, we note the study from which the raw data were extracted, list the values obtained from the study, note the figure or table from which the data were extracted, and show the steps of the calculations. In total, we included 35 production and decay coefficients in our model, which we derived from 23 published reports.

3.2.2 Chemotaxis

Table 1 lists the equations for migration kinetics of macrophages and SFs. We assumed that SF concentration was constant throughout each simulation, while we allowed the macrophage concentrations to vary.

In vitro experiments have demonstrated that macrophages migrate in response to signals from TGF-β and TNF-α (Pai, Ha, Kirschenbaum, & Kamanna, 1996; Wahl et al., 1987). Thus, we used chemotactic functions, $f_{TGF,M1}$ and $f_{TNF,M1}$, respectively, to incorporate migration into the present model. Appendix Table B.2 lists the parameters for these functions. However, like a previous *in silico* study (Nagaraja et al., 2014), we specified that these chemotactic functions would equal zero below a threshold platelet concentration ($10 * 10^{-12}$ cells/mL) to prevent non-physiological re-initiation of inflammation. While this concentration is not rooted in physiology, it is nonetheless useful computationally and has been established as a technique to prevent non-physiological re-initiation of inflammation in the model (Nagaraja et al., 2014).

Table 3.1: Equations for Cellular Migration

Model Variable	Initial Value	Concentration in Healthy Synovium	Equation
"Platelets"	$2 * 10^8 \frac{cells}{mL}$	$0 \frac{cells}{mL}$	$\frac{dC_P}{dt} = -k_{d,P}C_P$
M1 Macrophages	$0 \frac{cells}{mL}$	$0 \frac{cells}{mL}$	$\frac{dC_{M1}}{dt} = k_{M,in}(f_{TGF,M1} + f_{TNF,M1}) - k_{M1M2}f_{M1M2}C_{M1} - k_{d,M}C_{M1}$
M2 Macrophages	$0 \frac{cells}{mL}$	$0 \frac{cells}{mL}$	$\frac{dC_{M2}}{dt} = k_{M1M2}f_{M1M2}C_{M1} - k_{d,M}C_{M2}$
SFs	$5 * 10^5 \frac{cells}{mL}$		$\frac{dC_{SF}}{dt} = 0$

Formulations of $f_{TGF,M1}$ and $f_{TNF,M1}$, and the values of their parameters can be found in Appendix Table B.2.

3.2.3 Feedback modulation of concentrations

We used feedback functions to describe the changes in production of a given substance by other substances based on numerous cellular-level *in vitro* experiments, which we cite in Appendix Table B.2. In this procedure, we modeled negative feedback with the monotonically decreasing function

$$g_{j,x} = a * \exp(-b * C_j) + c \quad (3)$$

and we modeled positive feedback data with the monotonically increasing function

$$f_{j,x} = a * \frac{C_j}{1 + C_j} \tag{4}$$

where j is the modulatory substance, x is the substance being modulated, a, b, and c are fitting parameters, and C_j is the concentration of the modulatory substance. We incorporated the up-regulatory functions found with Eq. 4 into the model using the expression

$$g_{j,x} = 1 + f_{j,x}, \tag{5}$$

to represent a fractional increase above the baseline production. Appendix Table B.2 lists all the estimated parameters for chemotaxis functions and feedback functions. For clarity, we also included a detailed description of the process for generating feedback functions in the Appendix B. In total, we included 56 feedback coefficients in our model, which we derived from 24 published reports.

3.2.4 Time evolution of cytokine, MMP, and TIMP concentrations

We used the nominal production and decay coefficients that we found with Eqs. 1 and 2, respectively, along with the feedback functions (Eqs. 3-5) to model cellular production of cytokines, growth factors, and MMPs using the general form:

$$\frac{dC_x}{dt} = \left(\prod_j g_{j,x}\right) k_{x,M1} C_{M1} + k_{x,M2} C_{M2} + \left(\prod_n g_{n,x}\right) k_{x,SF} C_{SF} - k_{d,x} C_x \qquad (6)$$

where C_x is the concentration of substance x, $k_{x,M1}$ is the baseline production rate of substance x by M1 macrophages, $k_{x,M2}$ is the production rate of substance x by M2 macrophages, $k_{x,SF}$ is the baseline production rate of substance x by SFs, C_{M1} is the concentration of M1 macrophages, C_{M2} is the concentration of M2 macrophages, C_{SF} is the concentration of SFs, $k_{d,x}$ is the degradation rate for substance x, $g_{j,x}$ describes the feedback regulation of substance x by substance j in M1 macrophages, $g_{n,x}$ describes the feedback regulation of substance x by substance n in SFs, and $\prod_j$ is the product operator. Table 2 shows the specific equations for each substance using symbolic representation of the model parameters.

Table 3.2: Equations for Cellular Products

* In some cases, the margin of error for the measurements extended below a concentration of 0 pg/mL, suggesting that the experimental data may have been non-normally distributed, may have had extreme outliers, or may have been averaged over a small number of samples. However, very few studies report concentrations of cytokines in healthy joints, and the ones cited here serve as an adequate starting point for comparisons.

** Our estimate of initial MMP-9 concentration is lower than the concentration reported in a healthy knee. However, this will lead to a conservative estimate of its concentration once an inflammatory stimulus is included in the model.

*** Our estimate of TGF-β exceeds the concentration in a healthy joint. However, its initial value in the model is only about 1 % of its peak value, so we argue that its effect will be minimal.

Model Variable	**Initial Value (from Model Steady State)**	**Concentration in Healthy Synovium**	**Ref.**	**Equation**
IL-1β*	$0.037\ \frac{pg}{mL}$	$1 \pm 2\ \frac{pg}{mL}$	(Tsuchida et al., 2014)	$\frac{dC_{IL1}}{dt} = k_{IL1,M1} g_{IL10,IL1} g_{TGF,IL1} (1 + f_{E2,IL1})(1 + f_{IL6,IL1}) C_{M1} + k_{IL1,M2} C_{M2} + k_{IL1,SF}(1 + f_{TNF,IL1})(1 + f_{IL1,IL1}) C_{SF} - k_{d,IL1} C_{IL1}$

TNF-α	$0.155\ \frac{pg}{mL}$	$0\ \frac{pg}{mL}$	(Tsuchida et al., 2014)	$\frac{dC_{TNF}}{dt} = k_{TNF,M1}g_{IL10,TNF}g_{TGF,TNF}(1+f_{IL6,TNF})g_{T,TNF}g_{PR,TNF}C_{M1} + k_{TNF,M2}C_{M2} + k_{TNF,SF}(1+f_{IL1,TNF})C_{SF} - k_{d,TNF}C_{TNF}$
IL-6*	$0.023\ \frac{pg}{mL}$	$64 \pm 120\ \frac{pg}{mL}$	(Tsuchida et al., 2014)	$\frac{dC_{IL6}}{dt} = k_{IL6,M1}g_{IL10,IL6}(1+f_{TGF,IL6})g_{E,IL6}g_{PR,IL6}C_{M1} + k_{IL6,M2}C_{M2} + k_{IL6,SF}(1+f_{IL1,IL6})(1+f_{TNF,IL6})C_{SF} - k_{d,IL6}C_{IL6}$
IL-10*	$0.073\ \frac{pg}{mL}$	$1 \pm 6\ \frac{pg}{mL}$	(Tsuchida et al., 2014)	$\frac{dC_{IL10}}{dt} = k_{IL10,M1}(1+f_{TGF,IL10})(1+f_{T,IL10})(1+f_{IL6,IL10})g_{E2,IL10}C_{M1} + k_{IL10,M2}C_{M2} + k_{IL10,SF}C_{SF} - k_{d,IL10}C_{IL10}$
TGF-β***	$5.684\ \frac{pg}{mL}$	$0\ \frac{pg}{mL}$	(M. Fang et al., 2013)	$\frac{dC_{TGF}}{dt} = k_{TGF,P}C_P + k_{TGF,M1}C_{M1} + k_{TGF,M2}C_{M2} + k_{TGF,SF}(1+f_{TNF,TGF})C_{SF} - k_{d,TGF}C_{TGF}$
TIMP-1	$2.42 * 10^5\ \frac{pg}{mL}$	$1.24 * 10^5\ \frac{pg}{mL}$	(Heard et al., 2012)	$\frac{dC_{TIMP}}{dt} = k_{TIMP,M1}g_{TNF,TIMPa}g_{IL1,TIMPa}g_{IL10,TIMP}C_{M1} + k_{TIMP,M2}C_{M2} + k_{TIMP,SF}(1+f_{TNF,TIMPb})(1+f_{IL1,TIMPb})(1+f_{IL6,TIMP})C_{SF} - k_{d,TIMP}C_{TIMP}$
MMP-9**	$0\ \frac{pg}{mL}$	$960\ \frac{pg}{mL}$	(Haller et al., 2015)	$\frac{dC_{MMP9}}{dt} = k_{MMP9,M1}(1+f_{IL1,MMP9})(1+f_{TNF,MMP9})g_{IL6,MMP9}C_{M1} + k_{MMP9,M2}C_{M2} - k_{d,MMP9}C_{MMP9}$
MMP-1	$1413\ \frac{pg}{mL}$	$3729\ \frac{pg}{mL}$	(Heard et al., 2012)	$\frac{dC_{MMP1}}{dt} = k_{MMP1,M1}C_{M1} + k_{MMP1,SF}(1+f_{TNF,MMP1})(1+f_{IL1,MMP1})C_{SF} - k_{d,MMP1}C_{MMP1}$

Here, we illustrate how we formulated the kinetic equations for IL-1β, relating the general form that we present in Eq. 6 to the specific equations in Table 2. First, we found the coefficients that described

baseline IL-1β production by M1, M2, and SFs using Eq. 1 and data from published reports (Byrne & Reen, 2002; T. L. Huang, Hsu, Yang, & Lin, 2011), which we cited in Appendix Table B.1. This procedure led to numerical values for the coefficients $k_{IL1,M1}$, $k_{IL1,M2}$, and $k_{IL1,SF}$, which were also listed in Appendix Table B.1. Second, we used data from another published report (Klapproth, Castell, Geiger, Andus, & Heinrich, 1989) (also cited in Appendix Table B.1) to formulate the decay coefficient, $k_{d,IL1}$, using Eq. 2. Third, we formulated the functions that describe feedback regulation of IL-1β production in M1 macrophages. In these cells, IL-1β is down regulated by IL-10 and TGF-β and up regulated by estrogen (E2) and IL-6 (see Figure 3.1). We used Eq. 3 and previously reported *in vitro* data from two studies to estimate the feedback parameters for IL-10 and TGF-β down regulation of IL-1β in M1 macrophages (Chantry, Turner, Abney, & Feldmann, 1989; Thomassen, Divis, & Fisher, 1996), leading to the expressions $g_{IL10,IL1}$ and $g_{TGF,IL1}$. We used Eq. 4 and previously reported *in vitro* data from two other studies to estimate the feedback parameters for E2 and IL-6 up regulation of IL-1β (D'Agostino et al., 1999; Schindler et al., 1990), leading to the expressions $f_{E2,IL1}$ and $f_{IL6,IL1}$, which we incorporate into Eq. 5 to obtain the feedback up regulation functions $g_{E2,IL1} = 1 + f_{E2,IL1}$ and $g_{IL6,IL1} = 1 + f_{IL6,IL1}$. Fourth, we formulated the functions that describe feedback regulation of IL-1β production by SFs. In the case of IL-1β feedback regulation in SFs, all of the regulators are positive, so we use Eqs. 4 and 5 and data from published *in vitro* studies to obtain the feedback functions $g_{TNF,IL1} = 1 + f_{TNF,IL1}$, and $g_{IL1,IL1} = 1 + f_{IL1,IL1}$ (Ganesan, Balachandran, Manohar, & Puvanakrishnan, 2012; T. L. Huang et al., 2011). These functions represented up regulation of SF IL-1β production by TNF-α and IL-1β, respectively. Finally, we combined terms to obtain the final equation for IL-1β concentration. We obtained the first additive term, $k_{IL1,M1} g_{IL10,IL1} g_{TGF,IL1} (1 + f_{E2,IL1})(1 + f_{IL6,IL1}) C_{M1}$, by multiplying the M1 production coefficient for IL-1β ($k_{IL1,M1}$) by all four M1 feedback functions ($\prod_j g_{j,x}$) and the concentration of M1 macrophages (see Appendix Table B.2 for a list of feedback functions and their parameters). We obtained the second additive term by multiplying the M2 IL-1β production coefficient ($k_{IL1,M2}$) by the concentration of M2

macrophages (C_{M2}). We obtained the third additive term by multiplying the SF production coefficient for IL-1β ($k_{IL1,SF}$) by the SF feedback functions ($\prod_n g_{n,x}$) and the concentration of SFs, C_{SF}, leading to the term $k_{IL1,SF}\left(1 + f_{TNF,IL1}\right)\left(1 + f_{IL1,IL1}\right)C_{SF}$. And we obtained the final additive term by multiplying the negative of the decay coefficient for IL-1β ($- k_{d,IL1}$) by the present concentration of IL-1β (C_{IL1}), leading to the term $-k_{d,IL1}C_{IL1}$. Summing all of these additive terms led to the expression for the change in concentration of IL-1β listed in Table 2 and follows from Eqs. 1-6. We used this same procedure to find the rest of the equations in Table 2 and listed the resulting parameters and feedback functions in Appendix Tables B.1 and B.2.

To summarize our approach for formulating the equations that describe time evolution of concentration, we note that there are four key calculations required to formulate the parameters for each substance in the model: 1) calculation of the production coefficients, 2) calculation of the degradation coefficients, 3) calculation of feedback down-regulation functions, and 4) calculation of feedback up-regulation functions. To clarify this procedure and facilitate reproducibility, we demonstrate an example of each of these calculations in S1 Text, which also includes the citations for the studies we used to estimate the parameters. Using the parameters calculated with these steps, we implement the differential equations in an open-source code (S1 Scripts).

3.2.5 Determination of initial conditions

The first step toward understanding the cascade of inflammation after an injury is understanding the initial conditions in the healthy joint before injury has occurred. We attempted to reflect the cellular environment of a healthy knee with our model by running a preliminary simulation in which we only allowed the SFs to produce cytokines in the absence of macrophages. We then used the steady-state concentrations that resulted from this simulation as the initial conditions for subsequent simulations where

we included macrophages. This technique for finding initial conditions has been described previously (Kar et al., 2016).

SF concentration in a healthy joint is not well defined. Therefore, for lack of better information, we used a typical experimental *in vitro* cellular concentration of SFs, $5 * 10^5$ cells/mL (H. F. Huang et al., 2004). Additionally, we used a platelet concentration of $2 * 10^8$ platelets/mL to initiate the inflammation (Nagaraja et al., 2014).

3.2.6 Probabilistic modeling and analysis

We used Latin Hypercube Sampling, a statistical sensitivity analysis method commonly used in computer simulation applications, to account for uncertainty in the nominal parameters that we found using Eqs. 1-5. With Latin Hypercube Sampling, we randomly varied each production and decay coefficient within a range of ±60% of its nominal value (Appendix Table B.1), generating 2000 unique parameter sets and 2000 corresponding solutions of the differential equations. We next determined the median and interquartile range for each respective cytokine at every time point to generate margins of error for our results. Figure 3.2 schematically depicts this statistical sampling technique. We generated these margins of error in the absence of hormones to facilitate comparisons with independent *in vivo* data that did not account for hormonal effects (Irie et al., 2003).

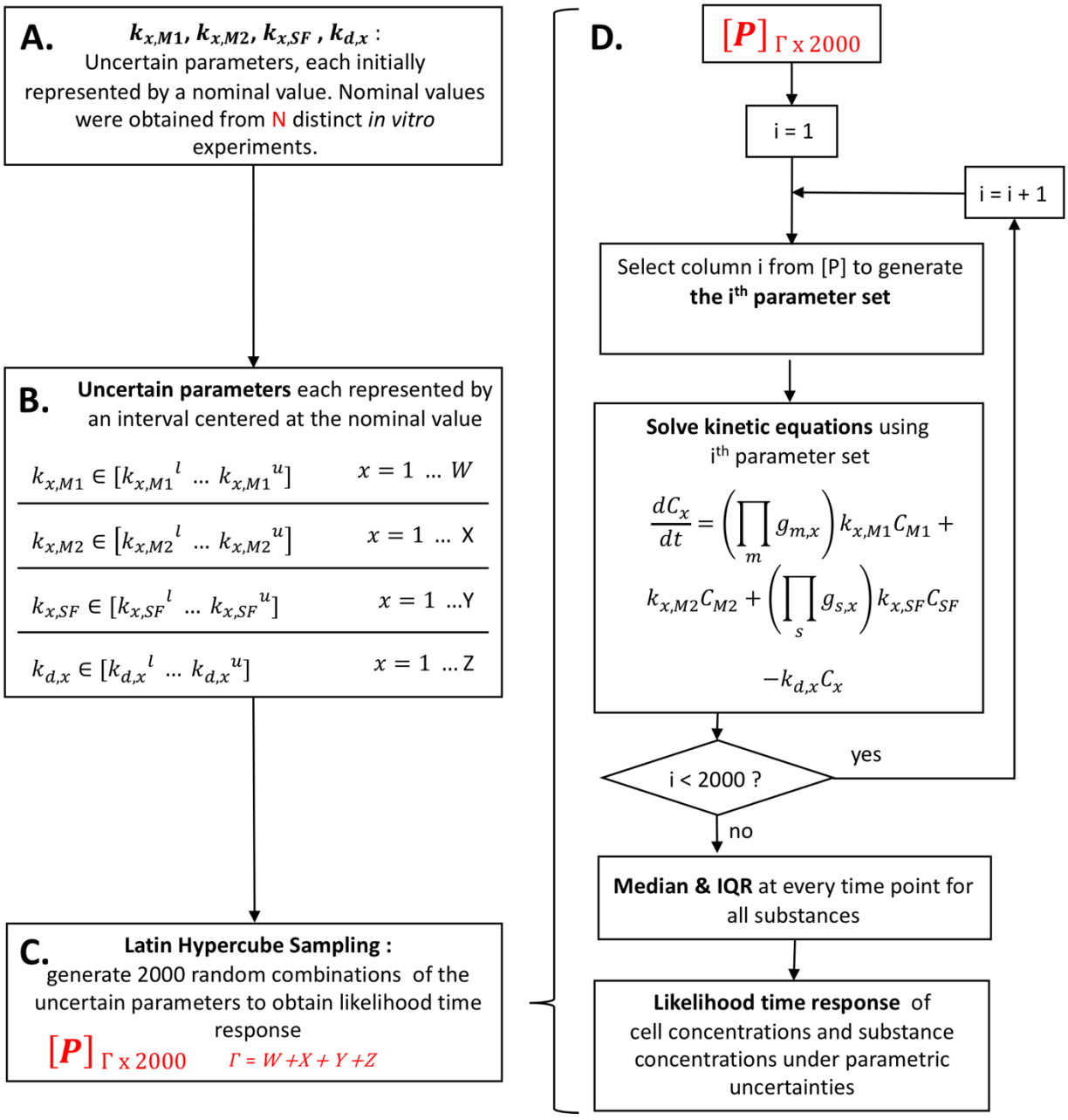

Figure 3.2. Latin Hypercube Sampling approach. A. Estimation of Nominal Parameter Values. The first step in the modeling process was to estimate the nominal production and decay rate coefficients (see section 2.1) from N = 23 published *in vitro* studies (cited in Appendix Table B.1). **B. Parametric Variations.** We varied these parameters between 40 % and 160% (±60%) of their nominal values, generating a 2000 element row vector associated with every parameter. The values in these row vectors

were evenly spaced and sorted in ascending order. **C. Parameter Matrix [P].** Next, we randomized the order of each individual row vector before stacking the vectors into a Γ by 2000 matrix, [P], where Γ represented the number of nominal parameters (and, therefore, the number of row vectors) in the model. Because of the randomization and stacking, each individual column in [P] represented a randomly varied parameter set that we could use in the differential equations. **D. Latin Hypercube Sampling Process.** We selected column i from [P] to generate the ith parameter set and solved the differential equations. After solving the equations with all 2000 randomly varied parameter sets, we determined the median and interquartile range of the results at every time point for every substance, generating the likelihood time responses for concentration under parametric uncertainties. This parametric uncertainty analysis helped us account for uncertainties in the *in vitro* experiments that we used to estimate the nominal values, such as varied experimental conditions and limited numbers of samples. Furthermore, this analysis helped us account for biological differences that exist between the *in vitro* experiments from which we formulated the parameters and the *in vivo* states that we sought to model.

We then performed two analyses of hormonal effects on the post-injury inflammatory response using concentrations reported in (Greenspan & Gardner, 2004). First, we used the nominal parameter set to examine the effects of isolated hormones at single concentrations using three scenarios: 1) estrogen alone (143 pM); 2) estrogen plus progesterone (143 pM and 990 pM, respectively); and 3) testosterone alone (20 nM). Second, after examining the effects of isolated hormone concentrations at single concentrations with the nominal parameter set, we performed simulations with combined estrogen and testosterone with ranges of possible concentrations, since males have non-negligible levels of circulating estrogen and females have detectable concentrations of testosterone in the blood (Greenspan & Gardner, 2004). Using Latin Hypercube Sampling, we varied estrogen and testosterone within physiological ranges for both females and males and simultaneously varied the model coefficients in a balanced fashion, varying the coefficients by

±20% in this analysis. We included two female conditions: 1) "Female Peak E" with low testosterone concentrations and the highest 20% of estrogen concentrations observed during the female menstrual cycle and 2) "Female Low E" with low testosterone concentrations and the lowest 20 % of estrogen concentrations observed during the cycle. In addition, we incorporated a condition with high testosterone and low estrogen to represent male concentrations ("Male"). Table 3 shows these conditions and the corresponding hormone ranges.

Table 3.3: Estrogen and testosterone ranges for males and females. These concentrations were obtained from (Greenspan & Gardner, 2004).

	Minimum E (pM)	Maximum E (pM)	Minimum T (nM)	Maximum T (nM)
Male	1.0	106	8.7	38.1
Female Low E	143	673	0.069	1.38
Female Peak E	2266	2797	0.069	1.38

3.2.7 *In vivo* verification literature

We reviewed the literature to obtain *in vivo* studies that examined the time-course of inflammation in the knee joint after ACL injury (the state we sought to examine) by searching the PubMed database, using the "Best Match" and "Most Recent" features. For each substance, we searched keywords such as "cytokine concentration synovial fluid," "MMP concentration synovial fluid," and "in vivo synovial cytokine concentration," where the word "cytokine" could be replaced with the name of any individual

cytokine. We combined these terms with "ACL injury" and "healthy" to obtain studies of synovial cytokine concentration in the states that we simulated with the model.

3.2.8 Statistical analysis

We used Kruskal-Wallis to test for differences between "Female Peak E," "Female Low E," and "Male" at a t = 1 day and Mann-Whitney U testing with the Bonferroni correction to do pairwise hypothesis testing *post hoc*. We then repeated these tests at the start of each subsequent day up to t = 20 days using the MATLAB R2017b Statistics and Machine Learning Toolbox. S1 Scripts contains the .m file for this statistical analysis.

3.3 Results

3.3.1 Initial conditions

Table 2 ("Initial Value (from Model Steady State)" column) shows the initial conditions that resulted from running the simulation in the absence of an inflammatory stimulus (SFs only, no macrophages) and the column entitled, "Concentration in Healthy Synovium," shows the *in vivo* concentrations of these substances in healthy knee joints. Our data appear to capture the same order of magnitude as experimentally measured quantities in the cases of TIMP-1, MMP-1, and TNF-α. Our data also appear to be in the experimentally reported confidence intervals in the cases of IL-1β, IL-6, and IL-10. In the cases of TGF-β and MMP-9, our initial conditions do not appear to show close agreement.

3.3.2 Verification

The cytokine concentrations predicted by our model appear to be qualitatively consistent with independent *in vivo* experimental results (Irie et al., 2003) (Figure 3.3; Appendix Figure B.1 and Appendix Table B.4). Figure 3.3 shows that independent *in vivo* cytokine concentration data (that is, data not used for parameter estimation or model formulation) appear to confirm the salient features of the bottom-up model output: a peak concentration that occurs shortly after injury and a gradual decrease in concentration over 20 days. Further, we note that the bottom-up model results and the experimental values show approximate numerical agreement at most time points in Figure 3.3. Unfortunately, only one independent *in vivo* study reported the time-course of synovial cytokine concentration after ACL injury *in vivo* and that study did not include all the substances modeled here (Irie et al., 2003). Appendix Figure B.1 shows the time-course of concentrations for the substances that were not included in (Irie et al., 2003). However, while *in vivo* time-course data do not exist for some of the substances in the model, *in vivo* data for single time points after injury have been reported for the remaining substances. We include these data in Appendix Table B.4. The data in Appendix Table B.4 appear to show reasonable order-of-magnitude agreement with the concentrations of cytokines, MMPs, and TIMP-1 in Appendix Figure B.1.

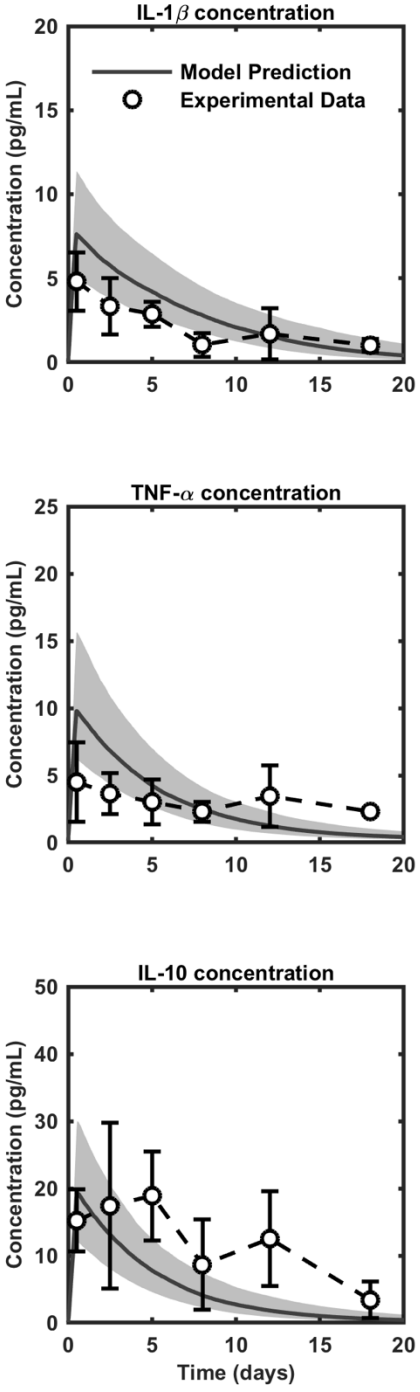

Figure 3.3: Model results for Latin Hypercube Sampling analysis of IL-1β, TNF-α, and IL-10 compared to independent *in vivo* synovial concentrations following anterior cruciate ligament (ACL) injury (Irie et al., 2003). Simulation results shown as median (solid gray lines) ± IQR (gray bands). In vivo

comparison data are shown as circles with error bars. See Appendix Figure B.1 and Appendix Table B.4 for independent comparisons of the rest of the substances in the model.

3.3.3 Hormonal considerations

Figure 3.4 demonstrates that isolated estrogen leads to higher concentrations of IL-1β and TNF-α, as well as lower IL-10 concentration compared with male levels of isolated testosterone. Progesterone does not appear to attenuate the pro-inflammatory effects of estrogen at a physiologically relevant concentration.

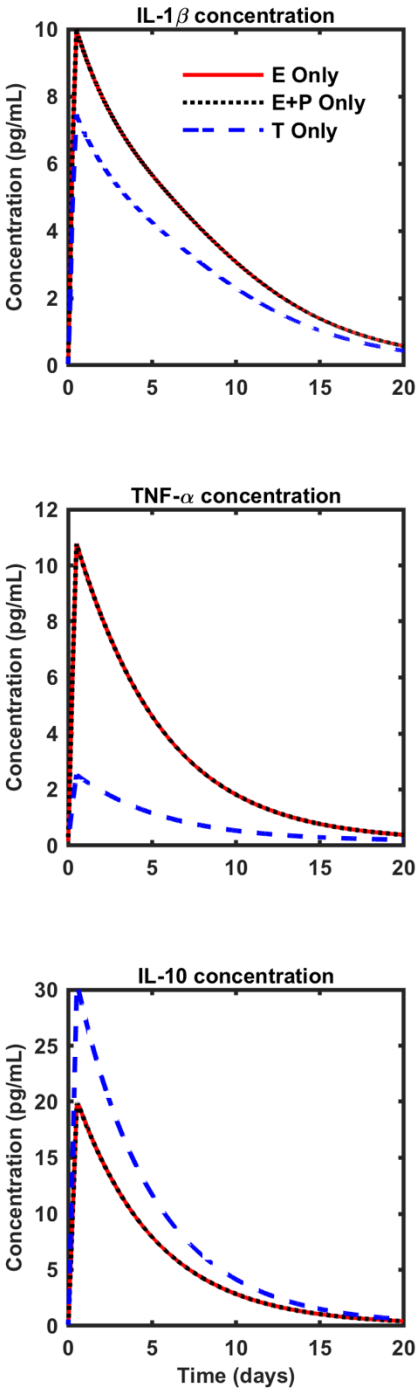

Figure 3.4: Using the nominal parameter set, sex hormones modulate post-injury IL-1β, TNF-α, and IL-10. E Only: low estrogen concentration, as for the early follicular phase (143 pM); E + P: low levels of

estrogen and progesterone, as for the early follicular phase (143 pM estrogen, 990 pM progesterone); T Only: testosterone concentration in the normal range for an adult male (20 nM).

Figure 3.5 shows the median and interquartile range for cytokine concentrations when the model parameters and sex hormone concentrations are varied simultaneously. The “Female Peak E” condition leads to significant elevation of IL-1β and MMP-1, and significant suppression of IL-10 compared to the “Male" condition. The “Female Low E” condition also appears to elevate IL-1β and MMP-1 and suppress IL-10 compared to the “Male” condition, but to a lesser degree than the “Female Peak E” condition. Nonetheless, the differences between “Female Low E” and “Male” remain significant through the duration of the simulation for IL-1β and IL-10 and until t = 19 days for MMP-1. Both “Female Peak E” and “Female Low E” lead to significantly elevated TNF-α concentration compared to the “Male” condition throughout the time frame of the analysis. Conversely, TNF-α concentration did not significantly differ between “Female Peak E” and “Female Low E” at any time point.

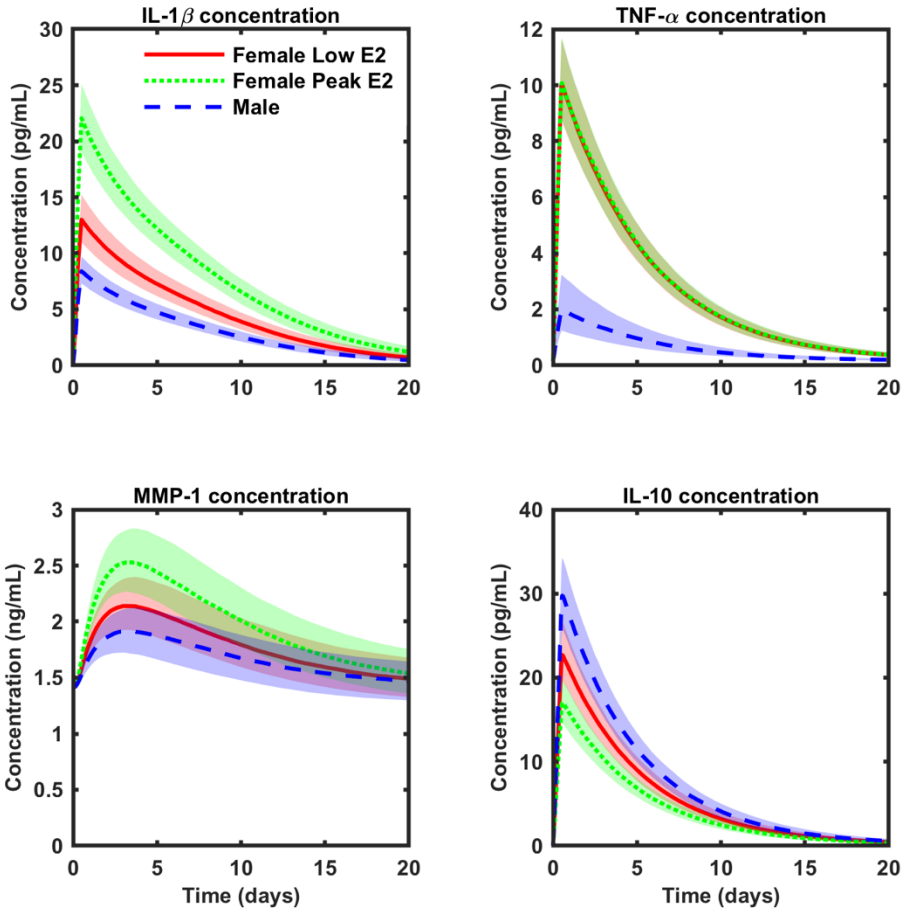

Figure 3.5: Effects of combined estrogen and testosterone at physiological levels for males and females (median ± IQR). Blue: combined T and E at concentrations for adult males; red solid: females with combined T and E at concentrations for females in the early follicular phase (Female Low E); green dotted: combined T and E for females with a steady estrogen concentration that varies around the peak value of estrogen during the menstrual cycle (Female Peak E). Kruskal-Wallis testing and *post hoc* Mann-Whitney U testing (with the Bonferroni correction) reveal highly significant differences between hormonal conditions at nearly all time points for all substances (analysis included in S1 Scripts). For IL-1β, IL-10, and MMP-1, there are significant differences between every possible hormone pair: "Male" is significantly different from "Female Peak E;" "Male" is significantly different from "Female Low E;" and "Female Peak

E" is significantly different from "Female Low E." The difference in MMP-1 concentration between "Male" and "Female Low E" lose significance at t = 19 days and t = 20 days. TNF-α is the only exception, as it shows no significant differences between "Female Low E" and "Female Peak E" at any time point. Further, no differences exist between hormone conditions t = 0 days, since the initial conditions are the same, regardless of the hormone treatment.

3.4 Discussion

3.4.1 Summary of findings

In the present work, we examined the effects of the three principal sex hormones on inflammation and MMP production by macrophages and SFs using a systems biology approach. First, we formulated the model in the absence of hormonal effects, using data from more than 40 published reports of *in vitro* cellular studies to model the cellular and molecular processes that occur in concert in the knee joint after injury. After estimating the nominal parameters from these *in vitro* studies, we performed Latin Hypercube sampling to account for uncertainties in our estimated parameters, generating 2000 model solutions. We used the results from those 2000 statistically varied solutions to compare our model results to independent experimental data *post hoc*. For this comparison, we found that our results captured the salient features of data from the only available *in vivo* study that reported the time course of cytokine concentration in the synovium after an acute ACL injury (Irie et al., 2003) for a select subset of substances in our model (Figure 3.3). Further, we found that the rest of the substances in our model appear to agree with concentration data from single time points after ACL injury (Appendix Figure B.1 and Appendix Table B.4).

Following formulation, statistical variation, and comparison to independent experimental data, we used the model to investigate the effects of single concentrations of estrogen, estrogen plus progesterone,

and testosterone on the inflammatory response. Our simulation results indicated that estrogen led to a pro-inflammatory effect, testosterone led to an anti-inflammatory effect, and progesterone had little influence on the post-injury inflammatory response. However, because males and females have non-negligible levels of both estrogen and testosterone, we also used Latin Hypercube Sampling to generate a range of solutions that could result from typical hormone concentrations. We found that female combinations of estrogen and testosterone ("Female Low E" and "Female Peak E" conditions) both led to higher concentrations of pro-inflammatory IL-1β and TNF-α and lower concentrations of IL-10 compared to the "Male" condition. Further, model simulations indicated that the "Female Peak E" condition led to increased MMP-1 production compared with the "Male" condition. Together, these results suggest that estrogen, which varies in concentration through the menstrual cycle, has the potential to affect the course of the inflammatory process after knee injury. To our knowledge, this is the first model that can be used as a platform to study hormonal influences on post-injury inflammation while addressing some of the biological complexity of the post-injury synovium.

3.4.2 Model assumptions

Our systems biology approach is consistent with other *in silico* studies of inflammatory processes in other model systems (Anderson et al., 2015; Cobbold & Sherratt, 2000; Nagaraja et al., 2014). As such, the approach relies on estimated rate coefficients and feedback parameters, which we determined based on simplifying assumptions and limited data from numerous independent *in vitro* experiments. One simplifying assumption is that the effects seen in isolated *in vitro* experiments will not qualitatively change as the environment becomes more complex. For example, we assume that a parameter for uptake of one substance does not change in the presence of another substance, and that the functional forms of feedback regulation do not change as the environment changes. These assumptions make it tractable to study the

inflammatory response when multiple cell types and multiple hormones are present, since it is experimentally complex, even intractable, to conduct multi-variate *in vitro* experiments that emulate the real biological state of the injured knee joint. Thus, we argue that the present model represents a first step toward understanding post-injury knee inflammation at the systems level that would otherwise be quite difficult to examine experimentally.

In our model of the acutely ACL-injured knee joint, we included a number of cytokines, chemokines, and growth factors that contribute to sex hormonal regulation of MMPs (Bigoni et al., 2013; D'Agostino et al., 1999; Irie et al., 2003; Lei et al., 2014; Sun et al., 2012), while we chose to exclude other cytokines and molecules implicated in joint inflammation. For example, we did not include IL-8 (also known as CXCL8), even though, in some cases, it has been detected in the knee joint after injury (Bigoni et al., 2013). Traditionally, IL-8 acts primarily as a chemoattractant for neutrophils (Harada et al., 1994), but evidence suggests neutrophils do not infiltrate the knee joint after ACL injury and during OA (de Lange-Brokaar et al., 2012; Della Beffa et al., 2013; Kou et al., 2015; Little et al., 2014; Murakami et al., 1995). Thus, the exact purpose of IL-8 in the ACL-injured synovium is unclear, making unclear why IL-8 has been detected in the joint after injury and making it difficult to justify its inclusion in our model. Furthermore, we chose to exclude damage associated molecular patterns (DAMPs) from our analysis, even though they can play an important role in the joint after ACL injury and during the initiation and progression of OA. DAMPs, which can result from tissue damage, can activate toll-like receptors (TLRs) and perpetuate inflammation in the long term (Rosenberg, Rai, Dilisio, & Agrawal, 2017). Unfortunately, not enough quantitative data exist to allow us to formulate parameters that describe this process, so we were unable to include DAMPs in the present model.

In the present model, we included "platelets" as a tool to initiate the inflammatory response because the cellular and molecular initiators of the inflammatory response after joint injury are not well understood (Lieberthal, Sambamurthy, & Scanzello, 2015). However, we did not investigate clotting nor other effects

of platelets. We specified that the platelets would release TGF-β, then rapidly decrease in concentration to negligible levels within hours of the onset of inflammation. Those cells were labeled as platelets because the model parameters for the release of TGF-β, an important driver of macrophage chemotaxis (Wahl et al., 1987), were derived from experiments with platelets (Grainger, Wakefield, Bethell, Farndale, & Metcalfe, 1995; Wakefield, Smith, Flanders, & Sporn, 1988). Further, we note that the inclusion of platelets as a trigger to inflammation has also been reported by other investigators (Nagaraja et al., 2014).

To account for experimentally observed effects of sex hormones on inflammation, we incorporated specific hormonal feedback functions in the model and used the framework described in the methodology. We assumed that synovial concentrations were equal to serum concentrations of hormones, since no significant difference exists between serum and synovial concentrations (Rovensky et al., 2004). We also assumed that estrogen was pro-inflammatory, and that progesterone and testosterone were anti-inflammatory in the environment of the injured knee based on published data from cellular level experiments (Calippe et al., 2010; D'Agostino et al., 1999; Lei et al., 2014; L. Liu et al., 2014; Sun et al., 2012).

3.4.3 Model contextualization

We selected estrogen concentrations to match the concentration of freely circulating estrogen in non-pregnant, pre-menopausal females, and those concentrations were within the range where the hormone produces a pro-inflammatory response (Straub, 2007). The relationship between macrophage production of IL-1β and estrogen appears to be non-monotonic, leading to a pro-inflammatory effect at menopausal to peri-ovulatory concentrations, but a suppressive effect at pregnancy concentrations (Straub, 2007). That is, estrogen may be pro- or anti-inflammatory, depending on the cell types and estrogen concentrations present. Several factors may contribute to these discrepancies, including method of macrophage polarization,

relative expressions of estrogen receptor (ER)-α and ER-β, and estrogen dosage. However, for the cell types involved in post-injury joint inflammation and the estrogen concentrations in the synovium for men and non-pregnant pre-menopausal women, estrogen is likely pro-inflammatory.

Additionally, the present work only addresses hormonal effects associated with pre-menopausal females that do not use exogenous hormones (hormonal contraceptives). We narrowed the focus of this study to this group for several reasons. First, post-menopausal females appear to have increased risk of osteoarthritis for reasons that are not completely understood (Cimmino & Parodi, 2005), and those risk factors may affect the inflammatory response under investigation. Second, formulations of hormonal contraceptives vary widely, particularly for the progestins. Some formulations of progestin have androgenic effects while others appear to have anti-androgenic effects (Sitruk-Ware & Nath, 2010). In either case, the research community does not quantitatively understand the effects of the synthetic progestins on macrophage and SF production of cytokines and MMPs well enough to allow a thorough, model-based synthesis. Finally, we did not examine the effects of hormonal fluctuations associated with the menstrual cycle, though these effects are the subject of ongoing work. Such investigations are beyond the scope of the present work, which sought to establish a model to examine hormonal effects and examine potential differences in the male and female inflammatory response in the synovium after ACL injury.

Emerging research seems to indicate that hormonal effects *in vitro* may not only depend on the hormones and cell types present, but also may depend on the sex of the donor of the cells; the cellular responses will differ for XX cells compared to XY cells (Shah, McCormack, & Bradbury, 2014). The results of these studies represent an important step in our understanding of cellular behavior and we should ultimately incorporate them into multi-factorial kinetic models like the present model. However, we could not include the effect of cell sex in this study because most *in vitro* studies give no clear classification of the sex of the animal or human cell donor (see Appendix Tables B.1 and B.2; n.r. indicates that sex was not reported in the cited study). Nonetheless, the present model represents an important first step toward

understanding hormonal contributions to the inflammation that occurs in the knee synovium after an ACL injury, and may serve as a building block for future work that can also account for sex differences in the cellular responses.

The model may also serve as a building block that could help inform the design of future *in vivo* or *in vitro* experiments by identifying the relative contributions of hormones, cells, cytokines, and time analytically. When designing experimental studies of cytokines, it can be difficult to pinpoint which cytokines are most important to investigate, and experimental costs can rise quickly if too many cytokines are investigated. To narrow the scope of such experiments, *in silico* models such as this one could be used to help determine which subset of cytokines will be most critical to the *in vivo* and *in vitro* processes of interest.

3.4.4 Verification considerations

Running the model in the absence of an inflammatory stimulus, we found that most our predictions agreed reasonably with experimentally reported concentrations in healthy knees (Table 2). However, we note that the experimental confidence intervals for IL-1β, IL-6, and IL-10 extended below zero; that is, the measured error was larger than the mean value of the measurements. For example, the mean concentration of IL-6 was 64 pg/mL while its standard deviation was 120 pg/mL. Such large errors may be a result of non-normally distributed data or small sample sizes. However, despite large variability, these data serve as important points of comparison because few studies report the concentrations of synovial cytokines in healthy knee joints.

We found that our estimate of MMP-9 in the absence of inflammation did not appear to agree with experimental measurements from healthy knees. This discrepancy may have arisen either because our model did not incorporate all possible cell types in the healthy joint or because of experimental uncertainties

in the study that reported MMP-9 concentration in the healthy joint. In our model, we only incorporated SFs during the simulation of the healthy joint and did not include potential effects of the resident macrophages during this particular analysis. While the resident macrophages are not polarized toward an inflammatory phenotype in the healthy joint (Orlowsky & Kraus, 2015), it is possible that they may produce substances that the SFs do not, such as MMP-9. In that case, our model would not have been able to capture the concentration of MMP-9 in the healthy joint because it did not include the synovial macrophages in the healthy state. However, experimental uncertainties may have also influenced the MMP-9 measurement, causing experimental concentrations to disagree with the model predictions. For example, the study that measured MMP-9 might have left variables uncontrolled that had the potential to influence cytokine and MMP-9 concentrations. Such variables may include undetected sub-acute joint inflammation, activity levels on the day of testing, or use of external stimuli like caffeine or alcohol (Horrigan, Kelly, & Connor, 2006; Pedersen, 2017; Szabo & Saha, 2015). However, it is not entirely clear whether experimental uncertainties or model shortcomings were responsible for the observed discrepancy in MMP-9 concentration in the healthy joint.

Our estimate of TGF-β concentration in the healthy state also differed from experimental measurements of its concentration in healthy knees. However, we argue that this discrepancy between concentrations in the healthy state is unimportant in the context of the inflammatory process, since the discrepancy of 5.7 pg/mL is only about 1% of the peak concentration of TGF-β. Indeed, despite some discrepancies between our estimates and experimental data in the healthy state, the model appears to appropriately capture important aspects of experimentally measured data when we examine the inflammatory response.

The results from our systems biology model appeared to capture the salient features of an independent *in vivo* experiment (that is, an experiment that was not used in the formulation of our model) (Irie et al., 2003), as shown Figure 3.3. However, some differences existed between the model results and

the experimentally measured quantities. These differences may have arisen because of the model limitations discussed above, or due to experimental constraints of the *in vivo* study. The experimental constraints included the small sample size and the cross-sectional study design in which a different group of people was tested at each time point, making it difficult to infer the time course of cytokine concentrations for a single subject. In addition, the experiments utilized mixed groups of males and females, not accounting for hormonal effects. Uncontrolled hormonal influences in the *in vivo* data may have been responsible for the deviations of experimental data from the model results, which we calculated without hormonal influences for the comparison analysis. Ideally, the results from the present study could be compared to an experiment that separates males and females and controls for female hormone levels, but no such study exists as of yet. The *in vivo* study by Irie et al. appears to be the only study that reports the time course of cytokine concentration in the synovium after injury, and even so, it reports only a subset of the cytokines that we modeled (Irie et al., 2003).

Irie et al. reported the time course of concentration for IL-6 in addition to the time course for IL-1β, TNF-α, and IL-10 (Irie et al., 2003). However, the concentrations for IL-6 in their time course data appear to be two orders of magnitude higher than other reported IL-6 concentrations in the synovium at single time points after ACL injury and in other joint pathologies (see Appendix Table B.4), while the concentrations of IL-1β, TNF-α, and IL-10 appear to be consistent with numerical values from comparable measurements (Appendix Table B.4). Thus, due to the disagreement in experimental IL-6 concentrations, it is impossible to make a confident comparison of our data. Nevertheless, we note that our results, shown in Appendix Figure B.1, seem to quantitatively agree with several other IL-6 measurements from synovial fluid, which we report in Appendix Table B.4.

3.4.5 Implications of findings and conclusion

After verification of the model, we performed a preliminary analysis where we considered the effects of sex hormones at single concentrations using the nominal parameter set. The purpose of this analysis was to assess whether sex hormones would have any appreciable effect on inflammation before proceeding to a more thorough analysis in which we varied both the model parameters and the hormonal concentrations. The preliminary analysis revealed that estrogen treatment increased IL-1β and TNF-α and decreased IL-10 compared to testosterone treatment, suggesting that females, who have higher levels of estrogen than males, may be prone to a stronger inflammatory response after injury compared to males. However, females have non-negligible concentrations of testosterone and males have non-negligible concentrations of estrogen, so analysis of isolated hormone effects is inadequate for studying sex differences in the post-injury inflammatory response. Thus, we performed analysis where we simultaneously considered estrogen and testosterone at concentrations relevant for males and females.

In our preliminary analysis of isolated hormones, we also found no discernible change in the inflammatory response when we compared the condition with estrogen alone to the condition with estrogen plus progesterone, suggesting that progesterone was unable to attenuate the effects of estrogen. This result contrasted with our hypothesis that the anti-inflammatory effects of progesterone would be beneficial in the environment of the injured knee. Further, this result was in direct contrast with the findings of other examinations of progesterone effects on inflammation (Lei et al., 2014; Salamonsen, 1998). Specifically, studies of the female reproductive system have shown that progesterone reduces inflammation at the concentrations found locally in the female reproductive system (Salamonsen, 1998). However, the concentrations in the reproductive tract are substantially higher than those in the synovium (and in our simulations), so it is possible that the concentrations in the synovium were too low to have a meaningful effect. Indeed, the anti-inflammatory effects of progesterone started to become apparent in our model at a concentration of 31.4 pg/mL (see Appendix Table B.3). However, because we saw no effect of progesterone

at concentrations relevant in the synovium, we did not include it in the subsequent analysis of combined hormones.

Our analysis of combined hormones revealed that a relative abundance of testosterone in males may reduce TNF-α concentrations, since the "Male" condition led to significantly lower TNF-α concentrations compared to both the "Female Peak E" and "Female Low E" conditions. Conversely, estrogen does not appear to have an effect on TNF-α, since no significant difference existed between the "Female Peak E" and "Female Low E" conditions at any time point for the cytokine. The lack of estrogen effect seems to suggest that testosterone is the key hormonal regulator of TNF-α in the present study. This reduction in TNF-α concentration for males may have the potential to improve post-injury outcomes, since the cytokine was recently identified as a marker for early osteoarthritis, a common long-term consequence of ACL injury (Edd et al., 2017).

Our analysis of combined hormones also revealed that elevated estrogen ("Female Peak E") seems to exacerbate inflammation compared to lower estrogen ("Female Low E"), even when we include the opposing effects of testosterone at concentrations relevant for females. Indeed, we observed that the "Female Peak E" condition led to significantly elevated IL-1β and MMP-1 and led to significantly reduced IL-10 concentrations compared to "Female Low E" at all time points. This result suggests that the severity of post-injury inflammation may depend not only on the sex of the patient, but also on estrogen concentration at the time of injury for female patients. This result may inform the design of future studies that seek to examine sex differences in post-injury outcomes, since it suggests that inflammation may differ among females, depending on their estrogen levels.

With this quantitative framework, we aimed to shed light on the mechanisms that may cause increased cartilage damage for females after knee injury. Our model results demonstrated that sex hormones could differentially regulate the inflammatory process after an injury and provided a quantitative framework

for studying the complexities of the inflammation that may occur after an injury. While the results of this study alone do not provide enough evidence to conclusively assert that estrogen will increase MMP production *in vivo* and, in turn, put females at higher risk of cartilage damage, the results do offer hints toward the mechanism that may underlie poorer post-injury outcomes for females. These hints may help inform the design of future *in vitro* and *in vivo* studies that will further improve our understanding of the factors that may put females at higher risk of damage to the cartilage and poor long-term joint health and may eventually serve as a basis for developing targeted treatments to reduce inflammation and MMPs, particularly for females.

Connecting text: on MMP diffusion and adsorption to collagen

Quantifying hormonal effects on synovial inflammation allows us to predict the resulting changes in MMP concentrations. However, the question remains: how could the hormone-induced changes in MMP concentrations lead to degradation of the cartilage and mechanical changes to the tissue? The MMPs produced by the invading macrophages and the resident synovial fibroblasts must diffuse from the synovium into the cartilage tissue and adsorb to the surface of the fibrillar collagen where they can cleave, denature, and reduce the mechanical integrity of the supporting collagen structure.

Numerous reports indicate that diffusion of MMPs into the cartilage is hindered by the presence of the aggrecans that surround the fibrillar collagen (Kar et al., 2016; Pratta et al., 2003). For articular cartilage, Li et al. 2015 demonstrated that fibrillar collagen degradation does not occur in the absence of aggrecanse, and that loss of fibrillar collagen lags several days behind aggrecan loss in bovine cartilage explants, suggesting that the aggrecans may protect the fibrillar collagen (Li et al., 2015). Another study showed similar behavior with bovine nasal cartilage, which lost no collagen until the tissue had lost a critical amount of aggrecan (Pratta et al., 2003). These studies reveal a need for models that can predict how MMPs will diffuse into the cartilage and eventually bind to the collagen surfaces.

Recently, a model of MMP diffusion into cartilage was formulated (Kar et al., 2016). In this work, data from an in vitro study was leveraged to formulate a system of diffusion-reaction equations that described the time course of IL-1α induction of aggrecanases and MMPs, aggrecanase diffusion, cleavage of aggrecans, MMP diffusion, and MMP cleavage of collagen, among other quantities. The model was designed to recapitulate experimental results (Li et al., 2015) and clarify the physical processes underlying experimental observations. The experiments were conducted by placing cylinders of bovine articular cartilage in culture plates, treating with IL-1α, and measuring the amount of collagen and radiolabeled

aggrecan in the supernatant over 4 weeks. The experimental metrics were then used as a guide for the formulation of a detailed computational model.

The model relied on the experimental conditions to specify the geometry, boundary conditions, and initial conditions to facilitate the study of the aggrecan and collagen destruction. The cylindrical geometry of the experimental specimens was simplified to a two-dimensional rectangle by assuming radial symmetry. The initial conditions were specified based on initial concentrations of each substance in the cartilage at the start of the experiment, and the boundary conditions were specified such that the simulation results matched experimental observations.

While multiple interacting processes were studied in their work, we will focus here on the process of MMP diffusion into the cartilage, noting other processes only as they relate to MMP diffusion. In their model, the effective diffusion coefficient for MMP was described by

$$D_{mmp}(t,r,z) = D^*_{mmp} e^{-95 * C_{agg}(t,r,z)} \quad (1)$$

where $D^*_{mmp} = 1 * 10^{-12}\ \frac{m^2}{s}$ is an approximation of the diffusion coefficient of MMP-1 on collagen substrate (Sarkar et al., 2012), $C_{agg}(t,r,z)$ is the concentration of aggrecan, t is time, and r and z denote radial and vertical spatial position, respectively. This formulation of the effective diffusion coefficient was parameterized to take into account the physical barrier that aggrecans present to MMPs, and the form of this expression suggests that effective diffusion coefficient of MMPs is low when aggrecan concentration is high and vice versa. It is worth noting that the effective diffusion coefficient will vary throughout the thickness of the cartilage specimen based on the spatial distribution of aggrecans, which will also vary in time due to aggrecanase action. In this model, the complexity of MMP diffusion into cartilage was modeled by a simple expression that phenomenologically accounts for experimental findings.

In addition to diffusion, their full model accounted for production and binding of MMPs and other processes, which we will not discuss in detail here. The finite element analysis solution to the model adequately recapitulated the results of the experimental study (Li et al., 2015), and revealed the time-course of MMP diffusion in the cartilage. This modeling approach or a similar one could serve as a link between the conditions in the synovial fluid and the attachment of MMPs to the fibrillar collagen, a critical connection between our model of hormonal effects on MMPs and our model of collagen fibril degradation.

The diffusion model discussed above represents a useful building block that will facilitate further analysis of MMP diffusion in cartilage but relies on simplifying assumptions that may obscure complexities of the process that arise because of the intricate organization of the collagen fibrils in the tissue. One such assumption is that the diffusivity of MMPs in the cartilage only changes with the aggrecan concentration at a particular location, implying that the geometry of the surrounding collagen fibers will not affect diffusion. However, analyses of neutral solutes diffusing through cartilage suggest that the diffusivity of the solute will vary substantially in the different zones of the cartilage (Arbabi, Pouran, Weinans, & Zadpoor, 2015, 2016), which can be delineated based on the orientation of the collagen fibers. In addition, the model of Kar et al. (2015) assumes that diffusion will be equal in all directions for any given value of the diffusivity, which seems unlikely given the orthotropic or fully anisotropic organization of the collagen fibers in the different zones for neutral solutes. These potential complexities of MMP diffusion into cartilage could be addressed using finite element modeling (FEM) by modifying existing models. Indeed, Arbabi et al. have developed a finite element model of cartilage that recapitulates experimental diffusion measurements made with computed tomography for neutral solutes (Arbabi et al., 2015, 2016), though this model also assumes that the diffusion only occurs in the vertical (axial) direction and does not explicitly account for collagen fiber organization. While diffusion of MMPs into cartilage has not been fully characterized, many existing approaches could be used or modified to predict how MMPs move from the synovial fluid into the cartilage itself.

We point out that the model by Kar et al. describes processes that are quite similar to those we address in this body of work. However, key differences exist between the diffusion-reaction model and the models we describe. First, the model by Kar et al. addresses IL-1α induction of MMPs by chondrocytes, a process similar to what we presented in the previous chapter, though not identical. Our model focuses on the inflammatory response mounted in the synovium after an injury and the numerous feedback mechanisms involved, while the Kar model focuses more narrowly on the chondrocyte response to a single substance, IL-1α. In addition, Kar et al. describe the aggregate degradation of collagen using the diffusion reaction model, and we describe collagen degradation in subsequent chapters using a different approach. But our model explores the mechanisms underlying degradation of a single fibril by collagenase and gelatinase, instead of using a phenomenological approach to predict aggregate metrics of degradation. Nevertheless, we refer to the diffusion-reaction model as a potential means of estimating the concentration of MMPs in the cartilage as a function of the MMP concentration in the synovial fluid.

Once we know the concentration of MMPs in the cartilage as a function of their concentration in the synovial fluid, we also know the concentration of MMPs to which a single fibril will be exposed at a particular point in the cartilage, which will dictate the number of MMPs that will eventually adsorb to the collagen. However, the process of MMP adsorption onto collagen fibrils is not well understood at the nanoscale. Early studies of collagenase measured adsorption of MMPs onto gelled collagen as a function of MMP concentration in the surrounding solution (Welgus et al., 1980). However, these studies did not provide the thermodynamic quantities that would be necessary to model the process at the fibril level.

In the subsequent chapters, we examine collagen degradation and the resulting changes in mechanical properties using a dynamic Metropolis Monte Carlo model and a coarse-grained molecular dynamics approach, respectively. We first develop the degradation model, then utilize it in conjunction with the existing molecular dynamics mechanical model to predict changes in fibril tensile strength.

Chapter 4: Effect of collagenase to gelatinase ratio on collagen fibril degradation and mechanics: a combined Monte Carlo-Molecular Dynamics study

Abstract

Loading in cartilage is supported primarily by fibrillar collagen, and damage will impair the function of the tissue, leading to pathologies such as osteoarthritis. Damage is initiated by two types of matrix metalloproteinases (MMPs), collagenase and gelatinase, that cleave and denature the collagen fibrils in the tissue. Experimental and modeling studies have revealed insights into the individual contributions of these two types of MMPs, as well as the mechanical response of intact fibrils and fibrils that have experienced random surface degradation. However, no research has comprehensively examined the combined influences of collagenases and gelatinases on collagen degradation, nor studied the mechanical consequences of biological degradation of collagen fibrils. Such pre-clinical examinations are required to gain insights into understanding, treating, and preventing degradation-related cartilage pathology. To develop these insights, we use sequential Monte Carlo and Molecular Dynamics simulations to probe the effect of enzymatic degradation on the structure and mechanics of a single collagen fibril. We find that the mechanical response depends on the ratio of collagenase to gelatinase - not just the amount of lost fibril mass - and we provide a possible mechanism underlying this phenomenon. From our results, we conclude that future experimental examinations of MMP effects on collagen degradation and mechanics must consider the effects of both collagenases and gelatinases on fibril degradation, not just the effects of one or the other. Further, such studies should also account for possible differences in degradation that may result from different collagenase-to-gelatinase ratios. Overall, by characterizing the combined influences of collagenases and gelatinases on fibril degradation and mechanics at the pre-clinical research stage, we gain

insights that may facilitate the development of targeted interventions to prevent the damage and loss of mechanical integrity that can lead to cartilage pathology.

*Note: This work was performed in collaboration with David Malaspina, who ran the molecular dynamics simulations, generated many of the figures, and aided in the design of this work. His contributions to this chapter were equal to the contributions of this author.

4.1 Introduction

In healthy tissue, collagen production is typically balanced by collagen degradation mediated by matrix metalloproteinases (MMPs), enzymes that bind and cleave the triple helical collagen molecule. This balance is disrupted in many disease states, including arthritis, cancer, and fibrosis (Cawston & Wilson, 2006; Clark et al., 2008; Giannandrea & Parks, 2014; Malemud, 2006; Mancini & Di Battista, 2006). When the balance favors destruction, permanent structural changes can occur, especially in tissues that are metabolically mostly quiescent, such as articular cartilage (Maroudas, Palla, & Gilav, 1992; Verzijl et al., 2000). Such damage can lead to changes in mechanical properties that impair the function of the tissue.

At the molecular level, collagen degradation is mediated by two MMPs subfamilies: collagenases and gelatinases. Single-molecule tracking techniques reveal that collagenases (MMP-1) adsorb on collagen and then spend the majority of their time in paused states where cleavage eventually occurs (Sarkar et al., 2012). Once collagenase has cleaved a tropocollagen molecule, the tropocollagen begins to denature and becomes susceptible to gelatinase cleavage. Employing a single molecule tracking paradigm, Rosenblum and colleagues reported that gelatinase (MMP-9) does not efficiently bind to the native triple helical structure, but tends to bind and cleave the partially denatured fragments that collagenases create (Rosenblum et al., 2010). While the isolated interactions of MMPs with their substrates have been

experimentally characterized, the combined influences of collagenase and gelatinase on the structural and mechanical properties of an isolated collagen fibril have not been established.

Several experimental examinations have shown that protease-mediated collagen degradation produces a dramatic decrease in the mechanical strength and toughness of collagen fibers (Laasanen et al., 2003; Panwar et al., 2013; Panwar et al., 2015; Park et al., 2008). But, while connections between the molecular structure and the strength and toughness of collagen have been drawn in some of these studies (Panwar et al., 2013; Panwar et al., 2015), the precise nature of the relationship between MMP-induced structural changes and the mechanical properties of collagen fibrils has not been comprehensively studied. In our recent work (Malaspina et al., 2017), we employed a coarse-grained molecular dynamics model (Depalle, Qin, Shefelbine, & Buehler, 2015) to examine how random surface degradation influenced the mechanical response of a collagen fibril. We showed that the surface degradation (determined using a solvent-accessible surface area constraint) produced dramatic changes in the toughness of the collagen fibril consistent with experimental observations (Laasanen et al., 2003; Panwar et al., 2013; Panwar et al., 2015; Park et al., 2008). These findings align with the hypothesis that the molecular organization of the fibril exerts a strong influence over the mechanical strength (Fratzl, 2008) and a small disruption of the structure leads to a large reduction of the fibril toughness. However, although the model yielded important insights into the relationship between degraded fibril structure and mechanical properties, our previous work did not account for the complexity of structural changes that may stem from the underlying biology and the thermodynamics of degradation, which includes the combined action of the two MMP subtypes, collagenase and gelatinase.

Accordingly, our purpose is to examine the combined effect of collagenase and gelatinase on collagen fibril structure and obtain the associated changes in the mechanical properties using molecular simulations. To do so, we developed a Metropolis Monte Carlo approach to examine the process of biological degradation of a collagen fibril by collagenase MMP-1 and gelatinase MMP-9. The structures

obtained by the Monte Carlo approach were then used as inputs to the coarse-grained Molecular Dynamics model (Malaspina et al., 2017) to examine the changes in the mechanical response of the fibril that resulted from MMP-induced structural changes. We hypothesized that a higher ratio of collagenases to gelatinases would lead to reduced toughness of the fibril at a fixed amount of degradation, since an increase in the number of collagenases would increase the number of cleaved bonds that cannot bear load. Further, we examined the time dependence of degradation, hypothesizing that the time course of degradation would differ based on the absolute number of collagenases and gelatinases on the fibril as well as the ratio of collagenases to gelatinases. To our knowledge, this is the first study to examine the relative influences of collagenases and gelatinases acting simultaneously on a collagen fibril and the first study to quantify their relative effects on fibril mechanical integrity. We argue that this computational construct will help inform future experimental designs and consequently serve as a bridge between experimental observations and molecular mechanisms. Our results demonstrate that the ratio of collagenase to gelatinase dictates fibril degradation and mechanical integrity. The findings presented herein could eventually inform future experiments that may provide targeted clinical treatment strategies, which would likely hinge on the relative effects of local collagenase and gelatinase inhibition on degradation and mechanics.

4.2 Methods

4.2.1 Dynamic Metropolis Monte Carlo degradation model

A coarse-grained lattice model was used to represent the structural hierarchy of collagen, which is depicted in Figure 4.1. Enzymes were randomly selected and placed on empty lattice sites using random selection of position indices on the surface of the fibril. A detailed description of the structure and the initial placement of the enzymes can be found in Appendix C. Briefly, the lattice was organized according to experimental reports of collagen fibril organization, which includes tropocollagen molecules arranged into

microfibrils and microfibrils arranged into a fibril. This structure served as the basis for a dynamic Metropolis Monte Carlo approach, depicted in Figure 4.1 A-D.

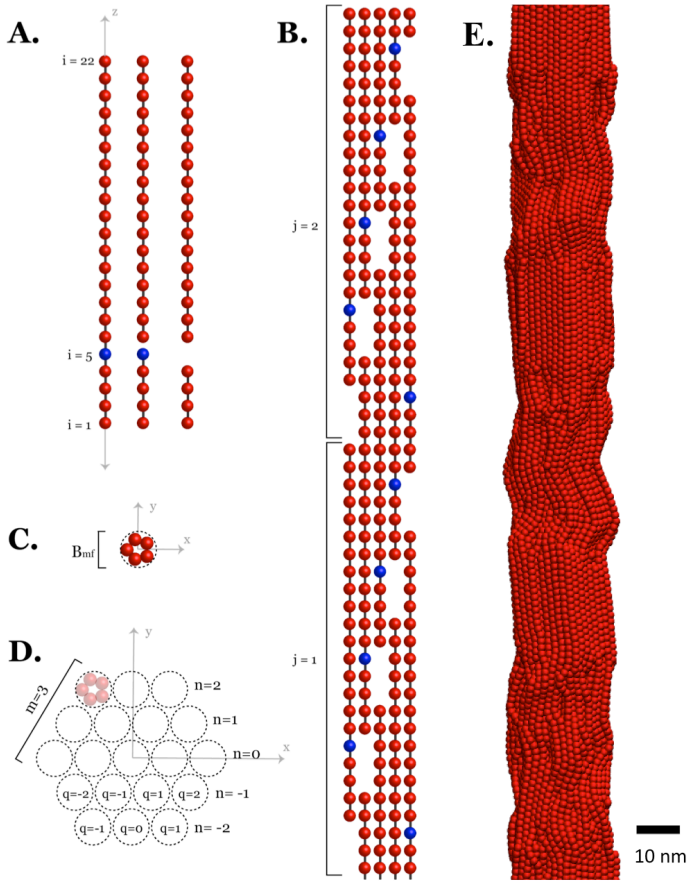

Figure 4.1. Illustrations of the components of the fibril Monte Carlo lattice structure and resulting Molecular Dynamics structure. A) Illustration of the individual tropocollagen molecule. An intact molecule is shown on the far left, a molecule that has been cleaved at the collagenase cleavage site is shown in the middle, and a molecule with a removed lattice site is shown on the far right. The blue site denotes the position where collagenase binds with high affinity and eventually cleaves. **B) Illustration of the microfibril structure (length-wise).** The pattern of gaps and staggering of the tropocollagen molecules is shown in this flattened depiction. The index j indicates the vertical position of an individual tropocollagen

within a microfibril. **C) Illustration of the microfibril cross-section.** B_{mf} is the diameter of a single microfibril. **D) Illustration of the fibril cross-section when m=3** (in the simulations presented in the results, m=4). The index m is the number of microfibrils per edge on a fibril, and n and q are indices of microfibril position within the fibril. Refer to Appendix C for more details on the indices used to describe the structure. **E) Snapshot of a section of the fibril equilibrated by molecular dynamics simulation.** The cleaved and removed sites were obtained from the results of the Monte Carlo simulations.

4.2.1.1 MMP-Collagen interaction energies

When an MMP occupied a lattice site on a given tropocollagen, it bound to the site with an energy that depended on the type of MMP, its position on the tropocollagen, and whether the tropocollagen molecule had been cleaved by a collagenase. The interaction energy between collagenase and the collagen lattice sites was described by

$$\mathrm{E_{C,colla}} = \begin{cases} 0, \mathrm{i} \leq 4 \\ -2\mathrm{kT}, \mathrm{i} = 5 \\ 0, \mathrm{i} > 5 \end{cases} \qquad (1)$$

where the first subscript C denotes the enzyme type, collagenase, the second subscript colla denotes the substrate, collagen, k is the Boltzmann constant, T is the temperature, and i is the index of vertical position along a tropocollagen. These interaction energies were estimated by running the MC model with a single collagenase on the fibril, calculating the percent of steps where the collagenase was paused at its characteristic cleave site (i = 5). The energy was adjusted until the collagenase remained at the characteristic cleave site during approximately 18 % of the total simulation steps, since Sarkar et al. (2012) observed that collagenases adsorbed to a fibril spend 18 % of their time paused at exposed collagenase cleave sites, which they denoted as “class II pauses” (Sarkar et al., 2012). Further, experiments indicate that collagenases are

unable to diffuse over cleaved sites and have lower affinity for gelatin (Saffarian et al., 2004; Sarkar et al., 2012), therefore

$$E_{C,Ccl} = \infty$$
$$E_{C,gela} = 0.5kT, 1 \leq i \leq 22 \quad (2)$$

where C denotes collagenase, Ccl denotes a cleaved lattice site and the subscript gela denotes gelatin (a tropocollagen molecule with at least one cleaved site). While the exact change in collagenase affinity for collagen after cleavage is unknown, we incorporated an increase in the interaction energy to phenomenologically incorporate qualitatively observed collagenase behavior.

Gelatinase interactions with collagen and gelatin, respectively, were described by the equations

$$E_{G,colla} = 0, 1 \leq i \leq 22$$
$$E_{G,gela} = -0.5kT, 1 \leq i \leq 22 \quad (3)$$

where the subscript G indicates gelatinase, colla denote an uncleaved tropocollagen and the subscript gela indicates a cleaved tropocollagen or gelatin. Again, the exact change in the gelatinase affinity for collagen after cleavage is unknown, but we incorporated a decrease in the interaction energy to phenomenologically take experimental observations into account (Rosenblum et al., 2010).

4.2.1.2 Dynamic Metropolis Monte Carlo moves

A dynamic Metropolis Monte Carlo approach was used to simulate the interactions between the MMPs and the collagen to capture the stochastic, time-dependent nature of the collagen degradation process.

For each step of the simulation, an enzyme was randomly selected from the ensemble of collagenases and gelatinases, and the selected enzyme attempted to move vertically or horizontally or attempted to cleave. The movement attempts were accepted based on the Boltzmann factor of the change in energy between one lattice site and the next.

For vertical motion, trial moves in the positive and negative z-direction were chosen with the same probability. In a similar way, trial moves were chosen with the same probability for 'left or right' movements for horizontal motion but constrained to remain on the outermost edge of the fibril. In accordance with experimental observations (Sarkar et al., 2012), the ratio of vertical to horizontal trial moves was selected in the model such that vertical movements were much more probable. Furthermore, the probabilities of displacement attempts were selected such that the enzymes would move with the diffusion coefficients reported in the literature (Collier et al., 2011).

For cleave attempts, the model presented here was parameterized to mimic experimental observations (Rosenblum et al., 2010; Sarkar et al., 2012). Collagenase cleavage only occurred when collagenases were positioned on the lattice site 66 nm from the C-terminus of an individual tropocollagen (i=4), and gelatinase cleavage only occurred when gelatinases were positioned on a tropocollagen that had already been cleaved by a collagenase (Fields, 2013; Rosenblum et al., 2010). When the enzymes were in the positions where cleavage could occur, cleavage succeeded at an overall rate of 0.35 s^{-1}(Sarkar et al., 2012). When cleavage occurred, a bond was broken between the N terminus of the occupied site and the C terminus of the site directly above the occupied site (Figure 4.1A).

Once a lattice site and its lower neighbor had been cleaved, that site became disconnected from the rest of the lattice and was removed from the system immediately (Figure 4.1A). As the removal progressed, some sets of lattice sites became detached from neighboring lattice sites and were removed from the system.

A set of lattice sites was considered detached when it had no vertical neighbors, and when it was not attached to at least two other beads horizontally.

A semi-quantitative verification of the MC simulations of the degradation process against experimental observations are shown in Appendix Figure C.1. Furthermore, Appendix C includes a detailed description of the MC model formulation.

4.2.1.3 Degradation conditions

The number of enzymes on the fibril was selected in a way that facilitated study of the relative effects of collagenases and gelatinases, since the patterns of cleavage differ for the two classes of MMPs. The amount of each type enzyme can be found in Table 4.1. For each enzyme surface coverage condition, the changes in fibril structure were recorded as the simulation progressed.

Table 4.1: Simulated systems and relative amounts of collagenases and gelatinases

Simulated system	Number of collagenases	Number of gelatinases	Ratio of collagenase to gelatinase
system 1 (c 4: g 4)	4	4	1
system 2 (c 8: g 8)	8	8	1

system 3 (c 6: g 2)	6	2	3
system 4 (c 2: g 6)	2	6	0.33

4.2.2 Mechanical analysis with coarse-grained Molecular Dynamics

The degraded structures from the Monte Carlo simulations were then used to perform mechanical analysis using molecular dynamics. The mapping of sites from the lattice Monte Carlo to the Molecular Dynamics model (Malaspina et al., 2017) is such that one site on the Monte Carlo structure is equivalent to ten sites in Molecular Dynamics structure. The simulation protocol is identical to the one used in our previous work (Malaspina et al., 2017) with a fibril that is ten times longer. The length was increased so that the size of the Molecular Dynamics structure would be equal to the Monte Carlo structure. In the Molecular Dynamics structure, which is depicted in Figure 4.1E, each tropocollagen is represented by a polymeric chain that contains 220 bonded beads. A total of 925 tropocollagen chains interact through a Lennard-Jones potential, in conjunction with a harmonic potential and a hyper-elastic bond energy. The force-field for the coarse-grained Molecular Dynamics model was developed by Buehler et al (Depalle et al., 2015) and is described in more detail in Appendix C.

The stress-strain response was assessed at 1.1% degradation for all treatment conditions, where percent degradation was defined as number of removed lattice sites divided by the initial number of lattice sites x 100. This amount of degradation (1.1%) was chosen based on a previous work (Malaspina et al., 2017) and represents the beginning of a plateau in the change of toughness of a collagen fibril as function of surface degradation. Since the Monte Carlo degradation simulation progressed at different rates for each

condition, the time required to reach 1.1% degradation differed for each system described in Table 4.1. Regardless of the time required to reach 1.1% degradation, the analysis was performed at a single instant in time, and no further enzyme-mediated degradation occurred as the tensile loading was applied.

For the quantification of the fibril stress-strain response to axial loading, the strain was computed by tracking the change in the size of the simulation box and the stress tensor was computed using the virial stress in the molecular dynamics package LAMMPS (Plimpton, 1995). The strain rate used in these simulations was $10^7\ s^{-1}$. In the current model, the abrupt fracture of the fibril does not occur because the fracture energy dissipation was constrained with a maximum velocity limit to avoid the collapse of the simulation at large strains.

We analyzed the strain distribution inside the fibril by calculating the tropocollagen bond length distributions. The distribution is calculated based on the length of bonds in the fibril structure at the different fibril bulk strain values. This distribution allows for the quantification of sliding and stretching of tropocollagen chains during the deformation of the fibril. We defined bonds as sliding bonds when their length during fibril deformation was comparable to their length in the undeformed fibril, and we defined bonds as stretching bonds when their length during fibril deformation was large compared to their length in the unstretched fibril.

4.3 Results

4.3.1 Fibril morphology after degradation

Figure 4.2 illustrates the complexity of the changes to the fibril structure when collagenases and gelatinases degrade a collagen fibril simultaneously, showing the cleaved and removed beads in the fibril for structures that had all experienced 1.1% degradation. Figures 4.2a and 4.2b show a snapshot of a section

of an equilibrated fibril (gray), removed beads (blue lines) and the beads with adjacent cleaved bonds (red spheres) and serves as an illustration of the general distribution of cleaved and removed bonds obtained from the MC simulation. Note that in the current study, one removed site in the MC simulation is equivalent to 10 sites in the MD simulation, which is why the removed sites are represented by blue lines instead of individual beads in the MD snapshot (Figure 4.2b). The heat maps shown in Figure 4.2c represent the spatial distribution of cleaved sites from the cross-sectional view of the fibril for all the systems. In a similar way, Figure 4.2d represents the spatial distribution of removed sites from the cross-sectional view of the fibril for all the systems. In both Figures 4.2c and 4.2d, the heatmaps are purposely arranged the lowest amount of collagenase (top panels) to the highest amount of collagenase (bottom panels) to better illustrate the behavior of the systems.

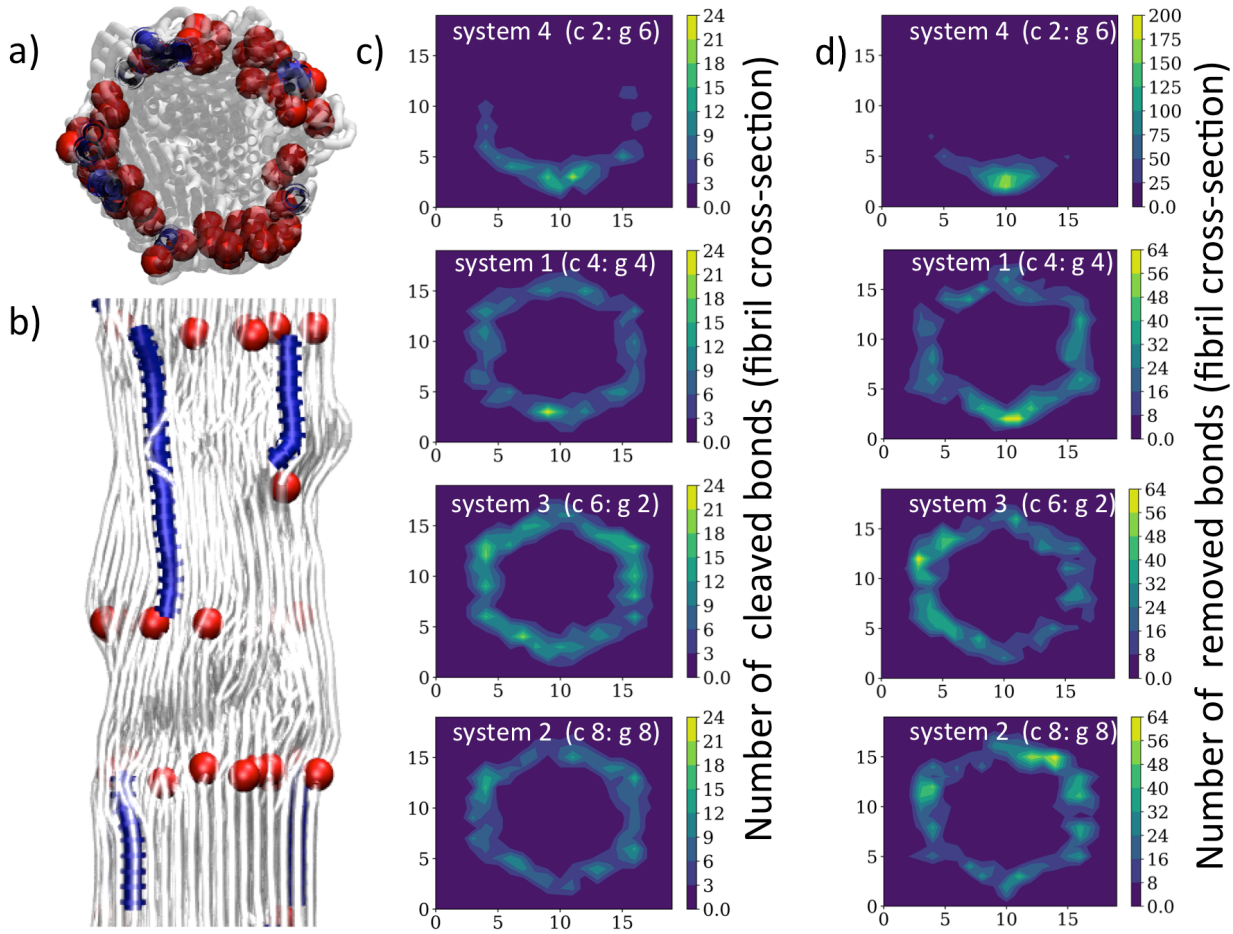

Figure 4.2: Representation of cleaved and removed sites for different conditions. **a) Snapshot of a crossectional view of the fibril** and **b) longitudinal view of the fibril.** In a) and b) removed sites are represented as blue tubes and cleaved sites are represented as red spheres. **c) Density map of cleaved sites** from the fibril crossectional view for system 4, 1, 3 and 2, ordered from top to bottom, respectively. **d) Density map of removed sites** from the fibril crossectional view for system 4, 1, 3 and 2, ordered from top to bottom respectively.

We note that the time course of degradation also appears to depend on the ratio of collagenases to gelatinases. Appendix Figure C.1 shows the time course of degradation for each system of collagenases and gelatinases. Degradation progresses most quickly when more gelatinases are present (system 4) and progresses most slowly when more collagenases are present (system 3) when the total number of enzymes on the surface is constant. However, when the the absolute number of enzymes on the fibril is increased, the degradation progresses more quickly (system 2).

The heatmaps in Figure 4.2c indicate that the density and location of cleaved bonds were highly dependent on the ratio of collagenase to gelatinase. System 4 (c 2: 6 g, top panel Figure 4.2c) had the smallest ratio collagenase to gelatinase and the most localization of cleaved bonds. As the ratio of collagenase to gelatinase increased, the distribution of cleaved bonds became more uniform across the outer surface of the fibril cross-section, as shown in System 1 (4 c: 4 g, second panel Figure 4.2c). As the ratio of collagenase to gelatinase continued to increase, the density of cleaved bonds increased around the outer surface of the fibril cross-section, as shown in System 3 (6 c: 2 g, third panel Figure 2c). Finally, System 2 (8 c: 8 g, bottom panel Figure 4.2c) showed a similar distribution and density of cleaved bonds compared to System 1 (4 c: 4 g, second panel Figure 4.2c), which had the same ratio of collagenase to gelatinase as System 2 but half the total number of enzymes. This observation indicates that, for the same amount of

degradation, the fibril had less connectivity (more cleaved bonds) on the surface as the ratio of collagenase to gelatinase increased. Moreover, for a small ratio of collagenase to gelatinase, the distribution of cleaved sites tended to be more localized.

The density map of removed beads (Figure 4.2d) appears to be related to the density map of cleaved bonds (Figure 4.2c), since gelatinase can remove a bead in the MC model only if a collagenase has previously cleaved a nearby bond. Thus, the location of removed bonds (Figure 4.2d) is similar to the density map of cleaved bonds (Figure 4.2c) but much more localized in certain regions. Note that the number of removed beads is the same for each of the panels in Figure 4.2d, but the distribution of the removed beads differs for each system. Moreover, the distribution appears to differ for a small ratio of collagenase to gelatinase (see system 4; c 2: 6 g, top panel Figure 4.2d), but the effect of the collagenase to gelatinase ratio is less evident in the other systems (Figure 4.2d, bottom 3 panels).

4.3.2 Toughness of the fibril

Figure 4.3 displays the stress-strain curves for the simulated systems in Table 4.1. As a reference, we included the stress-strain behavior of an intact fibril with its characteristic deformation regions (Depalle et al., 2015; Malaspina et al., 2017). The figure illustrates the abrupt change in the mechanical properties as a result of small amount of degradation and the shift in the yield strain for the degraded curves, characteristics consistent with our earlier report (Malaspina et al., 2017). One key observation is that the fibril toughness is progressively reduced as the collagenase to gelatinase ratio increases. Moreover, the stress-strain curves for a ratio of 1 (systems 1 & 2) are nearly identical, even though the absolute numbers of enzymes differ by a factor of two, indicating the stress-strain curves for a specified level of degradation appear to depend on the ratio of collagenases to gelatinases and not the total number of enzymes. The inset of Figure 4.3 shows that the yield stress is reduced by ~46% for the system with the smallest ratio of

collagenase to gelatinase (system 4) and ~36% for the system with the largest ratio collagenase to gelatinase (system 3).

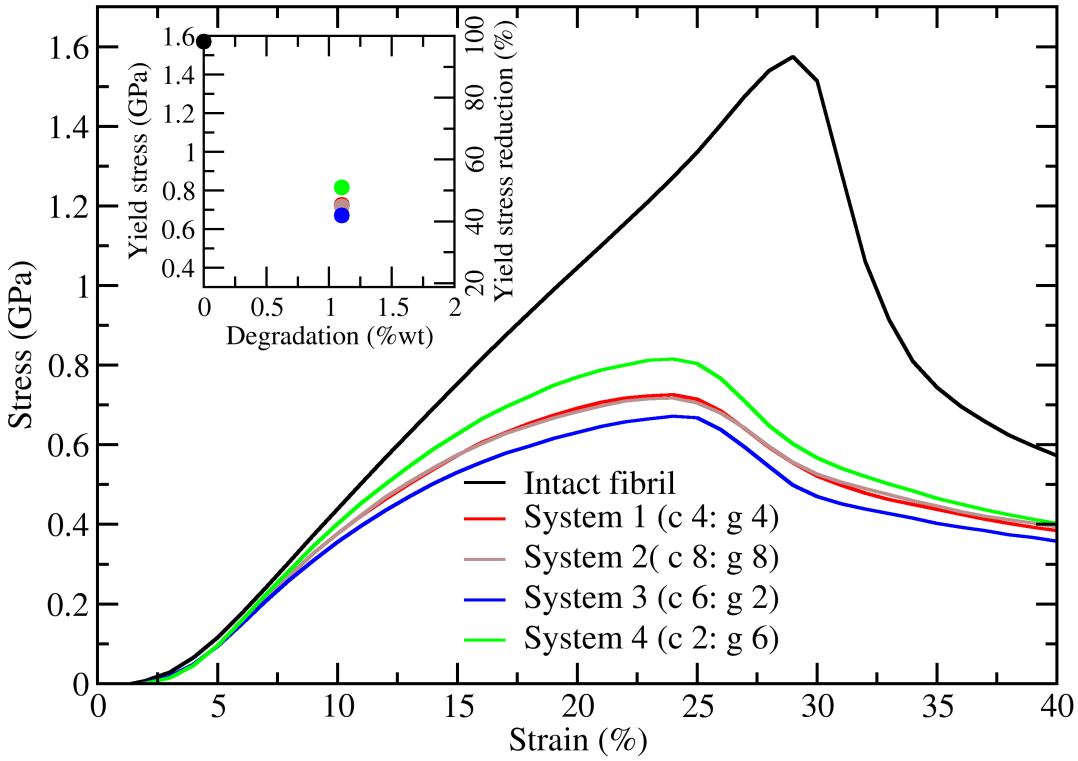

Figure 4.3: Stress-strain curves for different collagenase and gelatinase amounts at 1.1% degradation. Simulated system 1, 3 and 4 are represented in solid lines and system 2 is represented in blue dashed line to denote difference in total amount of enzymes. The stress-strain curve for the intact fibril is included in gray dashed lines.

4.3.3 Bond length distribution at fixed strain

Bond length distribution was examined to investigate the molecular origin of the change in toughness for the different stress-strain curves in Figure 4.3. These distributions provide the probabilities of tropocollagen stretching and tropocollagen sliding (Figure 4.4 inset schematic) and are related to the stress distribution inside the fibril. Figure 4.4 shows two populations of bond lengths for each structure when the strain is equal to 19%, a pre-yield state. The probability peak associated with the lower lengths is centered slightly above the equilibrium bond length of 14.7 Angstroms, indicating that minimal stretching has occurred and that the beads connected by those bonds are sliding with respect to the rest of the structure. The peak centered around higher lengths is associated with stretching of the bonds, indicating that the bonds connecting these beads can bear load (Malaspina et al., 2017). As the collagenase to gelatinase ratio increases, the proportion of un-stretched (sliding) bonds increases and the proportion of stretched bonds decreases. This trend suggests that fewer tropocollagen molecules bear load and more molecules passively slide apart as the ratio increases, which may explain why fibril toughness decreases as ratio increases.

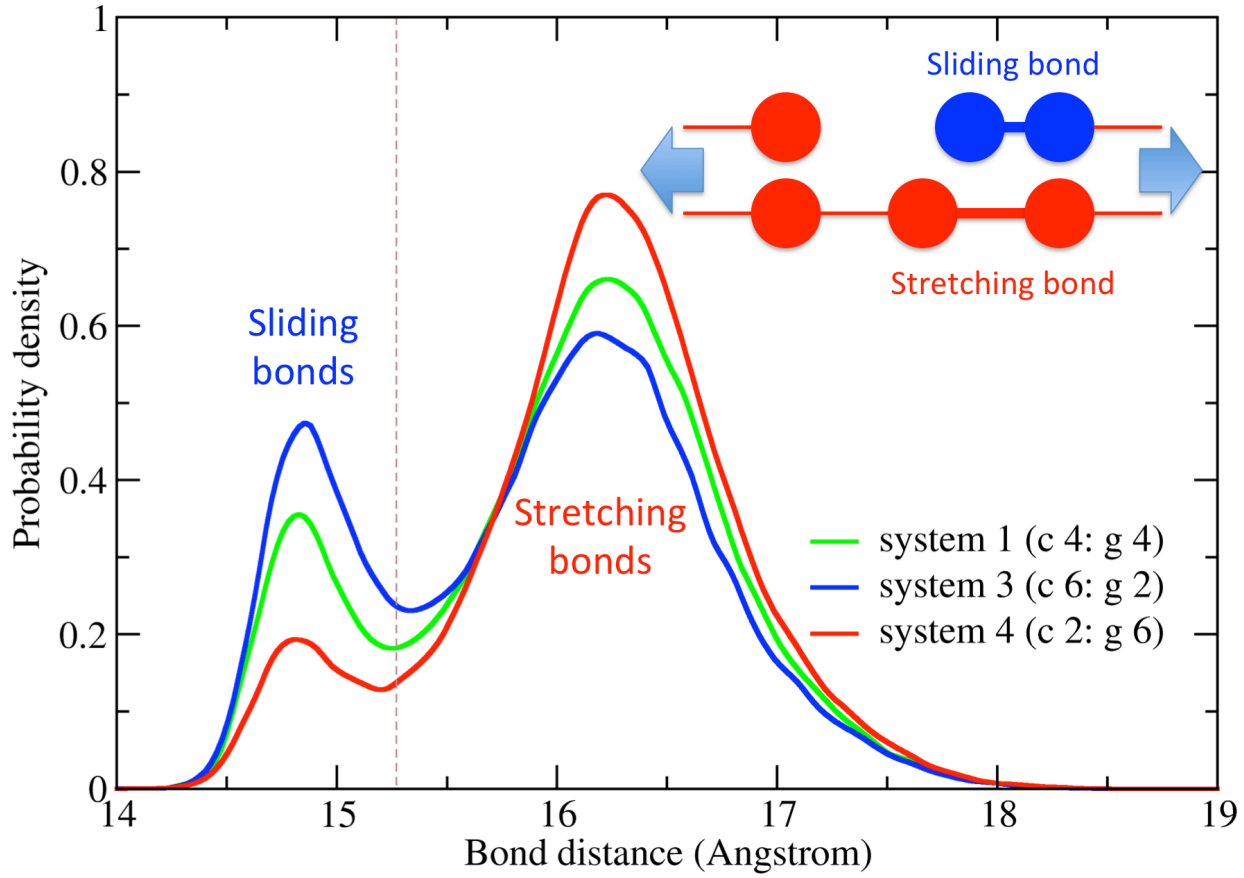

Figure 4.4: Distributions of tropocollagen bond lengths for systems 1, 3 and 4 described in Table 4.1. The distribution is evaluated at the same strain (19%) and same degradation (1.1 %wt). A grey dashed line represents the mean value where bonds transition from sliding to stretching. An inset scheme is included to show the difference between sliding and stretching bonds.

4.3.4 Bond length distribution vs. strain

The analysis of the bond length distribution was extended to the whole range of strains calculated in Figure 4.3. Figure 4.5 displays the distribution of bond lengths as a contour plot to identify how the distribution of bond lengths evolves as the fibril stretches. At low strains, the bond length distributions

show that almost all of the bonds are sliding bonds. As the strain increases, a bimodality in the distribution starts to develop, representing both stretching and sliding bonds. This bimodality can be identified in Figure 4.5 as the region containing a "hole" (dark blue) that represents the minimum between the sliding and stretching peaks (also shown in Figure 4.4). At midrange strains, system 3 appears to show this bimodality, while systems 1 and 4 do not appear to have as many sliding bonds in this range of strains before yield. However, as the strain increases beyond yield, the distributions of bond lengths shift back toward the equilibrium bond length of 14.7 Angstroms for all three systems.

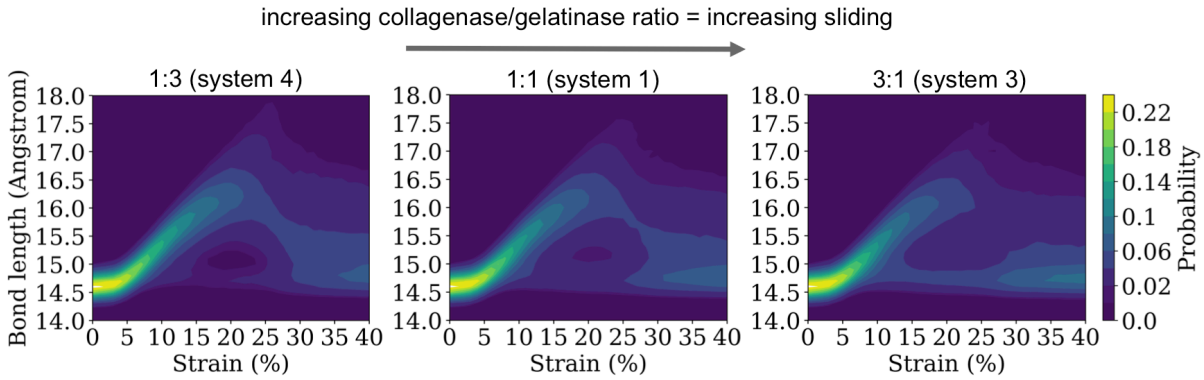

Figure 4.5: Contour plot of the distribution of bond lengths as a function of the strain for a collagen fibril at different collagenase/gelatinase ratios. The ratios are indicated above the plots, which are arranged in increasing ratio collagenase/gelatinase from left to right.

4.3 Discussion

4.4.1 Lessons learned

Using sequential Monte Carlo and Molecular Dynamics simulations, we probed the effect of enzymatic degradation on the structure and mechanics of a single collagen fibril. These models investigated the combined degradation behavior of collagenase and gelatinase and the molecular origin of the mechanical integrity of a degraded collagen fibril. Our MD simulations revealed that the loss of fibril mechanical integrity may depend not only on the number of removed beads, but also on the relative abundance of collagenase and gelatinase. An increase in the amount of collagenase increased the total number of cleaved bonds at a fixed amount of degradation. Further, the ratio of collagenase to gelatinase appeared to regulate the spatial distribution of the cleaved sites on the fibril surface, with a more diffuse pattern of cleaved bonds for higher ratios and a more localized pattern for low ratios. Finally, our examination of the bond length distribution demonstrated that the fibrils with reduced toughness had fewer stretched bonds and more sliding bonds compared to the tougher fibrils. These results, which demonstrated a complex interplay between collagenase and gelatinase effects on fibril degradation and mechanical integrity, could inform future experiments that would provide targeted clinical treatment strategies, which would likely hinge on the relative effects of local collagenase and gelatinase inhibition on degradation and mechanics.

The toughness of the fibril appeared to be linked to the connectivity of the fibril, which we characterized using bond length distributions (Figure 4.5). These distributions revealed that increases in the relative amount of collagenase led to more sliding bonds and fewer stretched bonds, which may help explain the reduced load-bearing capacity of fibrils that were exposed to higher ratios of collagenase to gelatinase. The sliding bonds only provided a small amount of resistance to fibril loading through non-bonded cohesive molecular forces within the fibril (hydrogen bonds, electrostatic and Van der Waals interactions). However, the stretched bonds provided greater resistance to load because they were connected by covalent bonds in addition to the cohesive molecular forces within the fibril. Thus, because sliding bonds indicate reduced

load-bearing capacity, the presence of more sliding bonds (shown in Figure 4.5) may help explain the overall reduction in toughness that was observed for systems with more collagenases (shown in Figure 4.3).

Our simulation results indicated that the relative abundance of collagenases and gelatinases affected the spatial distribution of fibril degradation (Figures 4.2c and 4.2d). It appeared that a low ratio would lead to damage that was more localized to one region of the fibril surface, while a higher ratio would lead to a more diffuse pattern of cleaved bonds and removed fragments. For lower ratios, the damage remained confined to a particular region of the fibril, which may have allowed more bonds in the undamaged regions to stretch and bear the applied load. Conversely, the diffuse pattern of cleaved sites may have disrupted the continuity of the molecular structure at more locations along the fibril surface and prevented the uptake of load by the individual tropocollagen molecules. Thus, multiple lines of evidence seem to help explain the observed differences in load-bearing capabilities for the systems with different ratios of collagenase to gelatinase (Figure 4.3).

Although the mechanical response of a fibril appeared to depend on the ratio of collagenases to gelatinases and not on the absolute number of enzymes after a fixed amount of degradation, the speed of degradation appeared to depend on both the absolute number of enzymes on the fibril and the ratio of collagenase to gelatinase. Appendix Figure C.1 shows that the time-course of degradation accelerated when the total number of enzymes increased (system 2) and when the collagenase to gelatinase ratio decreased (system 4). These two factors, MMP ratio and surface coverage, are likely regulated *in vivo* by local cellular production rate and clearance by the lymphatic system and may have important implications for the progression of damage in the joint. Thus, future investigations should attempt to holistically examine the progression of damage to the collagen by combining information about these two factors that influence degradation and mechanics with our understanding of the biological processes (cellular production and lymphatic clearance) that regulate the factors.

4.4.2 Model assumptions and limitations

The MC model of degradation employed in this study included a constant number of collagenases and gelatinases on the fibril surface and did include a relationship between this surface coverage and MMP concentration in adjacent solution. That is, the model neglected the processes of adsorption and desorption. Had the model included the adsorption and desorption processes, the total number of enzymes on the fibril would have remained constant on average but would have fluctuated around that average throughout the simulation. However, it would have been difficult to include these processes in the model because the interaction energies associated with the adsorption and desorption processes have not been experimentally reported in the context of MMP-tropocollagen interactions. Thus, it would not be possible to use information about the processes of adsorption and desorption to establish a functional relationship between MMP surface coverage and MMP concentration in solution at the single fibril level. At a coarser level, kinetic studies of collagenase and gelatinase have established such functional relationships for bulk solutions. However, the mean-field approximation underlying those approaches limits their utility at the nanoscale (Collier et al., 2001; Welgus et al., 1980). Nonetheless, the MC model could be adapted to examine adsorption/desorption if the necessary parameters become available.

In the present investigation, the computational framework assumes that the entire fibril is accessible to MMPs throughout the MC simulations. We recognize, however, that a single fibril in solution does not adequately represent the environment of a fibril that is incorporated into a tissue, such as cartilage, where degradation will proceed much more slowly. Indeed, numerous reports indicate that collagen fibrils in cartilage are protected by the glycosaminoglycan (GAG) molecules that surround them (Kar et al., 2016; Li et al., 2015; Pratta et al., 2003) and that the GAGs slow the degradation process such that it occurs over years and decades rather than minutes and hours. However, this slow degradation of GAG-protected tissues can be traced back to the degradation of collagen fibrils. Thus, we argue that it is necessary to gain a fundamental understanding of single fibril degradation to fully understand the degradation at larger scales.

4.4.3 Regarding verification

Multiple lines of evidence suggest that the MD model in this work adequately reflects experimental observations. In our previous work (Malaspina et al., 2017), we compared the results of simulated mechanical testing to experimental data obtained using axial extension tests (Svensson, Mulder, Kovanen, & Magnusson, 2013). While we were only able to compare the results for intact fibrils because axial extension tests have not been performed on degraded collagen fibrils, we observed reasonable agreement between experimental and simulated results for the intact fibril. Furthermore, the MD model has been successfully applied in different scenarios (Depalle et al., 2015; Depalle, Qin, Shefelbine, & Buehler, 2016) where it showed general agreement with experimental observations. Finally, recent work on collagen fascicles seems to corroborate our results that show damage to the fibril will reduce its mechanical strength (Zitnay et al., 2017). That work shows that collagen fascicles subjected to sub-yield loading conditions experience subtle damage that leads to reduced strength and toughness compared to intact specimens (Zitnay et al., 2017), though we note that the mechanism of damage differs between their experiment and our model. Despite the similarities between the MD model and experimental observations, the present model, which incorporates biological mechanisms of degradation, has not yet been validated thoroughly against experimental data and further verification is needed. However, such experiments would require examinations at the single fibril level, which is experimentally challenging (Laasanen et al., 2003; Panwar et al., 2013; Panwar et al., 2015). Some of these challenges include obtaining isolated fibrils, measuring enzyme adsorption and reaction, measuring collagen degradation, and measuring mechanical properties at the single fibril level.

A combination of approaches may be required to experimentally verify the predictions of the degradation model. Following treatment of isolated collagen fibrils with different ratios of collagenase to gelatinase, AFM imaging could be used to examine the resulting morphology of the fibrils. Indeed, high speed AFM imaging has been used to examine degradation of collagen micro-ribbons by bacterial collagenase in real time (Watanabe-Nakayama, Itami, Kodera, Ando, & Konno, 2016). Degradation rate

can also be verified by continually measuring the lost in mass of the fibril during a sustained MMPs exposure using sensitive microbalance technologies. However, these experiments may be difficult to interpret, since adsorption and desorption of the MMPs would also contribute to changes in weight. As indicated earlier, adsorption/desorption behavior of MMPs is not well understood and may be one of the key barriers in the validation of models exploring the enzyme-mediated changes in mechanical properties. While these advanced experimental approaches remain beyond the scope of the present work, the results of the model may serve as a guide to experiments that will further illuminate the combined influences of collagenase and gelatinase on the degradation of individual collagen fibrils.

4.4.4 Conclusion

In summary, this study is the first step toward revealing the individual roles of collagenases and gelatinases in the structural deterioration of fibrillar collagen. The ratio of collagenase to gelatinase appears to influence the structure and, consequently, the toughness of a fibril. This knowledge of the relative roles of collagenases and gelatinases may eventually help illuminate paths to targeted treatments that may prevent or reduce pathological collagen degradation and loss of mechanical integrity, particularly in articular cartilage.

Chapter 5: Conclusion and future work

5.1 Summary of goals

In this work, we presented several computational approaches designed to probe the mechanisms that underlie cartilage damage after a knee injury with an emphasis on sex hormone effects on the process. Because of the role that MMPs play in the initiation of damage to the cartilage, we began with a review of the effects of female sex hormones on MMP production at different spatial scales and in systems throughout the body. This review of literature highlighted the complexity and inhomogeneity of cellular responses to sex hormones throughout the body and hinted at a role for inflammation as an intermediary between hormone action and MMP production. We next examined sex hormone effects on inflammation and MMP production by macrophages and synovial fibroblasts using a systems biology modeling approach that aggregated and synthesized data from a number of well-controlled cellular studies. This analysis demonstrated how sex hormones can modulate the transient inflammatory response caused by an injury and subsequently elevate or reduce MMP production by the resident cells in the synovium. Finally, we developed a model of MMP-driven collagen fibril degradation, which we coupled with an existing coarse-grained molecular dynamics model to simulate the collagen fibril mechanical response. The analysis of degradation and mechanics provides a connection between hormonally modulated MMP production after injury and the resulting collagen destruction and loss of cartilage load-bearing capacity that impairs function of the knee joint after an injury. Together, the approaches presented in this work hold promise as tools that may eventually aid the development of targeted treatment strategies that will improve post-injury outcomes. Nevertheless, our work to understand sex differences in outcomes may be continued via multiple lines of inquiry.

5.2 Hormonal effects on inflammation

In this work, we presented a systems biology approach that synthesized information about components of the post-injury inflammatory response in the joint and examined the effects of the principal sex hormones estrogen, progesterone, and testosterone. With this approach, we quantified how MMP production and inflammation differed when male concentrations of hormones were present compared to female hormone concentrations and examined the potential differences in inflammation for concentrations of hormones associated with different phases of the menstrual cycle. We found that progesterone had little effect on the inflammatory response at the concentrations that would be expected in the knee joint. After making this observation, we excluded progesterone from the analysis and decided to assess the effects of estrogen and testosterone in three different cases: 1) low estrogen and low testosterone ("Female Low E"); 2) high estrogen and low testosterone ("Female High E"); 3) low estrogen and high testosterone ("Male"). Among these cases, the "Male" hormonal state led to the most subdued inflammatory response, with reduced TNF-α and increased IL-10. The "Female High E" condition led to the most pronounced inflammatory response and, importantly, increased production of MMP-1 compared to the other two cases. These findings indicated that inflammation and the resulting MMP production after an ACL injury may depend not only on the sex of the patient, but also on the exact concentration of estrogen at the time of injury, which may depend on timing within a female's menstrual cycle.

These results represent a framework for understanding the factors that influence the post-injury inflammatory response, providing a plausible mechanism that may underlie the differences in outcomes for males and females. Such knowledge may inform treatment in the first days after a knee injury. Further, these results may serve as the basis for the formulation of innovative treatments that may account for the hormonal contributions to inflammation.

In the future, the systems biology model of sex hormone effects on inflammation may also serve as a tool to explore the long-term post-injury outcomes for the cartilage and synovium. To perform such an analysis, other substances could be introduced into the model to account for the effects of damage associated molecular patterns (DAMPs) and other inflammatory signaling molecules that play a role in chronic

inflammation and OA initiation, but do not necessarily play a pronounced role in the initial inflammatory response (Rosenberg et al., 2017). Understanding the chronic inflammatory factors that may initiate OA may be one avenue for exploring new treatment approaches and preventative strategies. For example, the systems biology model could be extended to incorporate appropriate chronic inflammatory mediators and then used to predict which mediator or group of mediators have the strongest effect on long-term inflammation through sensitivity analysis. Based on the knowledge gleaned from such studies, therapies could eventually be developed to slow or inhibit the initiation and progression of OA.

While we were able to examine some potential sex differences in post-injury inflammation using a systems biology approach, we did not thoroughly investigate the effects of the female hormonal cycle, which may prove important to the post-injury inflammatory response. In the present work, we examined steady concentrations of sex hormones to provide upper and lower bounds on the possible inflammatory responses for females after knee injury. However, this approach could have obscured changes in the inflammatory response that could result from fluctuations in sex hormones after the initial injury. Our preliminary analyses of the influences of estrogen fluctuations on the inflammatory response suggest that the timing of an injury during the menstrual cycle may influence the severity of the inflammation response, particularly with regard to IL-1β and MMP-1. Future work will examine these effects, potentially improving our ability to assess how hormonal factors contribute to the inflammatory response in the knee after an injury.

5.3 Degradation and tensile mechanics

Here, we developed a dynamic Metropolis Monte Carlo (MC) algorithm to glean insights into the relative contributions of collagenases and gelatinases to the degradation of an isolated collagen fibril. Using the collagen fibril structures generated by the MC degradation model, we also examined the associated losses of mechanical integrity using a coarse-grained molecular dynamics approach that has been described

previously (Malaspina et al., 2017). These approaches allowed us to characterize the relative contributions of collagenases and gelatinases to the degradation and mechanical weakening of collagen fibrils. Our results indicated that the ratio of collagenases to gelatinases, not just the absolute amount of each, affected both degradation rate and the mechanical response. For a fixed total number of MMPs, the degradation rate was slowest when the number of collagenases exceeded the number of gelatinases. Conversely, the degradation rate was fastest when the number of gelatinases exceeded the number of collagenases (for a fixed number of total enzymes). At a fixed amount of degradation, the fibril toughness was lowest when the number of collagenases exceeded the number of gelatinases. These results suggest that the degradation and loss of mechanical integrity in the cartilage after ACL injury may depend not only on the concentrations of collagenases and gelatinases, but also on the ratio of the two.

Adsorption of MMPs onto a collagen fibril is an important link between the MMP production described by the systems biology model of inflammation and collagen fibril destruction described by the MC model. Ideally, we would be able to predict the surface coverage of MMPs on the collagen fibril based on the MMP concentration in the surrounding fluid. Previous reports have described the kinetics of MMP binding on collagen and gelatin (Collier et al., 2001; Welgus et al., 1980), but these kinetic data do not provide adequate thermodynamic information to predict MMP adsorption at the collagen fibril level. Early studies of collagenase characterized binding to collagen gels using Michaelis-Menten kinetics (Welgus et al., 1980), an approach relies on the mean-field approximation. However, the mean-field approximation makes the fundamental assumption that every individual interaction between adsorbing particles is equal to the mean value of all interactions between particles after averaging across the entire system. While this assumption is suitable when considering collagenase in bulk binding to a sufficiently large number of sites on collagen, the mean-field approximation blurs the molecular details that we seek to observe with the degradation model, and thus is not suitable for our purposes. Rather, Metropolis MC simulations represent a more appropriate way to assess adsorption and desorption of MMPs on an isolated collagen fibril, since they are able to probe the interactions of individual particles through the framework of statistical

thermodynamics. Therefore, the dynamic MC model we have developed in this work may be used as a tool to link MMP concentration in solution to surface coverage of MMPs on an individual collagen fibril, provided more information about the energetics of MMP binding becomes available.

Work to validate the models of degradation and mechanics is ongoing, though a number of technical issues remain unresolved (see Appendix D). We attempted re-create the conditions of the degradation model in the lab, then used AFM imaging and mechanical indentation to probe the mechanical response. Because mechanical indentation analysis is experimentally more tractable than tensile testing, we are also considering modifying the MD model of fibril mechanics so that we can perform equivalent indentation tests *in silico*, which would allow us to examine more carefully the strengths and weaknesses of our predictions. Future work should consider improved ways to isolate collagen fibrils, develop techniques for verifying that degradation has occurred after MMP treatment, and allow adequate time to master experimental approaches. These considerations will facilitate the next steps for experimentation and validation of the model predictions.

The findings we present may ultimately help clinicians assess the expected severity of collagen degradation based on MMP concentrations and may provide hints that will aid treatment of cartilage pathologies. For example, in the case of osteoarthritis, where damage and loss of mechanical integrity have already been initiated by collagenases, inhibiting gelatinase or its production may be advantageous to slow the progression of degradation. Conversely, inhibition of collagenase or its production may be advantageous after an injury to the knee when damage is still being initiated as a result of inflammation. The knowledge of the relative roles of collagenases and gelatinases may help illuminate paths to targeted treatments that could prevent or reduce pathological collagen degradation and loss of mechanical integrity, particularly in articular cartilage.

5.4 Other potential applications for systems biology and Monte Carlo models

Moving beyond the clinical problem presented herein, both the systems biology model of sex hormone effects on inflammation and the Metropolis MC model of collagen degradation could be readily modified for studies of inflammation and collagen degradation, respectively, in systems throughout the body, since both processes are ubiquitous in normal physiology as well as pathophysiology. For example, though we formulated the model of inflammation to be specific to the injured knee, knee-specific elements of the model (i.e., the effects of synovial fibroblasts) could be removed, allowing the study of sex hormone effects on any process where macrophages infiltrate. Additionally, other cell types could be easily added, provided adequate *in vitro* data exist to facilitate formulation of new kinetic parameters. Similarly, collagen degradation contributes to processes that range from cancer metastasis and fibrosis to aberrant ligament and tendon remodeling, making the MC model of collagen degradation a potentially valuable tool in examining these pathologies.

5.5 Final thoughts

This work is a step toward deeper understanding of the causes that underlie sex differences in outcomes after knee injury. The modeling approaches we presented here were intended to be building blocks that would allow us to learn about initiation of damage and associated loss of mechanical integrity in the injured knee, and how the process may differ due to the influences of sex hormones. Such knowledge could be used to identify key aspects of the post-injury inflammatory process in the knee joint to inform treatment strategies, which may include targeted anti-inflammatory treatments that disrupt the specific substances that enhance MMP production or local inhibition of MMPs in the joint. Ultimately, the purpose of this work was to develop tools that will help clinicians and researchers develop strategies to reduce or

prevent the cartilage damage that occurs as a result of injury, while accounting for hormonal contributions to the process, preventing the lifelong pain and dysfunction that can develop as early as the teenage years because of knee injury.

References

Ahlden, M., Sernert, N., Karlsson, J., & Kartus, J. (2012). Outcome of anterior cruciate ligament reconstruction with emphasis on sex-related differences. *Scand J Med Sci Sports, 22*(5), 618-626. doi:10.1111/j.1600-0838.2011.01306.x

Ahmad, N., Wang, W., Nair, R., & Kapila, S. (2012). Relaxin induces matrix-metalloproteinases-9 and -13 via RXFP1: induction of MMP-9 involves the PI3K, ERK, Akt and PKC-zeta pathways. *Mol Cell Endocrinol, 363*(1-2), 46-61. doi:10.1016/j.mce.2012.07.006

Amalinei, C., Caruntu, I. D., & Balan, R. A. (2007). Biology of metalloproteinases. *Rom J Morphol Embryol, 48*(4), 323-334.

Anderson, W. D., Makadia, H. K., Greenhalgh, A. D., Schwaber, J. S., David, S., & Vadigepalli, R. (2015). Computational modeling of cytokine signaling in microglia. *Mol Biosyst, 11*(12), 3332-3346. doi:10.1039/c5mb00488h

Arbabi, V., Pouran, B., Weinans, H., & Zadpoor, A. A. (2015). Transport of neutral solute across articular cartilage: the role of zonal diffusivities. *J Biomech Eng, 137*(7). doi:10.1115/1.4030070

Arbabi, V., Pouran, B., Weinans, H., & Zadpoor, A. A. (2016). Neutral solute transport across osteochondral interface: A finite element approach. *J Biomech, 49*(16), 3833-3839. doi:10.1016/j.jbiomech.2016.10.015

Asano, K., Sakai, M., Matsuda, T., Tanaka, H., Fujii, K., & Hisamitsu, T. (2006). Suppression of matrix metalloproteinase production from synovial fibroblasts by meloxicam in-vitro. *J Pharm Pharmacol, 58*(3), 359-366. doi:10.1211/jpp.58.3.0010

Baldwin, S. J., Quigley, A. S., Clegg, C., & Kreplak, L. (2014). Nanomechanical mapping of hydrated rat tail tendon collagen I fibrils. *Biophys J, 107*(8), 1794-1801. doi:10.1016/j.bpj.2014.09.003

Bani, D. (1997). Relaxin: a pleiotropic hormone. *Gen Pharmacol, 28*(1), 13-22.

Barbieri, R. L. (2014). The endocrinology of the menstrual cycle. *Methods Mol Biol, 1154*, 145-169. doi:10.1007/978-1-4939-0659-8_7

Bathgate, R. A., Halls, M. L., van der Westhuizen, E. T., Callander, G. E., Kocan, M., & Summers, R. J. (2013). Relaxin family peptides and their receptors. *Physiol Rev, 93*(1), 405-480. doi:10.1152/physrev.00001.2012

Bathgate, R. A., Ivell, R., Sanborn, B. M., Sherwood, O. D., & Summers, R. J. (2005). Receptors for relaxin family peptides. *Ann N Y Acad Sci, 1041*, 61-76. doi:10.1196/annals.1282.010

Batra, J., Robinson, J., Mehner, C., Hockla, A., Miller, E., Radisky, D. C., & Radisky, E. S. (2012). PEGylation extends circulation half-life while preserving in vitro and in vivo activity of tissue inhibitor of metalloproteinases-1 (TIMP-1). *PLoS One, 7*(11), e50028. doi:10.1371/journal.pone.0050028

Bertini, I., Fragai, M., Luchinat, C., Melikian, M., Toccafondi, M., Lauer, J. L., & Fields, G. B. (2012). Structural basis for matrix metalloproteinase 1-catalyzed collagenolysis. *J Am Chem Soc, 134*(4), 2100-2110. doi:10.1021/ja208338j

Bigoni, M., Sacerdote, P., Turati, M., Franchi, S., Gandolla, M., Gaddi, D., . . . Torsello, A. (2013). Acute and late changes in intraarticular cytokine levels following anterior cruciate ligament injury. *J Orthop Res, 31*(2), 315-321. doi:10.1002/jor.22208

Bjornstrom, L., & Sjoberg, M. (2005). Mechanisms of estrogen receptor signaling: convergence of genomic and nongenomic actions on target genes. *Mol Endocrinol, 19*(4), 833-842. doi:10.1210/me.2004-0486

Bobjer, J., Katrinaki, M., Tsatsanis, C., Lundberg Giwercman, Y., & Giwercman, A. (2013). Negative association between testosterone concentration and inflammatory markers in young men: a nested cross-sectional study. *PLoS One, 8*(4), e61466. doi:10.1371/journal.pone.0061466

Boccaccio, A., Lamberti, L., Papi, M., De Spirito, M., & Pappalettere, C. (2015). Effect of AFM probe geometry on visco-hyperelastic characterization of soft materials. *Nanotechnology, 26*(32), 325701.

Brailoiu, E., Dun, S. L., Brailoiu, G. C., Mizuo, K., Sklar, L. A., Oprea, T. I., . . . Dun, N. J. (2007). Distribution and characterization of estrogen receptor G protein-coupled receptor 30 in the rat central nervous system. *J Endocrinol, 193*(2), 311-321. doi:10.1677/JOE-07-0017

Bryant, A. L., Crossley, K. M., Bartold, S., Hohmann, E., & Clark, R. A. (2011). Estrogen-induced effects on the neuro-mechanics of hopping in humans. *Eur J Appl Physiol, 111*(2), 245-252. doi:10.1007/s00421-010-1647-8

Burrage, P. S., Mix, K. S., & Brinckerhoff, C. E. (2006). Matrix metalloproteinases: role in arthritis. *Front Biosci, 11*, 529-543.

Byrne, A., & Reen, D. J. (2002). Lipopolysaccharide induces rapid production of IL-10 by monocytes in the presence of apoptotic neutrophils. *J Immunol, 168*(4), 1968-1977.

Calippe, B., Douin-Echinard, V., Delpy, L., Laffargue, M., Lelu, K., Krust, A., . . . Gourdy, P. (2010). 17Beta-estradiol promotes TLR4-triggered proinflammatory mediator production through direct estrogen receptor alpha signaling in macrophages in vivo. *J Immunol, 185*(2), 1169-1176. doi:10.4049/jimmunol.0902383

Capellino, S., Straub, R. H., & Cutolo, M. (2014). Aromatase and regulation of the estrogen-to-androgen ratio in synovial tissue inflammation: common pathway in both sexes. *Ann N Y Acad Sci, 1317*, 24-31. doi:10.1111/nyas.12398

Casey, E., Hameed, F., & Dhaher, Y. Y. (2014). The muscle stretch reflex throughout the menstrual cycle. *Med Sci Sports Exerc, 46*(3), 600-609. doi:10.1249/MSS.0000000000000134

Cawston, T. E., & Wilson, A. J. (2006). Understanding the role of tissue degrading enzymes and their inhibitors in development and disease. *Best Pract Res Clin Rheumatol, 20*(5), 983-1002. doi:10.1016/j.berh.2006.06.007

Cha, H. S., Ahn, K. S., Jeon, C. H., Kim, J., Song, Y. W., & Koh, E. M. (2003). Influence of hypoxia on the expression of matrix metalloproteinase-1, -3 and tissue inhibitor of metalloproteinase-1 in rheumatoid synovial fibroblasts. *Clin Exp Rheumatol, 21*(5), 593-598.

Chantry, D., Turner, M., Abney, E., & Feldmann, M. (1989). Modulation of cytokine production by transforming growth factor-beta. *J Immunol, 142*(12), 4295-4300.

Charvolin, J., & Sadoc, J. F. (2012). About collagen, a tribute to Yves Bouligand. *Interface Focus, 2*(5), 567-574. doi:10.1098/rsfs.2012.0014

Chen, Q., Jin, M., Yang, F., Zhu, J., Xiao, Q., & Zhang, L. (2013). Matrix metalloproteinases: inflammatory regulators of cell behaviors in vascular formation and remodeling. *Mediators Inflamm, 2013*, 928315. doi:10.1155/2013/928315

Chow, B. S., Chew, E. G., Zhao, C., Bathgate, R. A., Hewitson, T. D., & Samuel, C. S. (2012). Relaxin signals through a RXFP1-pERK-nNOS-NO-cGMP-dependent pathway to up-regulate matrix metalloproteinases: the additional involvement of iNOS. *PLoS One, 7*(8), e42714. doi:10.1371/journal.pone.0042714

Chung, L., Dinakarpandian, D., Yoshida, N., Lauer-Fields, J. L., Fields, G. B., Visse, R., & Nagase, H. (2004). Collagenase unwinds triple-helical collagen prior to peptide bond hydrolysis. *EMBO J, 23*(15), 3020-3030. doi:10.1038/sj.emboj.7600318

Cimmino, M. A., & Parodi, M. (2005). Risk factors for osteoarthritis. *Semin Arthritis Rheum, 34*(6 Suppl 2), 29-34.

Claassen, H., Steffen, R., Hassenpflug, J., Varoga, D., Wruck, C. J., Brandenburg, L. O., & Pufe, T. (2010). 17beta-estradiol reduces expression of MMP-1, -3, and -13 in human primary articular chondrocytes from female patients cultured in a three dimensional alginate system. *Cell Tissue Res, 342*(2), 283-293. doi:10.1007/s00441-010-1062-9

Clark, I. M., Swingler, T. E., Sampieri, C. L., & Edwards, D. R. (2008). The regulation of matrix metalloproteinases and their inhibitors. *Int J Biochem Cell Biol, 40*(6-7), 1362-1378. doi:10.1016/j.biocel.2007.12.006

Cobbold, C. A., & Sherratt, J. A. (2000). Mathematical modelling of nitric oxide activity in wound healing can explain keloid and hypertrophic scarring. *J Theor Biol, 204*(2), 257-288. doi:10.1006/jtbi.2000.2012

Collier, I. E., Legant, W., Marmer, B., Lubman, O., Saffarian, S., Wakatsuki, T., . . . Goldberg, G. I. (2011). Diffusion of MMPs on the surface of collagen fibrils: the mobile cell surface-collagen substratum interface. *PLoS One, 6*(9), e24029. doi:10.1371/journal.pone.0024029

Collier, I. E., Saffarian, S., Marmer, B. L., Elson, E. L., & Goldberg, G. (2001). Substrate recognition by gelatinase A: the C-terminal domain facilitates surface diffusion. *Biophys J, 81*(4), 2370-2377. doi:10.1016/S0006-3495(01)75883-3

Cowin, S. C., & Doty, S. B. (2007). *Tissue mechanics*. New York: Springer.

Critchley, H. O., Kelly, R. W., Brenner, R. M., & Baird, D. T. (2001). The endocrinology of menstruation--a role for the immune system. *Clin Endocrinol (Oxf), 55*(6), 701-710.

D'Agostino, P., Milano, S., Barbera, C., Di Bella, G., La Rosa, M., Ferlazzo, V., . . . Cillari, E. (1999). Sex hormones modulate inflammatory mediators produced by macrophages. *Ann N Y Acad Sci, 876*, 426-429.

de Lange-Brokaar, B. J., Ioan-Facsinay, A., van Osch, G. J., Zuurmond, A. M., Schoones, J., Toes, R. E., . . . Kloppenburg, M. (2012). Synovial inflammation, immune cells and their cytokines in osteoarthritis: a review. *Osteoarthritis Cartilage, 20*(12), 1484-1499. doi:10.1016/j.joca.2012.08.027

Dedrick, G. S., Sizer, P. S., Merkle, J. N., Hounshell, T. R., Robert-McComb, J. J., Sawyer, S. F., . . . Roger James, C. (2008). Effect of sex hormones on neuromuscular control patterns during landing. *J Electromyogr Kinesiol, 18*(1), 68-78. doi:10.1016/j.jelekin.2006.09.004

Dehghan, F., Muniandy, S., Yusof, A., & Salleh, N. (2014). Testosterone reduces knee passive range of motion and expression of relaxin receptor isoforms via 5alpha-dihydrotestosterone and androgen receptor binding. *Int J Mol Sci, 15*(3), 4619-4634. doi:10.3390/ijms15034619

Della Beffa, C., Slansky, E., Pommerenke, C., Klawonn, F., Li, J., Dai, L., . . . Pessler, F. (2013). The relative composition of the inflammatory infiltrate as an additional tool for synovial tissue classification. *PLoS One, 8*(8), e72494. doi:10.1371/journal.pone.0072494

Depalle, B., Qin, Z., Shefelbine, S. J., & Buehler, M. J. (2015). Influence of cross-link structure, density and mechanical properties in the mesoscale deformation mechanisms of collagen fibrils. *J Mech Behav Biomed Mater, 52*, 1-13. doi:10.1016/j.jmbbm.2014.07.008

Depalle, B., Qin, Z., Shefelbine, S. J., & Buehler, M. J. (2016). Large Deformation Mechanisms, Plasticity, and Failure of an Individual Collagen Fibril With Different Mineral Content. *J Bone Miner Res, 31*(2), 380-390. doi:10.1002/jbmr.2705

Dimitrijevic, M., Stanojevic, S., Kustrimovic, N., Mitic, K., Vujic, V., Aleksic, I., . . . Leposavic, G. (2013). The influence of aging and estradiol to progesterone ratio on rat macrophage phenotypic profile and NO and TNF-alpha production. *Exp Gerontol, 48*(11), 1243-1254. doi:10.1016/j.exger.2013.07.001

Dragoo, J. L., Castillo, T. N., Braun, H. J., Ridley, B. A., Kennedy, A. C., & Golish, S. R. (2011). Prospective correlation between serum relaxin concentration and anterior cruciate ligament tears among elite collegiate female athletes. *Am J Sports Med, 39*(10), 2175-2180. doi:10.1177/0363546511413378

Duarte Campos, D. F., Drescher, W., Rath, B., Tingart, M., & Fischer, H. (2012). Supporting Biomaterials for Articular Cartilage Repair. *Cartilage, 3*(3), 205-221. doi:10.1177/1947603512444722

Edd, S. N., Favre, J., Blazek, K., Omoumi, P., Asay, J. L., & Andriacchi, T. P. (2017). Altered gait mechanics and elevated serum pro-inflammatory cytokines in asymptomatic patients with MRI evidence of knee cartilage loss. *Osteoarthritis Cartilage, 25*(6), 899-906. doi:10.1016/j.joca.2016.12.029

Emonard, H., Bellon, G., de Diesbach, P., Mettlen, M., Hornebeck, W., & Courtoy, P. J. (2005). Regulation of matrix metalloproteinase (MMP) activity by the low-density lipoprotein receptor-related protein (LRP). A new function for an "old friend". *Biochimie, 87*(3-4), 369-376. doi:10.1016/j.biochi.2004.11.013

Emonard, H., Theret, L., Bennasroune, A. H., & Dedieu, S. (2014). Regulation of LRP-1 expression: make the point. *Pathol Biol (Paris), 62*(2), 84-90. doi:10.1016/j.patbio.2014.02.002

Etique, N., Verzeaux, L., Dedieu, S., & Emonard, H. (2013). LRP-1: a checkpoint for the extracellular matrix proteolysis. *Biomed Res Int, 2013*, 152163. doi:10.1155/2013/152163

Evans, J., & Salamonsen, L. A. (2012). Inflammation, leukocytes and menstruation. *Rev Endocr Metab Disord, 13*(4), 277-288. doi:10.1007/s11154-012-9223-7

Fadok, V. A., Bratton, D. L., Konowal, A., Freed, P. W., Westcott, J. Y., & Henson, P. M. (1998). Macrophages that have ingested apoptotic cells in vitro inhibit proinflammatory cytokine production through autocrine/paracrine mechanisms involving TGF-beta, PGE2, and PAF. *J Clin Invest, 101*(4), 890-898. doi:10.1172/JCI1112

Fang, M., Wu, X. C., & Huang, W. (2013). Raloxifene upregulated mesangial cell MMP-2 activity via ER-beta through transcriptional regulation. *Cell Biochem Biophys, 67*(2), 607-613. doi:10.1007/s12013-013-9548-1

Fang, P. K., Ma, X. C., Ma, D. L., & Fu, K. Y. (1999). Determination of interleukin-1 receptor antagonist, interleukin-10, and transforming growth factor-beta1 in synovial fluid aspirates of patients with temporomandibular disorders. *J Oral Maxillofac Surg, 57*(8), 922-928; discussion 928-929.

Faryniarz, D. A., Bhargava, M., Lajam, C., Attia, E. T., & Hannafin, J. A. (2006). Quantitation of estrogen receptors and relaxin binding in human anterior cruciate ligament fibroblasts. *In Vitro Cell Dev Biol Anim, 42*(7), 176-181. doi:10.1290/0512089.1

Fields, G. B. (1991). A model for interstitial collagen catabolism by mammalian collagenases. *J Theor Biol, 153*(4), 585-602.

Fields, G. B. (2013). Interstitial collagen catabolism. *J Biol Chem, 288*(13), 8785-8793. doi:10.1074/jbc.R113.451211

Fratzl, P. (2008). *Collagen structure and mechanics*: Springer US.

Freeman, B. M., Mountain, D. J., Brock, T. C., Chapman, J. R., Kirkpatrick, S. S., Freeman, M. B., . . . Grandas, O. H. (2014). Low testosterone elevates interleukin family cytokines in a rodent model:

a possible mechanism for the potentiation of vascular disease in androgen-deficient males. *J Surg Res, 190*(1), 319-327. doi:10.1016/j.jss.2014.03.017

Friden, C., Hirschberg, A. L., Saartok, T., Backstrom, T., Leanderson, J., & Renstrom, P. (2003). The influence of premenstrual symptoms on postural balance and kinesthesia during the menstrual cycle. *Gynecol Endocrinol, 17*(6), 433-439.

Gaide Chevronnay, H. P., Selvais, C., Emonard, H., Galant, C., Marbaix, E., & Henriet, P. (2012). Regulation of matrix metalloproteinases activity studied in human endometrium as a paradigm of cyclic tissue breakdown and regeneration. *Biochim Biophys Acta, 1824*(1), 146-156. doi:10.1016/j.bbapap.2011.09.003

Gandhi, R., Santone, D., Takahashi, M., Dessouki, O., & Mahomed, N. N. (2013). Inflammatory predictors of ongoing pain 2 years following knee replacement surgery. *Knee, 20*(5), 316-318. doi:10.1016/j.knee.2012.10.015

Ganesan, K., Balachandran, C., Manohar, B. M., & Puvanakrishnan, R. (2012). Effects of testosterone, estrogen and progesterone on TNF-alpha mediated cellular damage in rat arthritic synovial fibroblasts. *Rheumatol Int, 32*(10), 3181-3188. doi:10.1007/s00296-011-2146-x

Giangrande, P. H., Kimbrel, E. A., Edwards, D. P., & McDonnell, D. P. (2000). The opposing transcriptional activities of the two isoforms of the human progesterone receptor are due to differential cofactor binding. *Mol Cell Biol, 20*(9), 3102-3115.

Giannandrea, M., & Parks, W. C. (2014). Diverse functions of matrix metalloproteinases during fibrosis. *Dis Model Mech, 7*(2), 193-203. doi:10.1242/dmm.012062

Goldsmith, L. T., & Weiss, G. (2005). Relaxin regulates endometrial structure and function in the rhesus monkey. *Ann N Y Acad Sci, 1041*, 110-117. doi:10.1196/annals.1282.015

Grainger, D. J., Wakefield, L., Bethell, H. W., Farndale, R. W., & Metcalfe, J. C. (1995). Release and activation of platelet latent TGF-beta in blood clots during dissolution with plasmin. *Nat Med, 1*(9), 932-937.

Grant, G. A., Eisen, A., Marmer, B., Roswit, W., & Goldberg, G. (1987). The activation of human skin fibroblast procollagenase. Sequence identification of the major conversion products. *Journal of Biological Chemistry, 262*(12), 5886-5889.

Greenspan, F. S., & Gardner, D. G. (2004). *Basic & clinical endocrinology* (7th ed.). New York: Lange Medical Books/McGraw-Hill.

Guccione, M., Silbiger, S., Lei, J., & Neugarten, J. (2002). Estradiol upregulates mesangial cell MMP-2 activity via the transcription factor AP-2. *Am J Physiol Renal Physiol, 282*(1), F164-169. doi:10.1152/ajprenal.00318.2000

Guery, J. C. (2012). Estrogens and inflammatory autoimmune diseases. *Joint Bone Spine, 79*(6), 560-562. doi:10.1016/j.jbspin.2012.09.010

Gupta, A., Shamseddin, M. K., & Khaira, A. (2011). Pathomechanisms of nephrogenic systemic fibrosis: new insights. *Clin Exp Dermatol, 36*(7), 763-768. doi:10.1111/j.1365-2230.2011.04136.x

Haller, J. M., Swearingen, C. A., Partridge, D., McFadden, M., Thirunavukkarasu, K., & Higgins, T. F. (2015). Intraarticular Matrix Metalloproteinases and Aggrecan Degradation Are Elevated After Articular Fracture. *Clin Orthop Relat Res, 473*(10), 3280-3288. doi:10.1007/s11999-015-4441-4

Halls, M. L., Bathgate, R. A., & Summers, R. J. (2006). Relaxin family peptide receptors RXFP1 and RXFP2 modulate cAMP signaling by distinct mechanisms. *Mol Pharmacol, 70*(1), 214-226. doi:10.1124/mol.105.021691

Harada, A., Sekido, N., Akahoshi, T., Wada, T., Mukaida, N., & Matsushima, K. (1994). Essential involvement of interleukin-8 (IL-8) in acute inflammation. *J Leukoc Biol, 56*(5), 559-564.

Heard, B. J., Martin, L., Rattner, J. B., Frank, C. B., Hart, D. A., & Krawetz, R. (2012). Matrix metalloproteinase protein expression profiles cannot distinguish between normal and early osteoarthritic synovial fluid. *BMC Musculoskelet Disord, 13*, 126. doi:10.1186/1471-2474-13-126

Heard, B. J., Solbak, N. M., Achari, Y., Chung, M., Hart, D. A., Shrive, N. G., & Frank, C. B. (2013). Changes of early post-traumatic osteoarthritis in an ovine model of simulated ACL reconstruction

are associated with transient acute post-injury synovial inflammation and tissue catabolism. *Osteoarthritis Cartilage, 21*(12), 1942-1949. doi:10.1016/j.joca.2013.08.019

Heeg, M. H., Koziolek, M. J., Vasko, R., Schaefer, L., Sharma, K., Muller, G. A., & Strutz, F. (2005). The antifibrotic effects of relaxin in human renal fibroblasts are mediated in part by inhibition of the Smad2 pathway. *Kidney Int, 68*(1), 96-109. doi:10.1111/j.1523-1755.2005.00384.x

Henmi, H., Endo, T., Nagasawa, K., Hayashi, T., Chida, M., Akutagawa, N., . . . Kudo, R. (2001). Lysyl oxidase and MMP-2 expression in dehydroepiandrosterone-induced polycystic ovary in rats. *Biol Reprod, 64*(1), 157-162.

Henneman, S., Bildt, M. M., Degroot, J., Kuijpers-Jagtman, A. M., & Von den Hoff, J. W. (2008). Relaxin stimulates MMP-2 and alpha-smooth muscle actin expression by human periodontal ligament cells. *Arch Oral Biol, 53*(2), 161-167. doi:10.1016/j.archoralbio.2007.08.010

Hertel, J., Williams, N. I., Olmsted-Kramer, L. C., Leidy, H. J., & Putukian, M. (2006). Neuromuscular performance and knee laxity do not change across the menstrual cycle in female athletes. *Knee Surg Sports Traumatol Arthrosc, 14*(9), 817-822. doi:10.1007/s00167-006-0047-4

Horrigan, L. A., Kelly, J. P., & Connor, T. J. (2006). Immunomodulatory effects of caffeine: friend or foe? *Pharmacology & therapeutics, 111*(3), 877-892.

Huang, H. F., Hong, L. H., Tan, Y., & Sheng, J. Z. (2004). Matrix metalloproteinase 2 is associated with changes in steroid hormones in the sera and peritoneal fluid of patients with endometriosis. *Fertil Steril, 81*(5), 1235-1239. doi:10.1016/j.fertnstert.2003.10.027

Huang, T. L., Hsu, H. C., Yang, K. C., & Lin, F. H. (2011). Hyaluronan up-regulates IL-10 expression in fibroblast-like synoviocytes from patients with tibia plateau fracture. *J Orthop Res, 29*(4), 495-500. doi:10.1002/jor.21261

Imada, K., Ito, A., Sato, T., Namiki, M., Nagase, H., & Mori, Y. (1997). Hormonal regulation of matrix metalloproteinase 9/gelatinase B gene expression in rabbit uterine cervical fibroblasts. *Biol Reprod, 56*(3), 575-580.

Inoue, H., Takamori, M., Nagata, N., Nishikawa, T., Oda, H., Yamamoto, S., & Koshihara, Y. (2001). An investigation of cell proliferation and soluble mediators induced by interleukin 1beta in human synovial fibroblasts: comparative response in osteoarthritis and rheumatoid arthritis. *Inflamm Res, 50*(2), 65-72. doi:10.1007/s000110050726

Irie, K., Uchiyama, E., & Iwaso, H. (2003). Intraarticular inflammatory cytokines in acute anterior cruciate ligament injured knee. *Knee, 10*(1), 93-96.

Jager, N. A., Wallis de Vries, B. M., Hillebrands, J. L., Harlaar, N. J., Tio, R. A., Slart, R. H., . . . Westra, J. (2016). Distribution of Matrix Metalloproteinases in Human Atherosclerotic Carotid Plaques and Their Production by Smooth Muscle Cells and Macrophage Subsets. *Mol Imaging Biol, 18*(2), 283-291. doi:10.1007/s11307-015-0882-0

Jha, A. K., Tharp, K. M., Browne, S., Ye, J., Stahl, A., Yeghiazarians, Y., & Healy, K. E. (2016). Matrix metalloproteinase-13 mediated degradation of hyaluronic acid-based matrices orchestrates stem cell engraftment through vascular integration. *Biomaterials, 89*, 136-147. doi:10.1016/j.biomaterials.2016.02.023

Jovanovic, D. V., Di Battista, J. A., Martel-Pelletier, J., Reboul, P., He, Y., Jolicoeur, F. C., & Pelletier, J. P. (2001). Modulation of TIMP-1 synthesis by antiinflammatory cytokines and prostaglandin E2 in interleukin 17 stimulated human monocytes/macrophages. *J Rheumatol, 28*(4), 712-718.

Kaneda, Y., Tsutsumi, Y., Yoshioka, Y., Kamada, H., Yamamoto, Y., Kodaira, H., . . . Mayumi, T. (2004). The use of PVP as a polymeric carrier to improve the plasma half-life of drugs. *Biomaterials, 25*(16), 3259-3266. doi:10.1016/j.biomaterials.2003.10.003

Kapila, S., Wang, W., & Uston, K. (2009). Matrix metalloproteinase induction by relaxin causes cartilage matrix degradation in target synovial joints. *Ann N Y Acad Sci, 1160*, 322-328. doi:10.1111/j.1749-6632.2009.03830.x

Kapila, S., & Xie, Y. (1998). Targeted induction of collagenase and stromelysin by relaxin in unprimed and beta-estradiol-primed diarthrodial joint fibrocartilaginous cells but not in synoviocytes. *Lab Invest, 78*(8), 925-938.

Kar, S., Smith, D. W., Gardiner, B. S., Li, Y., Wang, Y., & Grodzinsky, A. J. (2016). Modeling IL-1 induced degradation of articular cartilage. *Arch Biochem Biophys, 594*, 37-53. doi:10.1016/j.abb.2016.02.008

Kelly, R. W., King, A. E., & Critchley, H. O. (2001). Cytokine control in human endometrium. *Reproduction, 121*(1), 3-19.

Kim, K. S., Choi, H. M., Lee, Y. A., Choi, I. A., Lee, S. H., Hong, S. J., . . . Yoo, M. C. (2011). Expression levels and association of gelatinases MMP-2 and MMP-9 and collagenases MMP-1 and MMP-13 with VEGF in synovial fluid of patients with arthritis. *Rheumatol Int, 31*(4), 543-547. doi:10.1007/s00296-010-1592-1

Klapproth, J., Castell, J., Geiger, T., Andus, T., & Heinrich, P. C. (1989). Fate and biological action of human recombinant interleukin 1 beta in the rat in vivo. *Eur J Immunol, 19*(8), 1485-1490. doi:10.1002/eji.1830190821

Knowlton, A. A., & Korzick, D. H. (2014). Estrogen and the female heart. *Mol Cell Endocrinol, 389*(1-2), 31-39. doi:10.1016/j.mce.2014.01.002

Kong, R. C., Shilling, P. J., Lobb, D. K., Gooley, P. R., & Bathgate, R. A. (2010). Membrane receptors: structure and function of the relaxin family peptide receptors. *Mol Cell Endocrinol, 320*(1-2), 1-15. doi:10.1016/j.mce.2010.02.003

Kothari, P., Pestana, R., Mesraoua, R., Elchaki, R., Khan, K. M., Dannenberg, A. J., & Falcone, D. J. (2014). IL-6-mediated induction of matrix metalloproteinase-9 is modulated by JAK-dependent IL-10 expression in macrophages. *J Immunol, 192*(1), 349-357. doi:10.4049/jimmunol.1301906

Kou, X. X., Li, C. S., He, D. Q., Wang, X. D., Hao, T., Meng, Z., . . . Gan, Y. H. (2015). Estradiol promotes M1-like macrophage activation through cadherin-11 to aggravate temporomandibular joint inflammation in rats. *J Immunol, 194*(6), 2810-2818. doi:10.4049/jimmunol.1303188

Kovats, S. (2015). Estrogen receptors regulate innate immune cells and signaling pathways. *Cell Immunol, 294*(2), 63-69. doi:10.1016/j.cellimm.2015.01.018

Kuwata, H., Watanabe, Y., Miyoshi, H., Yamamoto, M., Kaisho, T., Takeda, K., & Akira, S. (2003). IL-10-inducible Bcl-3 negatively regulates LPS-induced TNF-alpha production in macrophages. *Blood, 102*(12), 4123-4129. doi:10.1182/blood-2003-04-1228

Laasanen, M. S., Toyras, J., Korhonen, R. K., Rieppo, J., Saarakkala, S., Nieminen, M. T., . . . Jurvelin, J. S. (2003). Biomechanical properties of knee articular cartilage. *Biorheology, 40*(1-3), 133-140.

Labombarda, F., Meffre, D., Delespierre, B., Krivokapic-Blondiaux, S., Chastre, A., Thomas, P., . . . Guennoun, R. (2010). Membrane progesterone receptors localization in the mouse spinal cord. *Neuroscience, 166*(1), 94-106. doi:10.1016/j.neuroscience.2009.12.012

Lauer-Fields, J. L., Juska, D., & Fields, G. B. (2002). Matrix metalloproteinases and collagen catabolism. *Biopolymers, 66*(1), 19-32. doi:10.1002/bip.10201

Laxdal, G., Kartus, J., Ejerhed, L., Sernert, N., Magnusson, L., Faxen, E., & Karlsson, J. (2005). Outcome and risk factors after anterior cruciate ligament reconstruction: a follow-up study of 948 patients. *Arthroscopy, 21*(8), 958-964. doi:10.1016/j.arthro.2005.05.007

Lee, Y. J., Lee, E. B., Kwon, Y. E., Lee, J. J., Cho, W. S., Kim, H. A., & Song, Y. W. (2003). Effect of estrogen on the expression of matrix metalloproteinase (MMP)-1, MMP-3, and MMP-13 and tissue inhibitor of metalloproternase-1 in osteoarthritis chondrocytes. *Rheumatol Int, 23*(6), 282-288. doi:10.1007/s00296-003-0312-5

Lei, B., Mace, B., Dawson, H. N., Warner, D. S., Laskowitz, D. T., & James, M. L. (2014). Anti-inflammatory effects of progesterone in lipopolysaccharide-stimulated BV-2 microglia. *PLoS One, 9*(7), e103969. doi:10.1371/journal.pone.0103969

Lekgabe, E. D., Kiriazis, H., Zhao, C., Xu, Q., Moore, X. L., Su, Y., . . . Samuel, C. S. (2005). Relaxin reverses cardiac and renal fibrosis in spontaneously hypertensive rats. *Hypertension, 46*(2), 412-418. doi:10.1161/01.HYP.0000171930.00697.2f

Li, J., Shao, X., Wu, L., Feng, T., Jin, C., Fang, M., . . . Yao, H. (2011). Honokiol: an effective inhibitor of tumor necrosis factor-alpha-induced up-regulation of inflammatory cytokine and chemokine

production in human synovial fibroblasts. *Acta Biochim Biophys Sin (Shanghai), 43*(5), 380-386. doi:10.1093/abbs/gmr027

Li, R. T., Lorenz, S., Xu, Y., Harner, C. D., Fu, F. H., & Irrgang, J. J. (2011). Predictors of radiographic knee osteoarthritis after anterior cruciate ligament reconstruction. *Am J Sports Med, 39*(12), 2595-2603. doi:10.1177/0363546511424720

Li, Y., Wang, Y., Chubinskaya, S., Schoeberl, B., Florine, E., Kopesky, P., & Grodzinsky, A. J. (2015). Effects of insulin-like growth factor-1 and dexamethasone on cytokine-challenged cartilage: relevance to post-traumatic osteoarthritis. *Osteoarthritis Cartilage, 23*(2), 266-274. doi:10.1016/j.joca.2014.11.006

Lieberthal, J., Sambamurthy, N., & Scanzello, C. R. (2015). Inflammation in joint injury and post-traumatic osteoarthritis. *Osteoarthritis Cartilage, 23*(11), 1825-1834. doi:10.1016/j.joca.2015.08.015

Little, J. P., Bleedorn, J. A., Sutherland, B. J., Sullivan, R., Kalscheur, V. L., Ramaker, M. A., . . . Muir, P. (2014). Arthroscopic assessment of stifle synovitis in dogs with cranial cruciate ligament rupture. *PLoS One, 9*(6), e97329. doi:10.1371/journal.pone.0097329

Liu, L., Zhao, Y., Xie, K., Sun, X., Jiang, L., Gao, Y., & Wang, Z. (2014). Estrogen inhibits LPS-induced IL-6 production in macrophages partially via the nongenomic pathway. *Immunol Invest, 43*(7), 693-704. doi:10.3109/08820139.2014.917095

Liu, Y., Ballarini, R., & Eppell, S. J. (2016). Tension tests on mammalian collagen fibrils. *Interface Focus, 6*(1), 20150080.

Lohmander, L. S., Englund, P. M., Dahl, L. L., & Roos, E. M. (2007). The long-term consequence of anterior cruciate ligament and meniscus injuries: osteoarthritis. *Am J Sports Med, 35*(10), 1756-1769. doi:10.1177/0363546507307396

Lohmander, L. S., Ostenberg, A., Englund, M., & Roos, H. (2004). High prevalence of knee osteoarthritis, pain, and functional limitations in female soccer players twelve years after anterior cruciate ligament injury. *Arthritis Rheum, 50*(10), 3145-3152. doi:10.1002/art.20589

Loparic, M., Wirz, D., Daniels, A., Raiteri, R., VanLandingham, M. R., Guex, G., . . . Stolz, M. (2010). Micro-and nanomechanical analysis of articular cartilage by indentation-type atomic force microscopy: validation with a gel-microfiber composite. *Biophysical journal, 98*(11), 2731-2740.

Lu, K. G., & Stultz, C. M. (2013). Insight into the degradation of type-I collagen fibrils by MMP-8. *J Mol Biol, 425*(10), 1815-1825. doi:10.1016/j.jmb.2013.02.002

Maeda, H., Kuwahara, H., Ichimura, Y., Ohtsuki, M., Kurakata, S., & Shiraishi, A. (1995). TGF-beta enhances macrophage ability to produce IL-10 in normal and tumor-bearing mice. *J Immunol, 155*(10), 4926-4932.

Mahmoodzadeh, S., Dworatzek, E., Fritschka, S., Pham, T. H., & Regitz-Zagrosek, V. (2010). 17beta-Estradiol inhibits matrix metalloproteinase-2 transcription via MAP kinase in fibroblasts. *Cardiovasc Res, 85*(4), 719-728. doi:10.1093/cvr/cvp350

Malaspina, D. C., Szleifer, I., & Dhaher, Y. (2017). Mechanical properties of a collagen fibril under simulated degradation. *J Mech Behav Biomed Mater, 75*, 549-557. doi:10.1016/j.jmbbm.2017.08.020

Malemud, C. J. (2006). Matrix metalloproteinases (MMPs) in health and disease: an overview. *Front Biosci, 11*, 1696-1701.

Mancini, A., & Di Battista, J. A. (2006). Transcriptional regulation of matrix metalloprotease gene expression in health and disease. *Front Biosci, 11*, 423-446.

Manka, S. W., Carafoli, F., Visse, R., Bihan, D., Raynal, N., Farndale, R. W., . . . Nagase, H. (2012). Structural insights into triple-helical collagen cleavage by matrix metalloproteinase 1. *Proc Natl Acad Sci U S A, 109*(31), 12461-12466. doi:10.1073/pnas.1204991109

Maroudas, A., Palla, G., & Gilav, E. (1992). Racemization of aspartic acid in human articular cartilage. *Connect Tissue Res, 28*(3), 161-169.

Matthews, J., & Gustafsson, J. A. (2003). Estrogen signaling: a subtle balance between ER alpha and ER beta. *Mol Interv, 3*(5), 281-292. doi:10.1124/mi.3.5.281

McCachren, S. S., Greer, P. K., & Niedel, J. E. (1989). Regulation of human synovial fibroblast collagenase messenger RNA by interleukin-1. *Arthritis Rheum, 32*(12), 1539-1545.

Menzies, F. M., Henriquez, F. L., Alexander, J., & Roberts, C. W. (2011). Selective inhibition and augmentation of alternative macrophage activation by progesterone. *Immunology, 134*(3), 281-291. doi:10.1111/j.1365-2567.2011.03488.x

Mihm, M., Gangooly, S., & Muttukrishna, S. (2011). The normal menstrual cycle in women. *Anim Reprod Sci, 124*(3-4), 229-236. doi:10.1016/j.anireprosci.2010.08.030

Miller, L., Alley, E. W., Murphy, W. J., Russell, S. W., & Hunt, J. S. (1996). Progesterone inhibits inducible nitric oxide synthase gene expression and nitric oxide production in murine macrophages. *J Leukoc Biol, 59*(3), 442-450.

Miller, L., & Hunt, J. S. (1998). Regulation of TNF-alpha production in activated mouse macrophages by progesterone. *J Immunol, 160*(10), 5098-5104.

Mrosewski, I., Jork, N., Gorte, K., Conrad, C., Wiegand, E., Kohl, B., . . . Schulze-Tanzil, G. (2014). Regulation of osteoarthritis-associated key mediators by TNFalpha and IL-10: effects of IL-10 overexpression in human synovial fibroblasts and a synovial cell line. *Cell Tissue Res, 357*(1), 207-223. doi:10.1007/s00441-014-1868-y

Murakami, S., Muneta, T., Furuya, K., Saito, I., Miyasaka, N., & Yamamoto, H. (1995). Immunohistologic analysis of synovium in infrapatellar fat pad after anterior cruciate ligament injury. *Am J Sports Med, 23*(6), 763-768. doi:10.1177/036354659502300622

Murphy, G., Stanton, H., Cowell, S., Butler, G., Knauper, V., Atkinson, S., & Gavrilovic, J. (1999). Mechanisms for pro matrix metalloproteinase activation. *APMIS, 107*(1), 38-44.

Nagaraja, S., Wallqvist, A., Reifman, J., & Mitrophanov, A. Y. (2014). Computational approach to characterize causative factors and molecular indicators of chronic wound inflammation. *J Immunol, 192*(4), 1824-1834. doi:10.4049/jimmunol.1302481

Naqvi, T., Duong, T. T., Hashem, G., Shiga, M., Zhang, Q., & Kapila, S. (2005). Relaxin's induction of metalloproteinases is associated with the loss of collagen and glycosaminoglycans in synovial joint fibrocartilaginous explants. *Arthritis Res Ther, 7*(1), R1-11. doi:10.1186/ar1451

Nelson, L. R., & Bulun, S. E. (2001). Estrogen production and action. *J Am Acad Dermatol, 45*(3 Suppl), S116-124.

Okada, Y. (2000). Matrix-degrading metalloproteinases and their roles in joint destruction. *Mod Rheumatol, 10*(3), 121-128. doi:10.3109/s101650070018

Okada, Y., Gonoji, Y., Naka, K., Tomita, K., Nakanishi, I., Iwata, K., . . . Hayakawa, T. (1992). Matrix metalloproteinase 9 (92-kDa gelatinase/type IV collagenase) from HT 1080 human fibrosarcoma cells. Purification and activation of the precursor and enzymic properties. *Journal of Biological Chemistry, 267*(30), 21712-21719.

Orgel, J. P., Irving, T. C., Miller, A., & Wess, T. J. (2006). Microfibrillar structure of type I collagen in situ. *Proc Natl Acad Sci U S A, 103*(24), 9001-9005. doi:10.1073/pnas.0502718103

Orlowsky, E. W., & Kraus, V. B. (2015). The role of innate immunity in osteoarthritis: when our first line of defense goes on the offensive. *J Rheumatol, 42*(3), 363-371. doi:10.3899/jrheum.140382

Overall, C. M. (2002). Molecular determinants of metalloproteinase substrate specificity: matrix metalloproteinase substrate binding domains, modules, and exosites. *Mol Biotechnol, 22*(1), 51-86. doi:10.1385/MB:22:1:051

Pai, R., Ha, H., Kirschenbaum, M. A., & Kamanna, V. S. (1996). Role of tumor necrosis factor-alpha on mesangial cell MCP-1 expression and monocyte migration: mechanisms mediated by signal transduction. *J Am Soc Nephrol, 7*(6), 914-923.

Panwar, P., Du, X., Sharma, V., Lamour, G., Castro, M., Li, H., & Bromme, D. (2013). Effects of cysteine proteases on the structural and mechanical properties of collagen fibers. *J Biol Chem, 288*(8), 5940-5950. doi:10.1074/jbc.M112.419689

Panwar, P., Lamour, G., Mackenzie, N. C., Yang, H., Ko, F., Li, H., & Bromme, D. (2015). Changes in Structural-Mechanical Properties and Degradability of Collagen during Aging-associated Modifications. *J Biol Chem, 290*(38), 23291-23306. doi:10.1074/jbc.M115.644310

Park, S., Nicoll, S. B., Mauck, R. L., & Ateshian, G. A. (2008). Cartilage mechanical response under dynamic compression at physiological stress levels following collagenase digestion. *Ann Biomed Eng, 36*(3), 425-434. doi:10.1007/s10439-007-9431-6

Pedersen, B. K. (2017). Anti-inflammatory effects of exercise: role in diabetes and cardiovascular disease. *European journal of clinical investigation, 47*(8), 600-611.

Pehrsson, M., Westberg, L., Landen, M., & Ekman, A. (2007). Stable serum levels of relaxin throughout the menstrual cycle: a preliminary comparison of women with premenstrual dysphoria and controls. *Arch Womens Ment Health, 10*(4), 147-153. doi:10.1007/s00737-007-0186-8

Perumal, S., Antipova, O., & Orgel, J. P. (2008). Collagen fibril architecture, domain organization, and triple-helical conformation govern its proteolysis. *Proc Natl Acad Sci U S A, 105*(8), 2824-2829. doi:10.1073/pnas.0710588105

Plimpton, S. (1995). Fast Parallel Algorithms for Short-Range Molecular Dynamics. *Journal of Computational Physics, 117*(1), 1-19. doi:10.1006/jcph.1995.1039

Potier, M., Elliot, S. J., Tack, I., Lenz, O., Striker, G. E., Striker, L. J., & Karl, M. (2001). Expression and regulation of estrogen receptors in mesangial cells: influence on matrix metalloproteinase-9. *J Am Soc Nephrol, 12*(2), 241-251.

Powell, B. S., Dhaher, Y. Y., & Szleifer, I. G. (2015). Review of the Multiscale Effects of Female Sex Hormones on Matrix Metalloproteinase− Mediated Collagen Degradation. *Critical Reviews™ in Biomedical Engineering, 43*(5-6 %@ 0278-940X).

Pratta, M. A., Yao, W., Decicco, C., Tortorella, M. D., Liu, R. Q., Copeland, R. A., . . . Arner, E. C. (2003). Aggrecan protects cartilage collagen from proteolytic cleavage. *J Biol Chem, 278*(46), 45539-45545. doi:10.1074/jbc.M303737200

Qu, L., Abe, M., Yokoyama, Y., & Ishikawa, O. (2006). Effects of 17beta-estradiol on matrix metalloproteinase-1 synthesis by human dermal fibroblasts. *Maturitas, 54*(1), 39-46. doi:10.1016/j.maturitas.2005.08.006

Rae, J. M., & Johnson, M. D. (2005). What does an orphan G-protein-coupled receptor have to do with estrogen? *Breast Cancer Res, 7*(6), 243-244. doi:10.1186/bcr1330

Regan, E. A., Bowler, R. P., & Crapo, J. D. (2008). Joint fluid antioxidants are decreased in osteoarthritic joints compared to joints with macroscopically intact cartilage and subacute injury. *Osteoarthritis Cartilage, 16*(4), 515-521. doi:10.1016/j.joca.2007.09.001

Reynolds, A., Rubin, J., Clermont, G., Day, J., Vodovotz, Y., & Bard Ermentrout, G. (2006). A reduced mathematical model of the acute inflammatory response: I. Derivation of model and analysis of anti-inflammation. *J Theor Biol, 242*(1), 220-236. doi:10.1016/j.jtbi.2006.02.016

Rosenberg, J. H., Rai, V., Dilisio, M. F., & Agrawal, D. K. (2017). Damage-associated molecular patterns in the pathogenesis of osteoarthritis: potentially novel therapeutic targets. *Mol Cell Biochem, 434*(1-2), 171-179. doi:10.1007/s11010-017-3047-4

Rosenblum, G., Van den Steen, P. E., Cohen, S. R., Bitler, A., Brand, D. D., Opdenakker, G., & Sagi, I. (2010). Direct visualization of protease action on collagen triple helical structure. *PLoS One, 5*(6), e11043. doi:10.1371/journal.pone.0011043

Rosenblum, G., Van den Steen, P. E., Cohen, S. R., Grossmann, J. G., Frenkel, J., Sertchook, R., . . . Sagi, I. (2007). Insights into the structure and domain flexibility of full-length pro-matrix metalloproteinase-9/gelatinase B. *Structure, 15*(10), 1227-1236. doi:10.1016/j.str.2007.07.019

Rovensky, J., Radikova, Z., Imrich, R., Greguska, O., Vigas, M., & Macho, L. (2004). Gonadal and adrenal steroid hormones in plasma and synovial fluid of patients with rheumatoid arthritis. *Endocr Regul, 38*(4), 143-149.

Russell, R. E., Culpitt, S. V., DeMatos, C., Donnelly, L., Smith, M., Wiggins, J., & Barnes, P. J. (2002). Release and activity of matrix metalloproteinase-9 and tissue inhibitor of metalloproteinase-1 by

alveolar macrophages from patients with chronic obstructive pulmonary disease. *Am J Respir Cell Mol Biol, 26*(5), 602-609. doi:10.1165/ajrcmb.26.5.4685

Saarialho-Kere, U. K., Welgus, H. G., & Parks, W. C. (1993). Distinct mechanisms regulate interstitial collagenase and 92-kDa gelatinase expression in human monocytic-like cells exposed to bacterial endotoxin. *J Biol Chem, 268*(23), 17354-17361.

Saffarian, S., Collier, I. E., Marmer, B. L., Elson, E. L., & Goldberg, G. (2004). Interstitial collagenase is a Brownian ratchet driven by proteolysis of collagen. *Science, 306*(5693), 108-111. doi:10.1126/science.1099179

Salamonsen, L. A. (1998). Current concepts of the mechanisms of menstruation: a normal process of tissue destruction. *Trends Endocrinol Metab, 9*(8), 305-309.

Salamonsen, L. A., Butt, A. R., Hammond, F. R., Garcia, S., & Zhang, J. (1997). Production of endometrial matrix metalloproteinases, but not their tissue inhibitors, is modulated by progesterone withdrawal in an in vitro model for menstruation. *J Clin Endocrinol Metab, 82*(5), 1409-1415. doi:10.1210/jcem.82.5.3920

Salamonsen, L. A., & Woolley, D. E. (1996). Matrix metalloproteinases in normal menstruation. *Hum Reprod, 11 Suppl 2*, 124-133.

Saren, P., Welgus, H. G., & Kovanen, P. T. (1996). TNF-alpha and IL-1beta selectively induce expression of 92-kDa gelatinase by human macrophages. *J Immunol, 157*(9), 4159-4165.

Sarkar, S. K., Marmer, B., Goldberg, G., & Neuman, K. C. (2012). Single-molecule tracking of collagenase on native type I collagen fibrils reveals degradation mechanism. *Curr Biol, 22*(12), 1047-1056. doi:10.1016/j.cub.2012.04.012

Sato, T., Ito, A., Mori, Y., Yamashita, K., Hayakawa, T., & Nagase, H. (1991). Hormonal regulation of collagenolysis in uterine cervical fibroblasts. Modulation of synthesis of procollagenase, prostromelysin and tissue inhibitor of metalloproteinases (TIMP) by progesterone and oestradiol-17 beta. *Biochem J, 275 (Pt 3)*, 645-650.

Schindler, R., Mancilla, J., Endres, S., Ghorbani, R., Clark, S. C., & Dinarello, C. A. (1990). Correlations and interactions in the production of interleukin-6 (IL-6), IL-1, and tumor necrosis factor (TNF) in human blood mononuclear cells: IL-6 suppresses IL-1 and TNF. *Blood, 75*(1), 40-47.

Schmal, H., Henkelmann, R., Mehlhorn, A. T., Reising, K., Bode, G., Sudkamp, N. P., & Niemeyer, P. (2015). Synovial cytokine expression in ankle osteoarthritis depends on age and stage. *Knee Surg Sports Traumatol Arthrosc, 23*(5), 1359-1367. doi:10.1007/s00167-013-2719-1

Sciore, P., Frank, C. B., & Hart, D. A. (1998). Identification of sex hormone receptors in human and rabbit ligaments of the knee by reverse transcription-polymerase chain reaction: evidence that receptors are present in tissue from both male and female subjects. *J Orthop Res, 16*(5), 604-610. doi:10.1002/jor.1100160513

Seliktar, D., Zisch, A. H., Lutolf, M. P., Wrana, J. L., & Hubbell, J. A. (2004). MMP-2 sensitive, VEGF-bearing bioactive hydrogels for promotion of vascular healing. *J Biomed Mater Res A, 68*(4), 704-716. doi:10.1002/jbm.a.20091

Selvais, C., Gaide Chevronnay, H. P., Lemoine, P., Dedieu, S., Henriet, P., Courtoy, P. J., . . . Emonard, H. (2009). Metalloproteinase-dependent shedding of low-density lipoprotein receptor-related protein-1 ectodomain decreases endocytic clearance of endometrial matrix metalloproteinase-2 and -9 at menstruation. *Endocrinology, 150*(8), 3792-3799. doi:10.1210/en.2009-0015

Serra, R., Al-Saidi, A. G., Angelov, N., & Nares, S. (2010). Suppression of LPS-induced matrix-metalloproteinase responses in macrophages exposed to phenytoin and its metabolite, 5-(p-hydroxyphenyl-), 5-phenylhydantoin. *J Inflamm (Lond), 7*, 48. doi:10.1186/1476-9255-7-48

Shah, K., McCormack, C. E., & Bradbury, N. A. (2014). Do you know the sex of your cells? *Am J Physiol Cell Physiol, 306*(1), C3-18. doi:10.1152/ajpcell.00281.2013

Silacci, P., Dayer, J. M., Desgeorges, A., Peter, R., Manueddu, C., & Guerne, P. A. (1998). Interleukin (IL)-6 and its soluble receptor induce TIMP-1 expression in synoviocytes and chondrocytes, and block IL-1-induced collagenolytic activity. *J Biol Chem, 273*(22), 13625-13629.

Silbiger, S., & Neugarten, J. (2008). Gender and human chronic renal disease. *Gend Med, 5 Suppl A*, S3-S10. doi:10.1016/j.genm.2008.03.002

Simpson, E. R. (2003). Sources of estrogen and their importance. *J Steroid Biochem Mol Biol, 86*(3-5), 225-230.

Sitruk-Ware, R., & Nath, A. (2010). The use of newer progestins for contraception. *Contraception, 82*(5), 410-417. doi:10.1016/j.contraception.2010.04.004

Smythies, L. E., Sellers, M., Clements, R. H., Mosteller-Barnum, M., Meng, G., Benjamin, W. H., . . . Smith, P. D. (2005). Human intestinal macrophages display profound inflammatory anergy despite avid phagocytic and bacteriocidal activity. *J Clin Invest, 115*(1), 66-75. doi:10.1172/JCI19229

Sniekers, Y. H., Weinans, H., Bierma-Zeinstra, S. M., van Leeuwen, J. P., & van Osch, G. J. (2008). Animal models for osteoarthritis: the effect of ovariectomy and estrogen treatment - a systematic approach. *Osteoarthritis Cartilage, 16*(5), 533-541. doi:10.1016/j.joca.2008.01.002

Sridhar, B. V., Brock, J. L., Silver, J. S., Leight, J. L., Randolph, M. A., & Anseth, K. S. (2015). Development of a cellularly degradable PEG hydrogel to promote articular cartilage extracellular matrix deposition. *Adv Healthc Mater, 4*(5), 702-713. doi:10.1002/adhm.201400695

Straub, R. H. (2007). The complex role of estrogens in inflammation. *Endocr Rev, 28*(5), 521-574. doi:10.1210/er.2007-0001

Sun, Y., Cai, J., Ma, F., Lu, P., Huang, H., & Zhou, J. (2012). miR-155 mediates suppressive effect of progesterone on TLR3, TLR4-triggered immune response. *Immunol Lett, 146*(1-2), 25-30. doi:10.1016/j.imlet.2012.04.007

Svensson, R. B., Mulder, H., Kovanen, V., & Magnusson, S. P. (2013). Fracture mechanics of collagen fibrils: influence of natural cross-links. *Biophys J, 104*(11), 2476-2484. doi:10.1016/j.bpj.2013.04.033

Szabo, G., & Saha, B. (2015). Alcohol's effect on host defense. *Alcohol research: current reviews, 37*(2), 159.

Tan, S. H., Lau, B. P., Khin, L. W., & Lingaraj, K. (2016). The Importance of Patient Sex in the Outcomes of Anterior Cruciate Ligament Reconstructions: A Systematic Review and Meta-analysis. *Am J Sports Med, 44*(1), 242-254. doi:10.1177/0363546515573008

Tarrant, J. M. (2010). Blood cytokines as biomarkers of in vivo toxicity in preclinical safety assessment: considerations for their use. *Toxicol Sci, 117*(1), 4-16. doi:10.1093/toxsci/kfq134

Thomassen, M. J., Divis, L. T., & Fisher, C. J. (1996). Regulation of human alveolar macrophage inflammatory cytokine production by interleukin-10. *Clin Immunol Immunopathol, 80*(3 Pt 1), 321-324.

Tourville, T. W., Poynter, M. E., DeSarno, M. J., Struglics, A., & Beynnon, B. D. (2015). Relationship between synovial fluid ARGS-aggrecan fragments, cytokines, MMPs, and TIMPs following acute ACL injury: A cross-sectional study. *J Orthop Res, 33*(12), 1796-1803. doi:10.1002/jor.22961

Troeberg, L., & Nagase, H. (2012). Proteases involved in cartilage matrix degradation in osteoarthritis. *Biochim Biophys Acta, 1824*(1), 133-145. doi:10.1016/j.bbapap.2011.06.020

Tsuchida, A. I., Beekhuizen, M., t Hart, M. C., Radstake, T. R., Dhert, W. J., Saris, D. B., . . . Creemers, L. B. (2014). Cytokine profiles in the joint depend on pathology, but are different between synovial fluid, cartilage tissue and cultured chondrocytes. *Arthritis Res Ther, 16*(5), 441. doi:10.1186/s13075-014-0441-0

Van den Steen, P. E., Proost, P., Grillet, B., Brand, D. D., Kang, A. H., Van Damme, J., & Opdenakker, G. (2002). Cleavage of denatured natural collagen type II by neutrophil gelatinase B reveals enzyme specificity, post-translational modifications in the substrate, and the formation of remnant epitopes in rheumatoid arthritis. *FASEB J, 16*(3), 379-389. doi:10.1096/fj.01-0688com

van der Rijt, J. A., van der Werf, K. O., Bennink, M. L., Dijkstra, P. J., & Feijen, J. (2006). Micromechanical testing of individual collagen fibrils. *Macromol Biosci, 6*(9), 697-702. doi:10.1002/mabi.200600063

Van Hove, A. H., Beltejar, M. J., & Benoit, D. S. (2014). Development and in vitro assessment of enzymatically-responsive poly(ethylene glycol) hydrogels for the delivery of therapeutic peptides. *Biomaterials, 35*(36), 9719-9730. doi:10.1016/j.biomaterials.2014.08.019

Vassilev, V., Pretto, C. M., Cornet, P. B., Delvaux, D., Eeckhout, Y., Courtoy, P. J., . . . Henriet, P. (2005). Response of matrix metalloproteinases and tissue inhibitors of metalloproteinases messenger ribonucleic acids to ovarian steroids in human endometrial explants mimics their gene- and phase-specific differential control in vivo. *J Clin Endocrinol Metab, 90*(10), 5848-5857. doi:10.1210/jc.2005-0762

Verzijl, N., DeGroot, J., Thorpe, S. R., Bank, R. A., Shaw, J. N., Lyons, T. J., . . . TeKoppele, J. M. (2000). Effect of collagen turnover on the accumulation of advanced glycation end products. *J Biol Chem, 275*(50), 39027-39031. doi:10.1074/jbc.M006700200

Vrtacnik, P., Ostanek, B., Mencej-Bedrac, S., & Marc, J. (2014). The many faces of estrogen signaling. *Biochem Med (Zagreb), 24*(3), 329-342. doi:10.11613/BM.2014.035

Wahl, S. M., Hunt, D. A., Wakefield, L. M., McCartney-Francis, N., Wahl, L. M., Roberts, A. B., & Sporn, M. B. (1987). Transforming growth factor type beta induces monocyte chemotaxis and growth factor production. *Proc Natl Acad Sci U S A, 84*(16), 5788-5792.

Wakefield, L. M., Smith, D. M., Flanders, K. C., & Sporn, M. B. (1988). Latent transforming growth factor-beta from human platelets. A high molecular weight complex containing precursor sequences. *J Biol Chem, 263*(16), 7646-7654.

Walter, H., Kawashima, A., Nebelung, W., Neumann, W., & Roessner, A. (1998). Immunohistochemical analysis of several proteolytic enzymes as parameters of cartilage degradation. *Pathol Res Pract, 194*(2), 73-81. doi:10.1016/S0344-0338(98)80073-3

Wang, W., Hayami, T., & Kapila, S. (2009). Female hormone receptors are differentially expressed in mouse fibrocartilages. *Osteoarthritis Cartilage, 17*(5), 646-654. doi:10.1016/j.joca.2008.09.015

Warden, S. J., Saxon, L. K., Castillo, A. B., & Turner, C. H. (2006). Knee ligament mechanical properties are not influenced by estrogen or its receptors. *Am J Physiol Endocrinol Metab, 290*(5), E1034-1040. doi:10.1152/ajpendo.00367.2005

Warren, M. P., & Fried, J. L. (2001). Temporomandibular disorders and hormones in women. *Cells Tissues Organs, 169*(3), 187-192. doi:47881

Watanabe-Nakayama, T., Itami, M., Kodera, N., Ando, T., & Konno, H. (2016). High-speed atomic force microscopy reveals strongly polarized movement of clostridial collagenase along collagen fibrils. *Sci Rep, 6*, 28975. doi:10.1038/srep28975

Welgus, H. G., Jeffrey, J. J., Stricklin, G. P., Roswit, W. T., & Eisen, A. Z. (1980). Characteristics of the action of human skin fibroblast collagenase on fibrillar collagen. *J Biol Chem, 255*(14), 6806-6813.

Wenger, M. P., Bozec, L., Horton, M. A., & Mesquida, P. (2007). Mechanical properties of collagen fibrils. *Biophys J, 93*(4), 1255-1263. doi:10.1529/biophysj.106.103192

Wiik, A., Ekman, M., Johansson, O., Jansson, E., & Esbjornsson, M. (2009). Expression of both oestrogen receptor alpha and beta in human skeletal muscle tissue. *Histochem Cell Biol, 131*(2), 181-189. doi:10.1007/s00418-008-0512-x

Wiik, A., Glenmark, B., Ekman, M., Esbjornsson-Liljedahl, M., Johansson, O., Bodin, K., . . . Jansson, E. (2003). Oestrogen receptor beta is expressed in adult human skeletal muscle both at the mRNA and protein level. *Acta Physiol Scand, 179*(4), 381-387. doi:10.1046/j.0001-6772.2003.01186.x

Wingrove, C. S., Garr, E., Godsland, I. F., & Stevenson, J. C. (1998). 17beta-oestradiol enhances release of matrix metalloproteinase-2 from human vascular smooth muscle cells. *Biochim Biophys Acta, 1406*(2), 169-174.

Wojtys, E. M., Huston, L. J., Boynton, M. D., Spindler, K. P., & Lindenfeld, T. N. (2002). The effect of the menstrual cycle on anterior cruciate ligament injuries in women as determined by hormone levels. *Am J Sports Med, 30*(2), 182-188.

Wong, S., Schwartz, R. C., & Pestka, J. J. (2001). Superinduction of TNF-alpha and IL-6 in macrophages by vomitoxin (deoxynivalenol) modulated by mRNA stabilization. *Toxicology, 161*(1-2), 139-149.

Xu, X., Chen, Z., Wang, Y., Yamada, Y., & Steffensen, B. (2005). Functional basis for the overlap in ligand interactions and substrate specificities of matrix metalloproteinases-9 and -2. *Biochem J, 392*(Pt 1), 127-134. doi:10.1042/BJ20050650

Yan, C., & Boyd, D. D. (2007). Regulation of matrix metalloproteinase gene expression. *J Cell Physiol, 211*(1), 19-26. doi:10.1002/jcp.20948

Yang, L., van der Werf, K. O., Dijkstra, P. J., Feijen, J., & Bennink, M. L. (2012). Micromechanical analysis of native and cross-linked collagen type I fibrils supports the existence of microfibrils. *J Mech Behav Biomed Mater, 6*, 148-158. doi:10.1016/j.jmbbm.2011.11.008

Yorifuji, M., Sawaji, Y., Endo, K., Kosaka, T., & Yamamoto, K. (2016). Limited efficacy of COX-2 inhibitors on nerve growth factor and metalloproteinases expressions in human synovial fibroblasts. *J Orthop Sci, 21*(3), 381-388. doi:10.1016/j.jos.2016.01.004

Zazulak, B. T., Paterno, M., Myer, G. D., Romani, W. A., & Hewett, T. E. (2006). The effects of the menstrual cycle on anterior knee laxity: a systematic review. *Sports Med, 36*(10), 847-862.

Zitnay, J. L., Li, Y., Qin, Z., San, B. H., Depalle, B., Reese, S. P., . . . Weiss, J. A. (2017). Molecular level detection and localization of mechanical damage in collagen enabled by collagen hybridizing peptides. *Nature Communications, 8*. doi:ARTN 14913

10.1038/ncomms14913

Zong, W., Meyn, L. A., & Moalli, P. A. (2009). The amount and activity of active matrix metalloproteinase 13 is suppressed by estradiol and progesterone in human pelvic floor fibroblasts. *Biol Reprod, 80*(2), 367-374. doi:10.1095/biolreprod.108.072462

Zuloaga, D. G., Yahn, S. L., Pang, Y., Quihuis, A. M., Oyola, M. G., Reyna, A., . . . Mani, S. K. (2012). Distribution and estrogen regulation of membrane progesterone receptor-beta in the female rat brain. *Endocrinology, 153*(9), 4432-4443. doi:10.1210/en.2012-1469

Appendices

Appendix A: Microscale hormone effects on MMP production

Appendix Table A.1: Summary of microscale effects of hormonal treatments on MMP production. *Fractional changes in MMP concentrations and activities are extracted from the cited references; + indicates supraphysiological dose hormone; - indicates subphysiological dose of hormone; n.s. = not significant; TMJ = temporomandibular joint.

Hormone	Hormone Concentration (ng/mL)	Type of MMP	Fractional Change in MMP*	MMP metric	Cell Type	Animal	Duration of Treatment	Reference
Estrogen	0.0272 -	proMMP-13	1.43	Protein expression	Pelvic Fibroblasts	Human	48 h	(Zong et al., 2009)
	0.272	proMMP-13	1.46	Protein expression	Pelvic Fibroblasts	Human	48 h	
	2.72 +	proMMP-13	1.51	Protein expression	Pelvic Fibroblasts	Human	48 h	
	0.0272 -	MMP-13	0.45	Protein expression	Pelvic Fibroblasts	Human	48 h	
	0.272	MMP-13	0.4	Protein expression	Pelvic Fibroblasts	Human	48 h	
	2.72 +	MMP-13	0.42	Protein expression	Pelvic Fibroblasts	Human	48 h	
	0.0272 -	MMP-13	0.33	MMP activity	Pelvic Fibroblasts	Human	48 h	
	0.272	MMP-13	0.39	MMP activity	Pelvic Fibroblasts	Human	48 h	
	2.72 +	MMP-13	0.53	MMP activity	Pelvic Fibroblasts	Human	48 h	
	272 +	MMP-1	0.19	mRNA	Cervical fibroblasts	Rabbit	24 h	(Sato et al., 1991)
	0.0272 -	MMP-1	1 (n.s.)	MMP activity	Cervical fibroblasts	Rabbit	24 h	
	2.72 +	MMP-1	0.49	MMP activity	Cervical fibroblasts	Rabbit	24 h	
	272 +	MMP-1	0.72 (n.s.)	MMP activity	Cervical fibroblasts	Rabbit	24 h	
	0.0272 -	proMMP-1	1.30 (n.s.)	Protein expression	Cervical fibroblasts	Rabbit	24 h	

	2.72 +	proMMP-1	0.48 (n.s.)	Protein expression	Cervical fibroblasts	Rabbit	24 h	
	272 +	proMMP-1	0.57 (n.s.)	Protein expression	Cervical fibroblasts	Rabbit	24 h	
	0.000272	proMMP-1	0.75	Protein expression	Dermal Fibroblasts	Human	6 h	(Qu et al., 2006)
	0.00272	proMMP-1	0.9	Protein expression	Dermal Fibroblasts	Human	6 h	
	0.0272	proMMP-1	0.77	Protein expression	Dermal Fibroblasts	Human	6 h	
	0.272	proMMP-1	0.92	Protein expression	Dermal Fibroblasts	Human	6 h	
	2.72	proMMP-1	0.83	Protein expression	Dermal Fibroblasts	Human	6 h	
	2720 +	MMP-1	0.21	mRNA levels	Articular Chondrocytes (female)	Human	1-3 wk	(Claassen et al., 2010)
	0.00272 -	MMP-13	0.55	mRNA levels	Articular Chondrocytes (female)	Human	1-3 wk	
	0.272	MMP-13	0.47	mRNA levels	Articular Chondrocytes (female)	Human	1-3 wk	
	27.2 +	MMP-13	0.42	mRNA levels	Articular Chondrocytes (female)	Human	1-3 wk	
	2720 +	MMP-13	0.38	mRNA levels	Articular Chondrocytes (female)	Human	1-3 wk	
	0.272	MMP-1	1.15 (n.s.)	mRNA levels	Articular Chondrocytes (male)	Human	1-3 wk	
	27.2 +	MMP-1	0.69 (n.s.)	mRNA levels	Articular Chondrocytes (male)	Human	1-3 wk	
	2720 +	MMP-1	0.49 (n.s.)	mRNA levels	Articular Chondrocytes (male)	Human	1-3 wk	
	0.00272	MMP-13	0.75 (n.s.)	mRNA levels	Articular Chondrocytes (male)	Human	1-3 wk	
	0.272	MMP-13	1.15 (n.s.)	mRNA levels	Articular Chondrocytes (male)	Human	1-3 wk	
	27.2 +	MMP-13	0.75 (n.s.)	mRNA levels	Articular Chondrocytes (male)	Human	1-3 wk	
	2720 +	MMP-13	0.59 (n.s.)	mRNA levels	Articular Chondrocytes (male)	Human	1-3 wk	
	0.05	MMP-1	0.92	Protein expression	OA Chondrocytes	Human	48 h	(Lee et al., 2003)
	0.5	MMP-1	0.76	Protein expression	OA Chondrocytes	Human	48 h	

	5	MMP-1	0.85 (n.s.)	Protein expression	OA Chondrocytes	Human	48 h	
	0.05	MMP-1	0.91 (n.s.)	MMP activity	OA Chondrocytes	Human	48 h	
	0.5	MMP-1	1.02 (n.s.)	MMP activity	OA Chondrocytes	Human	48 h	
	5	MMP-1	1.04 (n.s.)	MMP activity	OA Chondrocytes	Human	48 h	
	0.05	MMP-1	0.76 (n.s.)	mRNA	OA Chondrocytes	Human	48 h	
	0.5	MMP-1	0.84 (n.s.)	mRNA	OA Chondrocytes	Human	48 h	
	5	MMP-1	0.70 (n.s.)	mRNA	OA Chondrocytes	Human	48 h	
	20 +	MMP-1	1.42 (n.s.)	Protein expression	TMJ Fibrochondrocytes	Rabbit	24 h	(Kapila & Xie, 1998)
	20 +	MMP-1	0.86 (n.s.)	Protein expression	TMJ Synoviocytes	Rabbit	24 h	
	20 +	MMP-1	1.32 (n.s.)	MMP activity	TMJ Fibrocartilaginous Tissue	Rabbit	48 h	(Naqvi et al., 2005)
	0.1	MMP-13	1.67	mRNA	TMJ Disk Fibrochondrocytes	Mouse	48 h	(Kapila et al., 2009)
	0.1	MMP-9	2.23	mRNA	TMJ Disk Fibrochondrocytes	Mouse	48 h	
	0.0408	MMP-2	1.95	Protein expression	Vascular Smooth Muscle Cells	Mouse	72 h	(Wingrove et al., 1998)
	0.408	MMP-2	2.02	Protein expression	Vascular Smooth Muscle Cells	Mouse	72 h	
	4.08	MMP-2	2	Protein expression	Vascular Smooth Muscle Cells	Mouse	72 h	
	40.8	MMP-2	1.83	Protein expression	Vascular Smooth Muscle Cells	Mouse	72 h	
	408	MMP-2	1.41	Protein expression	Vascular Smooth Muscle Cells	Mouse	72 h	
	2.72+	MMP-2	0.84	mRNA	Cardiac Fibroblasts	Female Rat	24 h	(Mahmoodzadeh et al., 2010)
	2.72+	MMP-2	0.79	mRNA	Cardiac Fibroblasts	Male Rat	24 h	
	2.72+	MMP-2	0.56	Protein expression	Cardiac Fibroblasts	Rat	24 h	
	0.0272	MMP-9	1.42 (n.s.)	mRNA	Mesangial Cells	Mouse	24 h	

	0.272	MMP-9	1.7	mRNA	Mesangial Cells	Mouse	24 h	(Potier et al., 2001)
	2.72	MMP-9	1.77	mRNA	Mesangial Cells	Mouse	24 h	
	0.0272	MMP-9	1.08 (n.s.)	mRNA	Mesangial Cells	Mouse	72 h	
	0.272	MMP-9	1.21 (n.s.)	mRNA	Mesangial Cells	Mouse	72 h	
	2.72	MMP-9	1.34 (n.s.)	mRNA	Mesangial Cells	Mouse	72 h	
	0.0272	MMP-9	1.95	MMP activity	Mesangial Cells	Mouse	24 h	
	0.272	MMP-9	2.3	MMP activity	Mesangial Cells	Mouse	24 h	
	2.72	MMP-9	3.32	MMP activity	Mesangial Cells	Mouse	24 h	
Relaxin	1	proMMP-2	0.96 (n.s.)	Protein expression	Periodontal Ligament Fibroblasts	Human	48 h	(Henneman et al., 2008)
	10 +	proMMP-2	1 (n.s.)	Protein expression	Periodontal Ligament Fibroblasts	Human	48 h	
	25 +	proMMP-2	1.07 (n.s.)	Protein expression	Periodontal Ligament Fibroblasts	Human	48 h	
	50 +	proMMP-2	1.04 (n.s.)	Protein expression	Periodontal Ligament Fibroblasts	Human	48 h	
	100 +	proMMP-2	1.27 (n.s.)	Protein expression	Periodontal Ligament Fibroblasts	Human	48 h	
	250 +	proMMP-2	1.17 (n.s.)	Protein expression	Periodontal Ligament Fibroblasts	Human	48 h	
	500 +	proMMP-2	1.28 (n.s.)	Protein expression	Periodontal Ligament Fibroblasts	Human	48 h	
	1	MMP-2	1.37 (n.s.)	Protein expression	Periodontal Ligament Fibroblasts	Human	48 h	
	10 +	MMP-2	1.21 (n.s.)	Protein expression	Periodontal Ligament Fibroblasts	Human	48 h	
	25 +	MMP-2	1.44 (n.s.)	Protein expression	Periodontal Ligament Fibroblasts	Human	48 h	
	50 +	MMP-2	1.44 (n.s.)	Protein expression	Periodontal Ligament Fibroblasts	Human	48 h	
	100 +	MMP-2	1.72 (n.s.)	Protein expression	Periodontal Ligament Fibroblasts	Human	48 h	

	250 +	MMP-2	1.95	Protein expression	Periodontal Ligament Fibroblasts	Human	48 h	
	500 +	MMP-2	1.68 (n.s.)	Protein expression	Periodontal Ligament Fibroblasts	Human	48 h	
	0.01	MMP-1	1.55 (n.s.)	Protein expression	TMJ Fibrochondrocytes	Rabbit	24 h	(Kapila & Xie, 1998)
	0.1	MMP-1	2.4 (n.s.)	Protein expression	TMJ Fibrochondrocytes	Rabbit	24 h	
	1	MMP-1	3.51	Protein expression	TMJ Fibrochondrocytes	Rabbit	24 h	
	10 +	MMP-1	4.39	Protein expression	TMJ Fibrochondrocytes	Rabbit	24 h	
	100 +	MMP-1	3.34	Protein expression	TMJ Fibrochondrocytes	Rabbit	24 h	
	0.1	MMP-1	2.53	mRNA	TMJ Fibrochondrocytes	Rabbit	48 h	
	0.01	MMP-1	0.77 (n.s.)	Protein expression	TMJ Synoviocytes	Rabbit	24 h	
	0.1	MMP-1	0.73 (n.s.)	Protein expression	TMJ Synoviocytes	Rabbit	24 h	
	1	MMP-1	0.65 (n.s.)	Protein expression	TMJ Synoviocytes	Rabbit	24 h	
	10 +	MMP-1	0.64 (n.s.)	Protein expression	TMJ Synoviocytes	Rabbit	24 h	
	100 +	MMP-1	0.58 (n.s.)	Protein expression	TMJ Synoviocytes	Rabbit	24 h	
	0.1	MMP-13	1.49	mRNA	TMJ Disk Fibrochondrocytes	Mouse	48 h	(Kapila et al., 2009)
	0.1	MMP-9	1.83	mRNA	TMJ Disk Fibrochondrocytes	Mouse	48 h	
	0.1	MMP-13	1.8 to2.8	Protein expression	TMJ Disk Fibrochondrocytes	Mouse	48 h	(Ahmad et al., 2012)
	0.1	MMP-9	2 to 8	Protein expression	TMJ Disk Fibrochondrocytes	Mouse	48 h	
	0.1	MMP-1	1.58	MMP activity	TMJ Fibrocartilaginous Tissue	Rabbit	48 h	(Naqvi et al., 2005)

	0.5 mg/kg/d (~19 ng/mL serum)	proMMP-9	1 (n.s.)	Protein expression	Cardiac Fibroblasts	Rat	2 wk (in vivo)	(Lekgabe et al., 2005)
	0.5 mg/kg/d	proMMP-2	1.25	Protein expression	Cardiac Fibroblasts	Rat	2 wk (in vivo)	
	0.1	MMP-2	1.27	MMP activity	Renal Fibroblasts	Human	48 h	(Heeg et al., 2005)
	1	MMP-2	1.32	MMP activity	Renal Fibroblasts	Human	48 h	
	10 +	MMP-2	1.31	MMP activity	Renal Fibroblasts	Human	48 h	
	0.1	MMP-9	1.12 (n.s.)	MMP activity	Renal Fibroblasts	Human	48 h	
	1	MMP-9	1.17 (n.s.)	MMP activity	Renal Fibroblasts	Human	48 h	
	10 +	MMP-9	1.31 (n.s.)	MMP activity	Renal Fibroblasts	Human	48 h	
	10 +	MMP-1	1.55	MMP activity	Dermal Fibroblasts	Human	72 h	(Chow et al., 2012)
	10 +	MMP-2	1.81	MMP activity	Dermal Fibroblasts	Human	72 h	
	10 +	MMP-9	1.78	MMP activity	Dermal Fibroblasts	Human	72 h	
	10 +	MMP-13	1.96	MMP activity	Renal Myofibroblasts	Rat	72 h	
	10 +	MMP-2	2.3	MMP activity	Renal Myofibroblasts	Rat	72 h	
	10 +	MMP-9	2.61	MMP activity	Renal Myofibroblasts	Rat	72 h	
Progesterone	0.314 -	proMMP-13	1.39	Protein expression	Pelvic Fibroblasts	Human	48 h	(Zong et al., 2009)
	3.14	proMMP-13	1.46	Protein expression	Pelvic Fibroblasts	Human	48 h	
	31.4 +	proMMP-13	1.36	Protein expression	Pelvic Fibroblasts	Human	48 h	
	0.314 -	MMP-13	0.39	Protein expression	Pelvic Fibroblasts	Human	48 h	
	3.14	MMP-13	0.41	Protein expression	Pelvic Fibroblasts	Human	48 h	
	31.4 +	MMP-13	0.42	Protein expression	Pelvic Fibroblasts	Human	48 h	
	0.314 -	MMP-13	0.48	MMP activity	Pelvic Fibroblasts	Human	48 h	

	3.14	MMP-13	0.53	MMP activity	Pelvic Fibroblasts	Human	48 h	
	31.4 +	MMP-13	0.56	MMP activity	Pelvic Fibroblasts	Human	48 h	
	314	proMMP-9	0.39	mRNA levels	Cervical fibroblasts	Rabbit	24 h	(Imada et al., 1997)
	314 +	MMP-1	0.19	mRNA	Cervical fibroblasts	Rabbit	24 h	(Sato et al., 1991)
	0.0314 -	MMP-1	1.02 (n.s.)	MMP activity	Cervical fibroblasts	Rabbit	24 h	
	3.14	MMP-1	0.17	MMP activity	Cervical fibroblasts	Rabbit	24 h	
	314 +	MMP-1	0.21	MMP activity	Cervical fibroblasts	Rabbit	24 h	
	0.0314 -	proMMP-1	0.90 (n.s.)	Protein expression	Cervical fibroblasts	Rabbit	24 h	
	3.14	proMMP-1	0.44 (n.s.)	Protein expression	Cervical fibroblasts	Rabbit	24 h	
	314 +	proMMP-1	0.46	Protein expression	Cervical fibroblasts	Rabbit	24 h	
	10	MMP-13	0.4	mRNA	TMJ Disk Fibrochondrocytes	Mouse	48 h	(Kapila et al., 2009)
	10	MMP-9	1.15	mRNA	TMJ Disk Fibrochondrocytes	Mouse	48 h	
Estrogen + Relaxin	20 + 0.01	MMP-1	2.64 (n.s.)	Protein expression	TMJ Fibrochondrocytes	Rabbit	24 h	(Kapila & Xie, 1998)
	20 + 0.1	MMP-1	4.5	Protein expression	TMJ Fibrochondrocytes	Rabbit	24 h	
	20 + 1	MMP-1	4.26	Protein expression	TMJ Fibrochondrocytes	Rabbit	24 h	
	20 + 10 +	MMP-1	4.09	Protein expression	TMJ Fibrochondrocytes	Rabbit	24 h	
	20 + 100 +	MMP-1	3.64	Protein expression	TMJ Fibrochondrocytes	Rabbit	24 h	
	20 + 0.1	MMP-1	3.18	mRNA	TMJ Fibrochondrocytes	Rabbit	48 h	
	20 + 0.01	MMP-1	0.68 (n.s.)	Protein expression	TMJ Synoviocytes	Rabbit	24 h	
	20 + 0.1	MMP-1	0.62 (n.s.)	Protein expression	TMJ Synoviocytes	Rabbit	24 h	

	20 + 1	MMP-1	0.5 (n.s.)	Protein expression	TMJ Synoviocytes	Rabbit	24 h	
	20 + 10 +	MMP-1	0.46 (n.s.)	Protein expression	TMJ Synoviocytes	Rabbit	24 h	
	20 + 100 +	MMP-1	0.41 (n.s.)	Protein expression	TMJ Synoviocytes	Rabbit	24 h	
	20 + 0.1	MMP-1	1.64	MMP activity	TMJ Fibrocartilaginous Tissue	Rabbit	48 h	(Naqvi et al., 2005)
	0.1 + 0.1	MMP-13	2.14	mRNA	TMJ Disk Fibrochondrocytes	Mouse	48 h	(Kapila et al., 2009)
	0.1 + 0.1	MMP-9	2.53	mRNA	TMJ Disk Fibrochondrocytes	Mouse	48 h	
Estrogen + Progesterone	2.72 + 0.314	proMMP-13	1.52	Protein expression	Pelvic Fibroblasts	Human	48 h	(Zong et al., 2009)
	2.72 + 3.14	proMMP-13	1.38	Protein expression	Pelvic Fibroblasts	Human	48 h	
	2.72 + 31.4	proMMP-13	1.4	Protein expression	Pelvic Fibroblasts	Human	48 h	
	2.72 + 0.314	MMP-13	0.42	Protein expression	Pelvic Fibroblasts	Human	48 h	
	2.72 + 3.14	MMP-13	0.43	Protein expression	Pelvic Fibroblasts	Human	48 h	
	2.72 + 31.4	MMP-13	0.4	Protein expression	Pelvic Fibroblasts	Human	48 h	
	2.72 + 0.314	MMP-13	0.6	MMP activity	Pelvic Fibroblasts	Human	48 h	
	2.72 + 3.14	MMP-13	0.48	MMP activity	Pelvic Fibroblasts	Human	48 h	
	2.72 + 31.4	MMP-13	0.53	MMP activity	Pelvic Fibroblasts	Human	48 h	
	0.272 + 31.4	MMP-1	0.19	mRNA	Endometrial Tissue (Early/midsecretory)	Human	24 h	(Vassilev et al., 2005)
	0.272 + 31.5	MMP-1	0.049	mRNA	Endometrial Tissue (Late secretory)	Human	24 h	
	0.272 + 31.6	MMP-1	0.13	mRNA	Endometrial Tissue (Secretory)	Human	24 h	
	0.1 + 10	MMP-13	0.41	mRNA	TMJ Fibrochondrocytes	Mouse	48 h	(Kapila et al., 2009)
	0.1 + 10	MMP-9	1.15	mRNA	TMJ Fibrochondrocytes	Mouse	48 h	
Progesterone + Relaxin	10 + 0.1	MMP-13	0.66	mRNA	TMJ Disk Fibrochondrocytes	Mouse	48 h	

	10 + 0.1	MMP-9	1.21	mRNA	TMJ Disk Fibrochondrocytes	Mouse	48 h	(Kapila et al., 2009)

Appendix B: Supplementary information for chapter 3 (kinetic model)

B.1 Tables

Appendix Table B.1: Rate coefficients

Parameter	Notation	Value	Units	Sex	Citation
Platelet decay	$k_{d,P}$	0.69	hr^{-1}		(Nagaraja et al., 2014)*
M1 influx	$k_{M,in}$	400	mL^{-1}		(Nagaraja et al., 2014)*
M1/M2 clearance	k_{M1M2}	$8.30 * 10^{-3}$	hr^{-1}		(Cobbold & Sherratt, 2000)*
M1 to M2 rate	$k_{d,M}$	0.0833	hr^{-1}		Assumed
M1 production of IL-1β	$k_{IL1,M1}$	$1.23 * 10^{-6}$	$\frac{ng}{cell * hr}$	N.R.	(Byrne & Reen, 2002)*
M2 production of IL-1β	$k_{IL1,M2}$	$2.45 * 10^{-7}$	$\frac{ng}{cell * hr}$	N.R.	(Byrne & Reen, 2002)*
SF production of IL-1β	$k_{IL1,SF}$	$1.03 * 10^{-9}$	$\frac{ng}{cell * hr}$	M, F	(T. L. Huang et al., 2011)

IL-1β decay	$k_{d,IL1}$	13.9	hr^{-1}	M	(Klapproth et al., 1989)
M1 production of TNF-α	$k_{TNF,M1}$	$3.46 * 10^{-7}$	$\frac{ng}{cell * hr}$	N.R.	(Byrne & Reen, 2002)*
M2 production of TNF-α	$k_{TNF,M2}$	$4.29 * 10^{-8}$	$\frac{ng}{cell * hr}$	N.R.	(Byrne & Reen, 2002)*
SF production of TNF-α	$k_{TNF,SF}$	$2.58 * 10^{-9}$	$\frac{ng}{cell * hr}$	M, F	(T. L. Huang et al., 2011)
TNF-α decay	$k_{d,TNF}$	8.32	hr^{-1}	M, F	(Kaneda et al., 2004)
M1 production of IL-6	$k_{IL6,M1}$	$1.18 * 10^{-6}$	$\frac{ng}{cell * hr}$	N.R.	(Smythies et al., 2005)*
M2 production of IL-6	$k_{IL6,M2}$	$1.18 * 10^{-7}$	$\frac{ng}{cell * hr}$		(Nagaraja et al., 2014)*
SF production of IL-6	$k_{IL6,SF}$		$\frac{ng}{cell * hr}$	N.R.	(Inoue et al., 2001)
IL-6 decay	$k_{d,IL6}$	0.634	hr^{-1}	N.R.	(Wong, Schwartz, & Pestka, 2001)*

M1 production of IL-10	$k_{IL10,M1}$	$7.60 * 10^{-8}$	$\frac{ng}{cell * hr}$	N.R.	(Byrne & Reen, 2002)*
M2 production of IL-10	$k_{IL10,M2}$	$1.55 * 10^{-7}$	$\frac{ng}{cell * hr}$	N.R.	(Byrne & Reen, 2002)*
SF production of IL-10	$k_{IL10,SF}$	$3.06 * 10^{-10}$	$\frac{ng}{cell * hr}$	M, F	(T. L. Huang et al., 2011)
IL-10 decay	$k_{d,IL10}$	2.079	hr^{-1}		(Reynolds et al., 2006)
Platelet production of TGF-β	$k_{TGF,P}$	$1.25 * 10^{-8}$	$\frac{ng}{cell * hr}$	N.R.	(Grainger et al., 1995; Wakefield et al., 1988)*
M1 production of TGF-β	$k_{TGF,M1}$	$1.88 * 10^{-6}$	$\frac{ng}{cell * hr}$	N.R.	(Fadok et al., 1998)*
M2 production of TGF-β	$k_{TGF,M2}$	$1.60 * 10^{-8}$	$\frac{ng}{cell * hr}$	N.R.	(Fadok et al., 1998)*
SF production of TGF-β	$k_{TGF,SF}$	$3.15 * 10^{-8}$	$\frac{ng}{cell * hr}$	N.R.	(J. Li et al., 2011)
TGF-β decay	$k_{d,TGF}$	2.772	hr^{-1}	N.R.	(Tarrant, 2010)
M1 production of MMP-9	$k_{MMP9,M1}$	$6.77 * 10^{-6}$	$\frac{ng}{cell * hr}$	M, F	(Jager et al., 2016)

M2 production of MMP-9	$k_{MMP9,M2}$	$1.43 * 10^{-5}$	$\frac{ng}{cell * hr}$	M, F	(Jager et al., 2016)
MMP-9 decay	$k_{d,MMP9}$	0.099	hr^{-1}		(Saarialho-Kere, Welgus, & Parks, 1993)
M1 production of MMP-1	$k_{MMP1,M1}$	$2.00 * 10^{-8}$	$\frac{ng}{cell * hr}$	N.R.	(Serra, Al-Saidi, Angelov, & Nares, 2010)*
SF production of MMP-1	$k_{MMP1,SF}$	$7.24 * 10^{-8}$	$\frac{ng}{cell * hr}$	N.R.	(Cha et al., 2003)
MMP-1 decay	$k_{d,MMP1}$	0.0257	hr^{-1}	N.R.	(McCachren, Greer, & Niedel, 1989)
M1 production of TIMP-1	$k_{TIMP,M1}$	$3.89 * 10^{-7}$	$\frac{ng}{cell * hr}$	M, F	(Russell et al., 2002)
M2 production of TIMP-1	$k_{TIMP,M2}$	$2.59 * 10^{-7}$	$\frac{ng}{cell * hr}$	M, F	(Russell et al., 2002)
SF production of TIMP-1	$k_{TIMP,SF}$	$3.05 * 10^{-4}$	$\frac{ng}{cell * hr}$	F	(Asano et al., 2006)

TIMP-1 decay	$k_{d,TIMP}$	0.63	hr^{-1}	F	(Batra et al., 2012)
* Denotes parameters taken directly from (Nagaraja et al., 2014)					

Appendix Table B.2. Feedback functions and parameters

Effector	Affected substance	Equation	Notation	Value	Sex	Citation
IL-10 effect on	M1 TNF-α	$f_{IL10,TNF} = a * \exp(bC_{IL10}) + c$	$a_{IL10,TNF}$ $b_{IL10,TNF}$ $c_{IL10,TNF}$	0.467 −1.528 0.533	N.R.	(Thomassen et al., 1996)*
	M1 IL-1β	$f_{IL10,IL1} = a * \exp(bC_{IL10}) + c$	$a_{IL10,IL1}$ $b_{IL10,IL1}$ $c_{IL10,IL1}$	0.633 −1.794 0.367	N.R.	(Thomassen et al., 1996)*
	M1 IL-6	$f_{IL10,IL6} = a * \exp(bC_{IL10}) + c$	$a_{IL10,IL6}$ $b_{IL10,IL6}$ $c_{IL10,IL6}$	0.3298 −1.189 0.6695	N.R.	(Thomassen et al., 1996)*
	M1 MMP-9	$f_{IL10,MMP9} = \exp(aC_{IL10})$	$a_{IL10,MMP9}$	−0.0089	N.R.	(Kothari et al., 2014)
	M1 TIMP-1	$f_{IL10,TIMP} = \exp(aC_{IL10})$	$a_{IL10,TIMP}$	−0.0716	N.R.	(Jovanovic et al., 2001)
	M1/M2 transformation	$f_{M1M2} = \frac{a * C_{IL10}}{1 + a * C_{IL10}}$	a_{M1M2}	0.3213	N.R.	(Kuwata et al., 2003)
TGF-β effect on	M1 TNF-α	$f_{TGF,TNF} = a * \exp(bC_{TGF}) + c$	$a_{TGF,TNF}$ $b_{TGF,TNF}$ $c_{TGF,TNF}$	0.621 −0.831 0.447	N.R.	(Chantry et al., 1989)*
	M1 IL-1β	$f_{TGF,IL1} = a * \exp(bC_{TGF}) + c$	$a_{TGF,IL1}$ $b_{TGF,IL1}$	0.690 −20.37	N.R.	(Chantry et al., 1989)*

			$c_{TGF,IL1}$	0.310		
	M1 IL-10	$f_{TGF,IL10} = \frac{a * C_{TGF}}{1 + a * C_{TGF}}$	$a_{TGF,IL10}$	274.5	F	(Maeda et al., 1995)*
	M1 migration	$f_{TGF,M1} = r_{q1}C_{TGF}^2 + r_{q2}C_{TGF}$ $C_{TGF} \leq 1\ pg/mL$ $f_{TGF,M1} = r_{l1}C_{TGF} + r_{l2}$ $1\ pg/mL < C_{TGF} \leq 10\ pg/mL$	r_{q1} r_{q2} r_{l1} r_{l2}	-240.3 298.9 -0.593 60.59	N.R.	(Wahl et al., 1987)*
TNF-α effect on	M1 MMP-9	$f_{TNF,MMP9} = a * \frac{C_{TNF}}{1 + C_{TNF}}$	$a_{TNF,MMP9}$	1.531	N.R.	(Saren et al., 1996)
	M1 TIMP-1	$f_{TNF,TIMPa} = a * exp(bC_{TNF}) + c$	$a_{TNF,TIMPa}$ $b_{TNF,TIMPa}$ $c_{TNF,TIMPa}$	0.608 -3.683 0.392	N.R.	(Saren et al., 1996)
	SF MMP-1	$f_{TNF,MMP1} = a * \frac{C_{TNF}}{1 + C_{TNF}}$	$a_{TNF,MMP1}$	2.782	F	(Asano et al., 2006)
	SF TIMP-1	$f_{TNF,TIMPb} = a * \frac{C_{TNF}}{1 + C_{TNF}}$	$a_{TNF,TIMPb}$	0.586	F	(Asano et al., 2006)
	SF IL-1β	$f_{TNF,IL1} = a * \frac{C_{TNF}}{1 + C_{TNF}}$	$a_{TNF,IL1}$	3.078	F	(Ganesan et al., 2012)

	SF IL-6	$f_{TNF,IL6} = a * \frac{C_{TNF}}{1 + C_{TNF}}$	$a_{TNF,IL6}$	1.066	N.R.	(Mrosewski et al., 2014)
	SF TGF-β	$f_{TNF,TGF} = a * \frac{C_{TNF}}{1 + C_{TNF}}$	$a_{TNF,TGF}$	2.296	N.R.	(J. Li et al., 2011)
	M1 migration	$f_{TNF,M1} = r_1 C_{TNF}^2 + r_2 C_{TNF}$	r_1 r_2	-0.316 10.71	N.R.	(Pai et al., 1996)*
IL-1β effect on	M1 MMP-9	$f_{IL1,MMP9} = a * \frac{C_{IL1}}{1 + C_{IL1}}$	$a_{IL1,MMP9}$	4.325	N.R.	(Saren et al., 1996)
	M1 TIMP-1	$f_{IL1,TIMPa} = aexp(bC_{IL1}) + c$	$a_{IL1,TIMPa}$ $b_{IL1,TIMPa}$ $c_{IL1,TIMPa}$	0.610 -0.233 0.390	N.R.	(Saren et al., 1996)
	SF IL-6	$f_{IL1,IL6} = a * \frac{C_{IL1}}{1 + C_{IL1}}$	$a_{IL1,IL6}$	1.987	N.R.	(Inoue et al., 2001)
	SF MMP-1	$f_{IL1,MMP1} = a * \frac{C_{IL1}}{1 + C_{IL1}}$	$a_{IL1,MMP1}$	46.76	N.R.	(Yorifuji et al., 2016)
	SF TIMP-1	$f_{IL1,TIMPb} = a * \frac{C_{IL1}}{1 + C_{IL1}}$	$a_{IL1,TIMPb}$	0.237	M, F	(T. L. Huang et al., 2011)
	SF TNF-α	$f_{IL1,TNF} = a * \frac{C_{IL1}}{1 + C_{IL1}}$	$a_{IL1,TNF}$	2.903	M, F	(T. L. Huang et al., 2011)

	SF IL-1β	$f_{IL1,IL1} = a * \frac{C_{IL1}}{1 + C_{IL1}}$	$a_{IL1,IL1}$	10.11	M, F	(T. L. Huang et al., 2011)
IL-6 effect on	M1 IL-1β	$f_{IL6,IL1} = \frac{a * C_{IL6}}{a + C_{IL6}{}^{b}}$	$a_{IL6,IL1}$ $b_{IL6,IL1}$	4.459 0.1571	N.R.	(Schindler et al., 1990)*
	M1 TNF-α	$f_{IL6,TNF} = \frac{a * C_{IL6}}{a + C_{IL6}{}^{b}}$	$a_{IL6,TNF}$ $b_{IL6,TNF}$	4.488 0.1541	N.R.	(Schindler et al., 1990)*
	M1 IL-10	$f_{IL6,IL10} = \frac{a * C_{IL6}}{1 + a * C_{IL6}}$	$a_{IL6,IL10}$	0.1424	N.R.	(Kothari et al., 2014)
	SF TIMP-1	$f_{IL6,TIMP1} = a * \frac{C_{IL6}}{1 + C_{IL6}}$	$a_{IL6,TIMP1}$	0.2753	N.R.	(Silacci et al., 1998)
E effect on	M1 IL-1β	$f_{E2,IL1} = a * \frac{C_{E2}}{1 + C_{E2}}$	$a_{E2,IL1}$	5.337	F	(Calippe et al., 2010)
	M1 IL-6	$f_{E2,IL6} = \exp(a * C_{E2})$	$a_{E2,IL6}$	-0.0331	M	(L. Liu et al., 2014)
	M1 IL-10	$f_{E2,IL10} = \exp(a * C_{E2})$	$a_{E2,IL10}$	-0.139	N.R.	(D'Agostino et al., 1999)
T effect on	M1 TNF-α	$f_{T,TNF} = \exp(a * C_T)$	$a_{T,TNF}$	-0.0742	N.R.	(D'Agostino et al., 1999)
	M1 IL-10	$f_{T,IL10} = a * \frac{C_T}{1 + C_T}$	$a_{T,IL10}$	0.522	N.R.	(D'Agostino et al., 1999)

P effect on	M1 TNF-α	$f_{P,TNF} = \exp(a * C_P)$	$a_{P,TNF}$	-0.0478	N.R.	(Lei et al., 2014)
	M1 IL-6	$f_{P,IL6} = \exp(a * C_P)$	$a_{P,IL6}$	-0.1083		(Sun et al., 2012)
* Denotes parameters taken directly from (Nagaraja et al., 2014)						

Appendix Table B.3: Model sensitivity to progesterone	
Progesterone Concentration (ng/mL)	Peak TNF-a Concentration (pg/mL)
1.4	10.77
3.14	10.77
31.4	10.76
314	10.62
3140	9.29

Appendix Table B.4. Experimental Measurements of Synovial Fluid Concentrations of Cytokines, MMPs, and TIMP-1. The concentrations of substances in healthy knee joints are shown in **bold** type. These concentrations represent the physiological "initial conditions" prior to injury.

Substance	Average (pg/mL)	Error (pg/mL)	Condition	Number of Females / Total Participants	Citation
IL-1β	7.8	3.7	arthroscopy adolescent (<18 yo)	7 of 9	(Schmal et al., 2015)
	10.1	9.5	arthroscopy adult (>=18 yo)	11 of 40	
	15.3	6.9	acute acl tear	0 of 48	(Bigoni et al., 2013)
	24.9	7.5	acute acl tear + meniscal damage	0 of 48	
	15.6	9.8	early sub-acute acl tear	0 of 48	
	5.9	2.5	early sub-acute acl tear +meniscal damage	0 of 48	
	11	3.4	late sub-acute acl tear	0 of 48	

	13.1	7.3	late sub-acute acl tear +meniscus damage	0 of 48	
	14.2	10.8	chronic acl tear	0 of 48	
	9.5	3	chronic acl tear +meniscal damage	0 of 48	
	1.2	1.6	OA, pre-TKA	16 of 28	(Gandhi, Santone, Takahashi, Dessouki, & Mahomed, 2013)
	1	**2**	**healthy**	**n.r.**	(Tsuchida et al., 2014)
	15	18	cartilage defect	n.r.	
	8	16	OA	n.r.	
TNF-α	0.87	0.58	acute acl tear	0 of 48	(Bigoni et al., 2013)
	2.7	1.2	acute acl tear + meniscal damage	0 of 48	
	4.6	3.2	early sub-acute acl tear	0 of 48	

	5.6	1.7	early sub-acute acl tear +meniscal damage	0 of 48	
	3.1	1.3	late sub-acute acl tear	0 of 48	
	3	0.4	late sub-acute acl tear +meniscus damage	0 of 48	
	6.3	2.8	chronic acl tear	0 of 48	
	6.7	2	chronic acl tear +meniscal damage	0 of 48	
	2.7	1.2	OA, pre-TKA	16 of 28	(Gandhi et al., 2013)
	0	**0**	**healthy**	**n.r.**	(Tsuchida et al., 2014)
	2	8	cartilage defect	n.r.	
	4	20	OA	n.r.	
IL-10	29.14	1.8	acute acl tear	0 of 48	(Bigoni et al., 2013)
	28.3	3.4	acute acl tear + meniscal damage	0 of 48	

	36	21.9	early sub-acute acl tear	0 of 48	
	16.2	4	early sub-acute acl tear +meniscal damage	0 of 48	
	7.5	1.9	late sub-acute acl tear	0 of 48	
	10.8	1.7	late sub-acute acl tear +meniscus damage	0 of 48	
	3.3	3.3	chronic acl tear	0 of 48	
	5.5	2.8	chronic acl tear +meniscal damage	0 of 48	
	1	**6**	**healthy**	**n.r.**	(Tsuchida et al., 2014)
	0	0	cartilage defect	n.r.	
	9	35	OA	n.r.	
	0	0	TMD	24 of 31	(P. K. Fang, Ma, Ma, & Fu, 1999)
TGF-β	1970	530	healthy knee	6 of 12	

	2320	320	TKA	17 of 28	(Regan, Bowler, & Crapo, 2008)
	100.4	109.3	TMD	24 of 31	(P. K. Fang et al., 1999)
	0	0	Healthy TMJ	4 of 7	
IL-6	576.6	166.4	acute acl tear + meniscal damage	0 of 48	(Bigoni et al., 2013)
	504.4	247.8	early sub-acute acl tear	0 of 48	
	388.3	110.8	early sub-acute acl tear +meniscal damage	0 of 48	
	24.1	8.0	late sub-acute acl tear	0 of 48	
	298.1	141.1	late sub-acute acl tear +meniscus damage	0 of 48	
	193.4	110.7	chronic acl tear	0 of 48	
	114.9	72.5	OA, pre-TKA	16 of 28	(Gandhi et al., 2013)
	64	**120**	**healthy**	**n.r**	

	261	385	cartilage defect	n.r.	(Tsuchida et al., 2014)
	396	508	OA	n.r.	
	88.8	32.3	healthy knee	6 of 12	(Regan et al., 2008)
	281.2	48.3	TKA	17 of 28	
	38.2	115.9	< 6 mo. post ACL	29 of 67	(Tourville, Poynter, DeSarno, Struglics, & Beynnon, 2015)
MMP-9	110	220.1	OA, pre-TKA	16 of 28	(Gandhi et al., 2013)
	6520	n.r.	injured ankle	14 of 45	(Haller et al., 2015)
	960	n.r.	un-injured ankle	14 of 45	
	609	290	OA	n.r.	(Kim et al., 2011)
	9511	**n.r.**	**healthy**	**11 of 25**	(Heard et al., 2012)
	11007	n.r.	early OA	1 of 12	
	53391	n.r.	OA	9 of 17	
	0	0	< 6 mo. post ACL	29 of 67	(Tourville et al., 2015)
MMP-1	3890	n.r.	injured ankle	14 of 45	

	370	n.r.	un-injured ankle	14 of 45	(Haller et al., 2015)
	549200	273100	OA	n.r.	(Kim et al., 2011)
	3729	**n.r.**	**healthy**	**11 of 25**	(Heard et al., 2012)
	8982	n.r.	early OA	1 of 12	
	53563	n.r.	OA	9 of 17	
	4928	6112	< 6mo. post ACL	29 of 67	(Tourville et al., 2015)
TIMP-1	**123925**	**n.r.**	**healthy**	**11 of 25**	(Heard et al., 2012)
	115567	n.r.	early OA	1 of 12	
	707562	n.r.	OA	9 of 17	
	1841461	9405495	< 6 mo. post ACL	29 of 67	(Tourville et al., 2015)

B.2 Figure

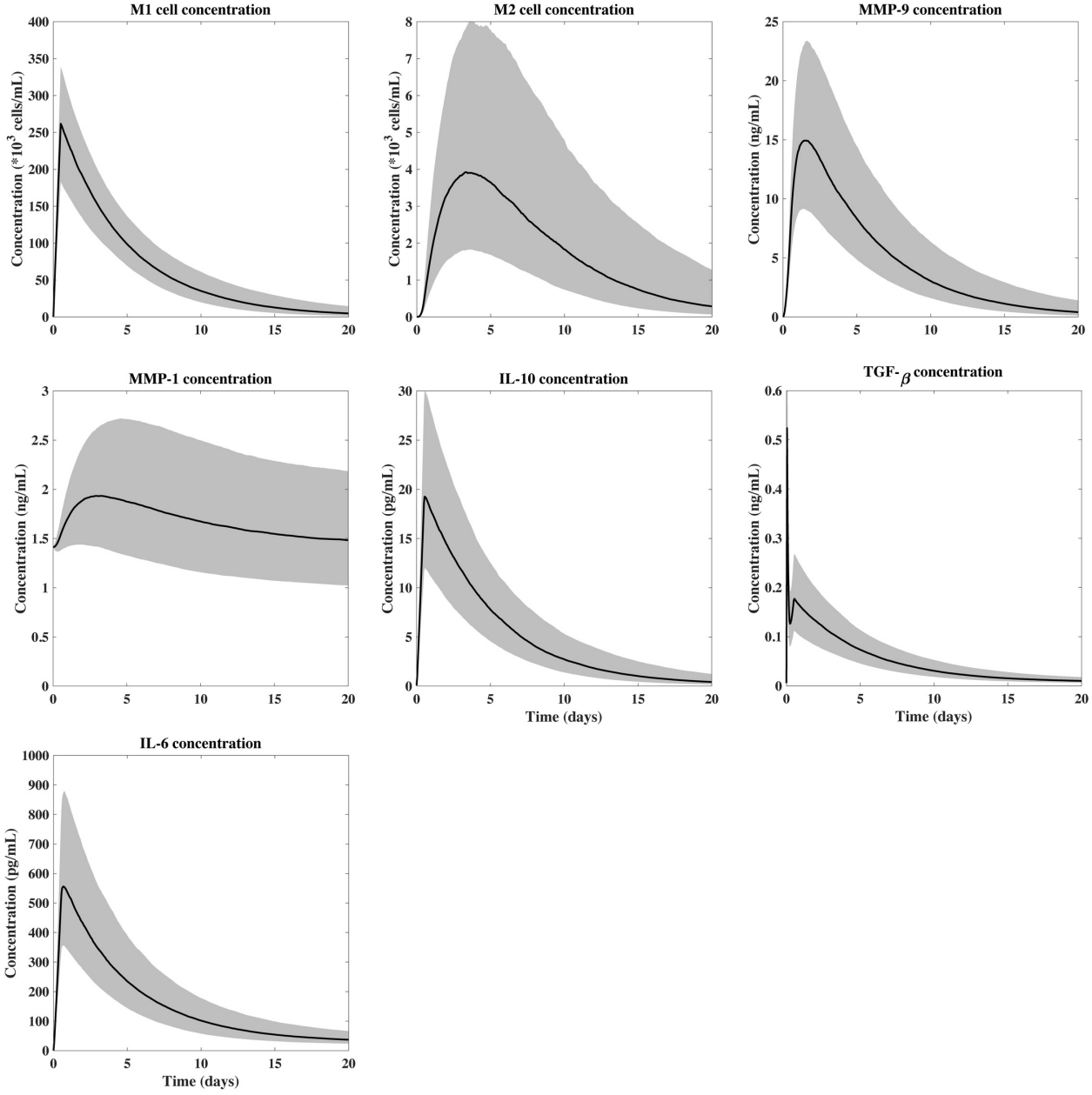

Appendix Figure B.1: Time evolution of concentration with error bands for M1, M2, TGF-β, IL-6 MMP-1, MMP-9, and TIMP-1 (median ± IQR). Confidence bands were generated by varying the parameters with

Latin hypercube sampling. All responses are in reasonable agreement with experimentally measured concentrations in the synovial fluid (see Appendix Table B.4, experimental values for each of these substances in the synovium).

B.3 Sample calculations

This procedure has been reported previously (Nagaraja et al., 2014).

Production coefficient estimation

- Coefficient of interest: TNF-a production by SFs
- Citation: Huang et al. 2011 (T. L. Huang et al., 2011)
- Table in citation: Table 3 (TNF-a for non-induced SFs)

$$C_{TNF} = 9.3\ \frac{pg}{mL}$$

$$C_{SF} = \ 3 \times 10^5\ \frac{cells}{well}$$

Assuming a volume of 2 mL per well in a six well plate,

$$C_{SF} = \ 1.5 \times 10^5\ \frac{cells}{mL}$$

$$t = 24\ h$$

$$k_{TGF,SF} = \frac{C_{TGF}}{C_{SF}t}$$

$$k_{TGF,SF} = \frac{0.0093\ \frac{ng}{mL}}{1.5 \times 10^5\ \frac{cells}{mL} * 24\ h}$$

$$\boldsymbol{k_{TGF,SF} = 2.58 \times 10^{-9}\ \frac{ng}{cell * h}}$$

We note that we had to make two assumptions here. First, we had to assume the volume for a six-well culture plate, which is typically between 1 mL and 2 mL. Second, we assumed that the SFs had not already assumed a pro-inflammatory phenotype (i.e., they were "non-induced"). However, we argue that such assumptions are justified because of our Latin Hypercube Sampling analysis, which varies all estimated parameters around their estimated values to account for the variability that arises from assumptions like these.

Degradation coefficient estimation

- Coefficient of interest: TNF-a degradation
- Citation: Kaneda et al. 2004 (Kaneda et al., 2004)
- Table in citation: Table 2 (TNF-a half-life)

$$t_{1/2} = 5\ min = 0.0833\ h$$

$$k_{d,TNF} = \frac{0.693}{t_{1/2}}$$

$$k_{d,TNF} = \frac{0.693}{0.0833\ h}$$

$$\boldsymbol{k_{d,TNF} = 8.32\ h^{-1}}$$

Up-regulation feedback parameter estimation

- Function of interest: TNF-a up-regulation of MMP-9 production by M1
- Citation: Saren et al. 1996 (Saren et al., 1996)
- Figure in citation: Figure 2
- Data points: (obtained from Saren et al. Fig. 2 using PlotDigitizer © 2000-2015, Joseph A. Huwaldt)

TNF-a (ng/mL)	MMP-9 (ug/ug DNA)	Normalized MMP-9
0	1.218	0
20	2.747	1.255
40	3.153	1.589

- Normalization of MMP-9 concentrations:

$$\{C_{MMP9,N}\} = \frac{\{C_{MMP9}\} - C_{MMP9,min}}{C_{MMP9,min}}$$

where $\{C_{MMP9,N}\}$ is the normalized vector of MMP-9 concentrations, $\{C_{MMP9}\}$ is the vector of un-normalized MMP-9 concentrations, and $C_{MMP9,min}$ is the smallest value in the un-normalized vector.

- General form of the up-regulation function

$$a * \frac{C_{TNF}}{1 + C_{TNF}}$$

- In the MATLAB curve fitting toolbox, use the vector of TNF-a concentrations as the X-data and the normalized MMP-9 vector as the Y-data. Next, change the fit type from Polynomial to Custom using the dropdown menu. Enter the general form of the equation in the textbox:

$$a * x/(1 + x)$$

- In the results box the value of *a* will be listed under coefficients. In this case, *a = 1.531*

Down-regulation feedback function parameter estimation

- Function of interest: TNF-a down-regulation of TIMP-1 production by M1
- Citation: Saren et al. 1996 (Saren et al., 1996)
- Figure in citation: Figure 7 (Data for LPS treatment alone with data for combined LPS+TNF-a treatment)
- Data points: (obtained from Saren et al. Fig. 7 using PlotDigitizer © 2000-2015, Joseph A. Huwaldt)

TNF-a (ng/mL)	TIMP-1 (ug/ug DNA)	Normalized TIMP-1
0 (LPS only)	0.181	1.00
2	0.071	0.392
20	0.071	0.392
40	0.071	0.392

- Normalization of TIMP-1 concentrations:

$$\{C_{TIMP1,N}\} = \frac{\{C_{TIMP1}\}}{C_{TIMP1,max}}$$

where $\{C_{TIMP1,N}\}$ is the normalized vector of TIMP-1 concentrations, $\{C_{TIMP1}\}$ is the vector of un-normalized TIMP-1 concentrations, and $C_{TIMP1,max}$ is the largest value in the un-normalized vector.

- General form of the down-regulation function

$$a * \exp(b * C_{TNF}) + c$$

- In the MATLAB curve fitting toolbox, use the vector of TNF-a as the X-data and use the normalized TIMP-1 vector as the Y-data. Next change the fit type from Polynomial to Custom using the dropdown menu. Enter the general form of the equation:

$$a * \exp(-b * x) + c$$

In the results box the value of *a* will be listed under coefficients. In this case, *a = 0.608, b = 3.721, c = 0.392*. Note that the fitted value for *b* can vary slightly. The value listed in Supplementary Table 2 is 3.683, while here it is 3.721. However, these small variations, in general, have very little effect on the model output.

B.4 Correction of hormonal concentrations

In order to calculate hormonal effects, we had to account for the differences in experimental techniques, some of which measured total hormonal concentrations in serum (Calippe et al., 2010; Greenspan & Gardner, 2004), and some of which reported free hormone concentrations (D'Agostino et al.,

1999; Lei et al., 2014). This distinction is important because free hormones only comprise 2% of the total serum concentration of hormones, and the other 98% are bound to sex hormone binding globulin, and are not capable of acting on cellular targets (Greenspan & Gardner, 2004) including cells in the synovium. Before calculating the parameters for the hormonal feedback functions, we determined what the corresponding total serum concentration would be for all experiments that reported free hormone concentration (including in vitro hormone experiments), according to the expression:

$$H_{free} = 0.02 * H_{total}$$

where H_{free} is the concentration of free hormone in the system and H_{total} is the total concentration (free + protein bound).

Appendix C: Supplementary information for chapter 4 (Monte Carlo and Molecular Dynamics models)

C.1 Appendix tables

Appendix Table C.1: Molecular Dynamics model parameters.

Model parameters	Value
ε – Lennard Jones [Kcal/mol]	6.87
σ – Lennard Jones [Å]	14.72
θ_0 – Equilibrium bending angle [degrees]	180
k_θ – Bending strength constant [Kcal/mol rad]	14.98
r_0 – Equilibrium distance (tropocollagen) [Å]	14.00
r_1 – Critical hypereslastic distance (tropocollagen) [Å]	18.20
r_{break} – Bond breaking distance (tropocollagen) [Å]	21.00
k_{T0} – Stretching strength constant (tropocollagen) [Å]	17.13
k_{T1}– Stretching strength constant (tropocollagen) [Å]	97.66
r_0 – Equilibrium distance (divalent crosslink) [Å]	10.00
r_1 – Critical hypereslastic distance (divalent crosslink) [Å]	12.00
r_{break} – Bond breaking distance (divalent crosslink) [Å]	14.68

k_{T0} – Stretching strength constant (divalent crosslink) [Å]	0.20
k_{T1} – Stretching strength constant (divalent crosslink) [Å]	41.84
r_0 – Equilibrium distance (trivalent crosslink) [Å]	8.60
r_1 – Critical hypereslastic distance (trivalent crosslink) [Å]	12.20
r_{break} – Bond breaking distance (trivalent crosslink) [Å]	14.89
k_{T0} – Stretching strength constant (trivalent crosslink) [Å]	0.20
k_{T1} – Stretching strength constant (trivalent crosslink) [Å]	54.60
m – mass tropocollagen beads [a.m.u]	1358.7

Appendix Table C.2: Number of cleaved (but not removed) bonds at 1.1% degradation.

	Number of Collagenases	Number of Gelatinases	Cleaved Sites
System 1	4	4	700
System 2	8	8	710
System 3	6	2	999
System 4	2	6	431

C.2 Appendix figures

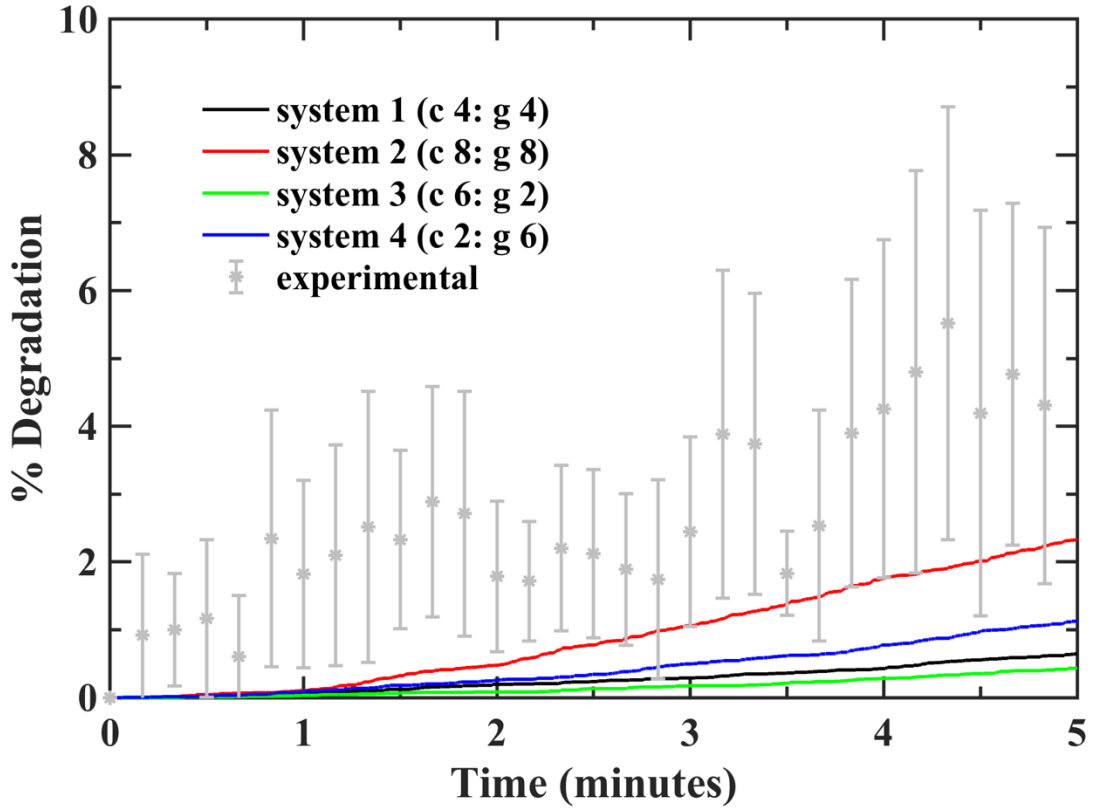

Appendix Figure C.1: Degradation of collagen fibril by collagenases and gelatinases as a function of time for different collagenase to gelatinase ratios.

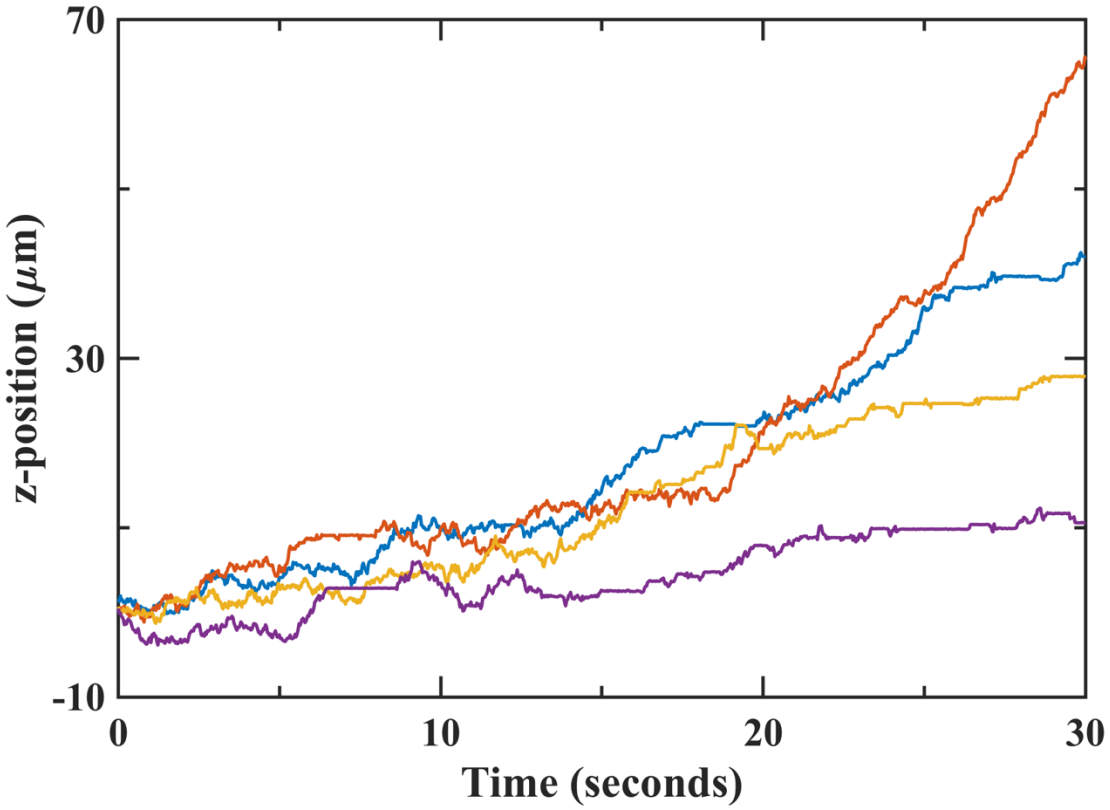

Appendix Figure C.2: Trajectories for Collagenases Moving Along the Long Axis of the Collagen Fibril for a System with 10 Collagenases and No Gelatinases. Each curve represents the path of one of the five collagenases, showing the directional motion observed in our simulations. Though we did not include a bias toward directional motion *a priori*, we observed an emergent directional motion of collagenases from the C-terminus toward the N-terminus for all of the systems under investigation. z = 0 corresponds to the C-terminus of the fibril.

C.3 Additional details for Monte-Carlo model formulation

C.3.1 Coarse-grained geometry

A coarse-grained lattice model was used to represent the structural hierarchy of collagen, which has been well characterized (Cowin & Doty, 2007). Detailed models of the collagen fibril structure have been reported (Charvolin & Sadoc, 2012; Orgel, Irving, Miller, & Wess, 2006), but we chose to use a simplified representation (Figure 4.1) to reduce computational cost and facilitate the study of aggregate degradation of the fibril. Each lattice site represents a segment of collagen with a length of 14 nm and a diameter of 1.5nm. Although each site represents a volume of collagen, a lattice site, or unit, is algorithmically described as a single (x, y, z) coordinate in the center of the volume.

The (x, y, z) coordinates of each lattice site are described by the following expressions:

$$z = (i-1)z^* + 25(j-1)z^* + 5(h-1), \quad \begin{cases} 1 \le i \le 22 \\ 1 \le j \le 5 \\ 1 \le h \le 5 \end{cases} \tag{1}$$

$$y = b\,[\sin(72°(h-1)) + \sin(r(n,q)°)] + B_{mf} n \sin(60°), \quad -(m-1) \le n \le m-1 \tag{2}$$

$$x = b\,[\cos(72°(h-1)) + \cos(r(n,q)°)] + B_{mf} q(n) \tag{3}$$

$$-[m - 0.5 * (|n|+1)] \le q(n) \le [m - 0.5 * (|n|+1)]$$

where i, j, and h are integers representing the vertical position of a lattice site within a single tropocollagen molecule, the vertical position of a tropocollagen within a microfibril, and the cross-sectional position of a tropocollagen within the microfibril, respectively. The integers n and q(n) describe the cross-sectional

positioning of a given microfibril within the fibril, specifying the row (n) and the position within row n (q(n)). The height of a single lattice site, 14 nm, was denoted as z*, and the diameters of tropocollagen molecules (1.5nm) and microfibrils (3.5nm) were denoted as b and Bmf, respectively. The random angle, r(n, q), rotates each microfibril about its long axis. A schematic of the fibril (without the random rotation of microfibrils) is depicted in Figure 4.1, illustrating the indices and measurements found in Eq. 1-3.

C.3.2 Initial MMP Placement

During the initial placement, enzymes were randomly selected and placed on empty lattice sites using random selection of position indices within a microfibril (defined in Eqs. 1-3)

$$\{i \mid 1 \leq i \leq 22\}$$
$$\{j \mid 1 \leq j \leq 5\} \qquad (4)$$
$$\{h \mid 1 \leq h \leq 5\}.$$

Next, to ensure that the enzymes were placed on the outer edge, the n and q(n) indices were randomly selected such that the selected microfibril had fewer than six nearest neighbors:

$$\{(n, q(n)) \mid NN(n, q(n)) < 6\} \qquad (5)$$

where NN(n,q(n)) is the number of nearest neighbors of the selected microfibril. A nearest neighbor microfibril was defined as any microfibril whose center in the xy-plane was a distance of B_{mf} away from the center of the selected microfibril and whose cross-section contained at least two tropocollagen lattice sites at the selected z-position. Once the enzymes were placed on the surface, a fixed number of them remained

on the fibril throughout the degradation simulations for the sake of computational simplicity, even though Watanabe-Nakayama et al. (Watanabe-Nakayama et al., 2016) showed collagenases adsorb and desorb on the surface of the fibril.

C.3.3 Further details of the dynamic Metropolis Monte Carlo algorithm

A dynamic Metropolis Monte Carlo approach, depicted in Figure 4.1, was used to simulate the interactions between the MMPs and the collagen to capture the stochastic, time-dependent nature of the collagen degradation process.

For each step of the simulation, an enzyme was randomly selected from the ensemble of collagenases and gelatinases, and the selected enzyme attempted to move vertically or horizontally or attempted to cleave. The movement attempts were accepted based on the Boltzmann factor of the change in energy between one lattice site and the next, defined as:

$$p = e^{\frac{-(E_s - E_{s-1})}{kT}} \qquad (6)$$

where p is the acceptance probability, E_s is the interaction energy between the enzyme and the lattice site it occupies on step s, and E_{s-1} is the interaction energy at the previous position.

The stepwise positions of the MMPs were dictated by the equation

$$f_s = f_{s-1} + g, \qquad (7)$$

for step s of the selected enzyme where f = i and g = ±1 for vertical displacement. For vertical motion, g was chosen using a random number generator that selected values on the uniform interval [0,1). A random

number in the range [0,0.5) led to a negative vertical displacement (g=-1), and a random number in the range [0.5,1) resulted in a positive vertical displacement (g=1). For horizontal motion, Eq. 7 is a vector equation where f = (n, q) and g is a two-element vector in which each element is a randomly selected integer on the interval [-1, 1]. Horizontal displacements were subject to the constraint that the selected microfibril was on the outermost edge of the fibril, as described by Eq. 5. Vertical movements were much more probable than horizontal movements, which occurred at the experimentally reported rate of 0.05 s^{-1} (Sarkar et al., 2012).

In some instances, a vertical step would cause an enzyme to step into a gap between tropocollagen molecules due to their vertical spacing within microfibrils. For this special case, the enzyme would move to another tropocollagen molecule within the current microfibril where

$$z_s = z_{s-1} + g * z^* \qquad (8)$$

where z_s is the newly selected z-position (according to Eq. 1) and z_{s-1} is the previous z-position for the selected enzyme. Due to the shift to the new tropocollagen, i, j, and h for step s will not be the same as they were in step s-1 and must be updated accordingly. If no neighbors were available in the current microfibril at z_s, the enzyme would move to the nearest unoccupied lattice site at the new z-position.

The probabilities of displacement attempts were selected such that the enzymes would move with the diffusion coefficients reported in the literature. Collier et al. (2011) summarized the reported diffusion coefficients for collagenases and gelatinases on collagen and gelatin, highlighting the fact that the diffusion of the enzymes depends on whether or not the substrate is intact or cleaved (Collier et al., 2011). These experimental diffusion coefficients are summarized in Table 4.1. Because the diffusion coefficients for collagenase and gelatinase are not equal, the duration required for each displacement was selected such that each enzyme type would diffuse with its experimentally reported diffusion coefficient according to the relationship:

$$\langle r(x,y,z)^2 \rangle = 4Dt, \qquad (9)$$

where r is the displacement, x, y, and z are the coordinates of the enzyme found with Eq. 1-3, D is the diffusion coefficient, and t is duration of the step. The two-dimensional formulation of this equation was chosen because the enzymes are constrained to diffuse on the surface of the fibril.

C.3.4 MMP cleavage properties

Patterns of collagenase and gelatinase cleavage have been described previously (Rosenblum et al., 2010; Sarkar et al., 2012), and the model presented here was parameterized to mimic experimental observations. Collagenase cleavage only occurred when collagenases were positioned on the lattice site 66 nm from the C-terminus of an individual tropocollagen (i=4), and gelatinase cleavage only occurred when gelatinases were positioned on a tropocollagen that had already been cleaved by a collagenase (Fields, 2013; Rosenblum et al., 2010). When the enzymes were in the positions where cleavage could occur, cleavage succeeded at an overall rate of 0.35 s^{-1} (Sarkar et al., 2012). When cleavage occurred, a bond was broken between the N terminus of the occupied site and the C terminus of the site directly above the occupied site.

C.3.5 Collagen fragment removal

Once a lattice site and its lower neighbor had been cleaved, that site became disconnected from the rest of the lattice and was removed from the system immediately, unless otherwise specified. The removal probabilities were defined as

$$\mathrm{P(remove)} = \begin{cases} \mathrm{a}, & \mathrm{i},\ \mathrm{i}+1 \text{ cleaved} \\ \mathrm{a}, & \mathrm{i}=22, \mathrm{i}-1 \text{ cleaved} \\ \mathrm{a}, & \mathrm{i}=1, \mathrm{i} \text{ cleaved} \\ 0, & \text{otherwise} \end{cases} \qquad (10)$$

where a=1, except where otherwise specified.

Occasionally, a removed fragment was occupied by a gelatinase, which remained in its vertical position and was moved horizontally to an adjacent microfibril or the nearest available lattice site if no available sites existed on adjacent microfibrils.

As the removal progressed, some groups of lattice sites became detached from neighboring lattice sites and were removed from the system. A set of lattice sites was considered detached when it had no vertical neighbors, and when it was not attached to at least two other segments horizontally.

C.4 Molecular Dynamics parameters

For the Molecular Dynamics simulations we used the parameters presented in Appendix Table C.1.

Coarse-grained Molecular Dynamics model: We implemented a collagen type I coarse grained, the parameters for the interaction potentials are given in Table 4.1. Tropocollagen is represented by a polymeric chain that contains 220 bonded beads units. Tropocollagen chains interact through a Lennard-Jones potential acting as the cohesive and repulsive force that keep the fibril together and prevent the interpenetration of beads, respectively. The potential is represented by the standard equation:

$$\mathrm{U_{LJ}} = 4\epsilon\left[\left(\frac{\sigma}{\mathrm{r}_{LJ}}\right)^{12} - \left(\frac{\sigma}{\mathrm{r}_{LJ}}\right)^{6}\right] \qquad (11)$$

Where U_{LJ} is the potential energy due to the interaction between two tropocollagen beads i and j, r_{LJ} distance apart. The parameter ε represents the strength of the potential and σ is related to the position of the minimum in potential energy.

The bending angle between beads is controlled by a harmonic potential with the following equation:

$$U_\theta = k_\theta(\theta - \theta_0)^2 \qquad (12)$$

Where U_θ is the potential energy of the bending angle between three consecutively bonded tropocollagen beads i, j and k forming an angle θ. The parameter k_θ represent the bending strength in energy units and θ_0 is the equilibrium angle.

The hyper-elastic bond (stretching) between tropocollagen beads is represented by 3-regime potential energy with a gradient defined by:

$$F_{bond} = \frac{\partial U_{bond}}{\partial r} = \begin{cases} k_{T0}(r - r_0) & if \quad r < r_1 \\ k_{T1}(r - r_0) & if \quad r_1 \le r < r_{break} \\ 0 & if \quad r > r_{break} \end{cases} \qquad (13)$$

Where r_0 is the equilibrium distance between the two beads, k_{T0} and k_{T1} are the spring constants acting at different distances between 0 to r_1 and r_1 to r_{break}, respectively. Note that the gradient of the potential energy represents the force of interactions between two given beads.

Simulation parameters: All the simulations were performed used LAMMPS molecular dynamics simulation package. The time step is 0.01 ps and the equations of motion are integrated with a Langevin thermostat that account for the implicit representation of water. The drag coefficient is 1000 ps and the temperature is 310K. A maximum velocity constraint is imposed to observe the breakage of the fibril without the collapse of the structure. The strains were applied in the axial direction with periodic boundary conditions. The strain rate used in these simulations was 10^7 s-1. This strain rate represents a speed of 3.4

m/s for the dimensions of our fibril. Due to computational constraints the loading speed used in the current model was faster than strain rates employed in experimental paradigms.

C.5 Supplemental results: degradation rate

The fibril degradation rate was dictated by the total number of enzymes on the fibril, as well as the ratio of collagenases to gelatinases. By comparing the progression of degradation for 4 collagenases and 4 gelatinases (system 1) and 8 collagenases and 8 gelatinases (system 2), we see in Figure 4.2 that the degradation progresses more rapidly when the number of MMPs is larger (system 2), as expected. However, when we compare systems with the same total number of enzymes (system 1, 3 and 4) we observe that the total amount of enzymes does not fully explain the rate of degradation. Rather, the ratio of collagenases to gelatinases appears to be the main contributor in the difference between systems. The rate of degradation increases as the ratio of collagenases to gelatinases decrease, this behavior is clearly observed in Appendix Figure C.1 systems 1, 3 and 4.

Appendix Figure C.1 also demonstrates semi-quantitative agreement between simulation results and experimental results for degradation, showing the mean $\pm$ s.d. for experimental measurements of degradation by Watanabe-Nakayama et al. (Watanabe-Nakayama et al., 2016) along with the simulated results for the present study. However, notable differences between the experimental and simulated systems preclude a direct comparison of the degradation. First, the simulated results are for the combined action of fibroblast collagenase and gelatinase, while the experimental data are for degradation by bacterial collagenase, which has both collagenolytic and gelatinolytic action; the mechanism of degradation differs between experiments and simulations. Furthermore, the experimental results were obtained by varying the concentration of enzymes in the solution, while the simulations in the present work were obtained by varying the number of enzymes on the surface of the fibril, again precluding a direct comparison of our

simulation results to the experimental results. For a discussion of the difficulties associated with quantifying the relationship between concentration of enzymes in solution and surface coverage of enzymes on the fibril, refer to the discussion section in the main text. Nevertheless, despite the differences between the experimental conditions and the conditions of our simulations, degradation in our simulations appears to progress in a manner consistent with the experimental observations.

Also, of note, System 2, with the larger number of MMPs, has a two-slope degradation behavior, with a first slow slope before 1 minute. This first slope is similar in value to the other systems, nevertheless the excess in enzymes seem to trigger an acceleration of the fibril degradation after 1 minute. Further analysis of this behavior will be necessary in future, though such analysis is beyond the scope of the present investigation.

Appendix Figure C.2 shows directional motion of collagenase toward the N-terminus of the fibril, an emergent property of our simulations that provides further semi-quantitative verification of our degradation model. This directional motion has been observed experimentally in a number of different systems, though some disagreement exists about the direction of the motion along the fibril (Saffarian et al., 2004; Sarkar et al., 2012; Watanabe-Nakayama et al., 2016). Sarkar et al. (2012) and Saffarian et al. (2004) observed directional of MMP-1 along a line pointing from the N-terminus to the C-terminus, while Watanabe-Nakayama et al. (2016) observed motion along a line pointing from the C-terminus to the N-terminus. In the present work, the directional motion was in agreement with the latter with collagenases moving from the C-terminus toward the N-terminus. Furthermore, Saffarian et al. (2004) reported a flow velocity on the order of micrometers per second for MMP-1, which appears to agree semi-quantitatively with our simulation results presented in Appendix Figure C.2 (Saffarian et al., 2004).

Appendix D: Toward model validation

Abstract

Computational approaches have provided a means to study fibril mechanics after degradation by MMPs, but the computational models have not yet been experimentally validated. In this appendix, we present pilot data for validation experiments that measure the collagen mechanical response after treatment of collagen with different ratios of collagenase to gelatinase using AFM imaging and indentation techniques. The experimental results described herein are inconclusive and incomplete, precluding our comparison of experimental results to our simulated predictions. However, this work lays the groundwork for future experiments that can be used to validate the models. Future work should consider improved ways to isolate collagen, develop techniques for monitoring degradation during MMP treatment, and allow adequate time to master experimental approaches.

*Note: This work was performed in collaboration with Franklyn Obi, who aided in the collection of experimental data.

D.1 Introduction

In this work, we leverage existing experimental techniques to study collagen mechanical properties as a step toward validating model predictions and toward a cohesive understanding of the processes that underlie pathologies of cartilage. We present pilot data for validation experiments that measure the collagen mechanical response after treatment of collagen with different ratios of collagenase to gelatinase using AFM imaging and indentation techniques. While we were unable to overcome numerous technical challenges and our present results are inconclusive, this work describes the process and pitfalls of our experimental approach and may be used by future researchers to formulate improved experimental validation approaches.

* Note: Franklyn Obi assisted with the execution of experiments, including collagen isolation, MMP activation and treatment, imaging with AFM, and indentation tests with AFM.

D.2 Materials and methods

D.2.1 Materials

Lyophilized MMP-1 and MMP-9 from Sigma. Trypsin to a final concentration of 10 ug/mL from Fisher Scientific, trypsin neutralizing solution (TNS 0.05% trypsin, 0.01% BSA) from Promocell GmbH. EDTA from Promega to a concentration of 20 mM. TNC buffer: 0.05 M tris-HCl, pH 7.5 with 0.01 M $CaCl_2$ and 0.15 M NaCl (Watanabe-Nakayama et al., 2016; Welgus et al., 1980). Tris-HCl, $CaCl_2$, and NaCl were obtained from Fisher Scientific.

D.2.2 Collagen extraction

Patellar tendons and medial collateral ligaments were obtained from OVX rats that were sacrificed for an unrelated experiment, and mechanical fibril extraction was performed according to the method of Wenger et al. 2007 (Wenger, Bozec, Horton, & Mesquida, 2007). Briefly, the tissue was mechanically separated into smaller sections. For each treatment condition, a small section of the tissue was placed on a mica surface and smeared along the surface to expose individual fibrils. The specimens were allowed to dry in air for at least 1 hour before treatment with MMPs.

D.2.3 MMP activation

MMPs were activated as previously described (Grant, Eisen, Marmer, Roswit, & Goldberg, 1987; Yasunori Okada et al., 1992). Lyophilized MMPs were reconstituted in TNC and diluted. Trypsin was

added to a final concentration of 10 ug/mL to activate the enzymes. For MMP-1, the activation reaction was performed at 25 deg. C for 20 minutes (Grant et al., 1987), and MMP-9 activation was performed at 37 deg. C for 2 hours (Yasunori Okada et al., 1992). The activation reaction was terminated by trypsin neutralizing solution.

D.2.4 MMP treatments

Activated MMP-1 and MMP-9 were added to the prepared collagen fibrils at the concentrations listed in tables D.1 and D.2. Samples were then heated to 37 deg. C to allow degradation to occur. After 20 minutes, the degradation reaction was terminated with EDTA to a final concentration of 20 mM. Excess liquid was then removed from the specimens using a pipette and the specimens were allowed to dry in air for at least 24 hours before further analysis.

D.2.5 AFM

AFM measurements were performed using an ICON atomic force microscope (Bruker). All measurements were taken at room temperature using a silicon probe with a nominal tip diameter of 7 nm and a standard (steep) tip geometry. Imaging and indentation were performed in tapping mode in air. Contact stiffness was calculated from the unloading portion of the force-displacement curves measured during the indentation process (Loparic et al., 2010). Although indentation speed and depth are known to influence the force-strain response (Boccaccio, Lamberti, Papi, De Spirito, & Pappalettere, 2015; Wenger et al., 2007), these quantities were not recorded.

Table D.1: MMP experimental concentrations		
	MMP-1	MMP-9
High Concentration (nM)	10	10
Low Concentration (nM)	1	1

Table D.2: MMP-1 and MMP-9 relative concentrations		
	MMP-1	MMP-9
Combination 1	High	High
Combination 2	Low	High
Combination 3	High	Low
Combination 4	Low	Low

D.3 Results

Figure D.1 shows an AFM image of dried intact collagen fibrils (no TNC added after fibril isolation). This figure demonstrates that the fibril isolation procedure did not produce individual fibrils on the mica substrate, as several individual fibrils can be identified together in the image. Table D.3 shows the contact stiffness for combinations 1, 2, and 4, showing that combination 4 has the highest stiffness, combination 1 has a stiffness that is slightly lower than combination 4, and combination 2 has the lowest stiffness of the three combinations. Fibrils could not be identified for combination 3. Additional fibrils could not be identified for combinations 1, 2, and 4, preventing the calculation of contact stiffness for more than a single fibril per condition.

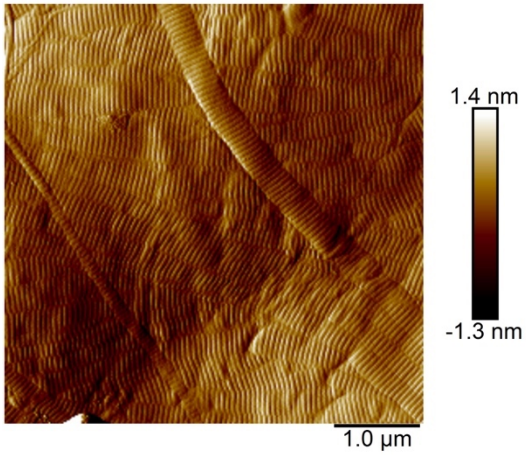

Figure D.1: AFM image of intact collagen fibrils (no TNC added after fibril isolation).

Table D.3: Contact stiffness for selected specimens.	
	Contact stiffness (N/m)
Combination 1	22.5
Combination 2	5.75
Combination 4	23.8

D.4 Discussion

D.4.1 Summary of findings

The results that we were able to obtain show that we did not isolate individual collagen fibrils from the rat connective tissue and that the contact stiffnesses do not follow the trends we predicted with our modeling approaches (see Chapter 4). We note that we were unable to calculate the elastic moduli from the measured contact stiffnesses because we did not record the depth of indentation. The relationship between

contact stiffness and elastic modulus depends on the projected area of the indenter, which depends on the depth of indentation. Thus, we reported contact stiffness, which can be calculated directly from the indentation force-displacement curves.

It is problematic that we did not isolate individual fibrils because layering of the fibrils may cause artifacts in the measurements. The layering could potentially influence the reaction force during the indentation by the AFM tip, causing deformation of multiple fibrils in series with one another. Ideally, the measurements would only provide the reaction force due to the molecular interactions within a single fibril (intramolecular). However, with layered fibrils, the reaction force from the specimen will be due to the intramolecular interactions as well as the interactions between fibrils (intermolecular), making it difficult to determine what portion of the reaction force stems from the intramolecular interactions in a single fibril.

Further, we were unable to obtain data for two conditions (combination 3 and a control specimen where the isolated fibrils were treated with TNC only) and we were unable to make replicate observations. In the cases where fibrils were identified, only one grouping of fibrils was found in each case, so we were unable to take measurements from more than one fibril per specimen and unable to account for fibril-to-fibril variations in degradation that may ultimately affect stiffness. In other conditions, we were unable to identify fibrils because the samples did not completely dry, even after weeks of drying time. The moisture in these cases prevented use of the AFM, though the issue may be avoided in the future by improved drying techniques (such as desiccation) or by using an AFM that can make measurements in solution instead of air.

The contact stiffnesses we obtained did not follow the trends predicted by the modeling approaches described in Chapter 4. Indeed, the stiffnesses for combinations 1 and 4 were nearly the same, even though combination 1 should have experienced substantially more degradation than combination 4 during the 20 minutes of MMP treatment. Our modeling approaches demonstrated that collagenase to gelatinase ratio will have an important effect on degradation rate and mechanical response. In both conditions 1 and 4, the ratio

is one, but in combination 1, the concentrations of both enzymes are substantially higher, so that combination should cause increased degradation compared to combination 4 in the same time span (see Appendix C). We also observed that collagenase to gelatinase ratio influences the mechanical response though our modeling approaches. Indeed, at a fixed percentage of degradation, the models predicted that the elastic modulus (which is linearly related to the stiffness) would vary with the ratio of collagenases to gelatinases but would not change based on the absolute number of enzymes on the surface (see Figure 4.3). However, in the present work, we are comparing the stiffnesses after a fixed duration of treatment, and not at a fixed percentage of degradation. Thus, the contact stiffness should be substantially lower for the specimen treated with combination 1 because it should have experienced the most degradation. Further, the stiffness for the specimen treated with combination 1 should be at least as low or lower than that of the specimen treated with combination 2, since the gelatinase concentration is equal in both cases and combination 1 has a greater collagenase concentration. However, this is not what we observed and further experimentation will be required to determine what factors caused these results to differ from the model predictions.

The unexpected stiffness values may be partially due to time-dependent effects of degradation, since degradation rate depends on collagenase to gelatinase ratio as well as the absolute value of enzyme surface coverage (see Appendix C) and degradation changes the stiffness (Malaspina et al., 2017). To account for the time-dependent effects of degradation, the rate of degradation could be monitored in real time to make sure that comparisons between model and experimental stiffness are made after approximately the same amount of degradation has occurred. Real-time monitoring of degradation has been accomplished by Watanabe-Nakayama et al. (2016) using high speed AFM on collagen microribbons treated with bacterial collagenase, an enzyme with both collagenolytic and gelatinolytic activity (Watanabe-Nakayama et al., 2016). Another method to measure degradation would be to employ a highly sensitive balance in combination with microfluidics to measure the loss of collagen from a fibril as fluid flows past, though this method has not been previously documented. These experimental approaches would serve to both account

for time-dependent effects of degradation and validate the model of fibril degradation presented in Chapter 4. However, these experiments would be difficult to interpret, since adsorption and desorption of the MMPs would also contribute to changes in weight, but thorough understanding of this process is lacking. Without an understanding of the adsorption/desorption behavior of MMPs, the results of such experiments could not be compared to the present model.

Further, two aspects of the indentation procedure could have contributed to the unexpected contact stiffness values. First, the speed of the indentation has been identified as a contributor to the force-strain response (Boccaccio et al., 2015), but the speed was not monitored in our experiments due to inexperience using the AFM. Second, the depth of indentation can also influence the force-strain response, since the underlying substrate (mica) will contribute to the reaction force if the AFM tip gets close to it (Wenger et al., 2007). Typically, indentation depth is kept to less than 10% of the total depth of the specimen (Wenger et al., 2007) to ensure that the AFM tip only experiences resistance due to the specimen (collagen, in our case) and not the stiffer substrate (mica). However, the indentations depths in the present experiment could not be determined because a reference force-strain measurement was not taken on a stiffer substrate, and the indentation depth is defined as the difference between the vertical piezo displacement for the sample and the vertical piezo displacement for a stiff reference material ((Wenger et al., 2007), Fig. 2b). These factors may be a few among many factors that confounded our results and must be appropriately controlled in future work.

D.4.2 Next steps and conclusion

Many opportunities for improvement exist in our experimental approach. A number of published reports have described the processes of collagen fibril isolation from connective tissues (Baldwin, Quigley, Clegg, & Kreplak, 2014; van der Rijt, van der Werf, Bennink, Dijkstra, & Feijen, 2006; Wenger et al., 2007; Yang, van der Werf, Dijkstra, Feijen, & Bennink, 2012), and these procedures should be explored

more thoroughly in the future, since our isolation procedure was unsuccessful. Though we followed a procedure that has been described previously, we were unable to replicate the result under the conditions of our experiments. We must also verify that the degradation is successful, monitoring the degradation for each condition. In addition, more time must be dedicated to learning the experimental techniques that are required for these experiments, particularly AFM, to allow time for mastery.

Finally, either the MD model of collagen mechanics or the experimental procedure must be adapted to facilitate comparisons between the experimental results and the model predictions of mechanical properties to ensure that the experimental paradigm and the model measure the same quantities. To adapt the model, we must define the tip geometry, account for its material properties, and define the tip-fibril interactions in the coarse-grained approach. Alternatively, we could adapt the AFM protocol to perform tensile tests on the fibrils to facilitate direct comparisons between experiments and the existing MD model. While tensile testing of intact collagen fibrils has been described (Y. Liu, Ballarini, & Eppell, 2016; van der Rijt et al., 2006), it remains technically challenging, so modifying the MD model may be a more pragmatic option than modifying the experimental procedure.

The experiments described herein led to inconclusive and incomplete results, which precluded our comparison of experimental results to our simulated predictions. However, this work has laid the groundwork for future experiments that can build on the information we described in this chapter. Future work should consider improved ways to isolate collagen, develop techniques for monitoring degradation during MMP treatment, and allow adequate time to master experimental approaches. These considerations will facilitate the next steps for experimentation and validation of the model predictions.

Vita

BETHANY SUSAN POWELL

1506 Sturdy Rd.

Valparaiso, IN 46383

913-961-9657

Bethany.Powell@valpo.edu

Employment

Instructor of Mechanical Engineering and Bioengineering August 2018 - present

Valparaiso University College of Engineering, Valparaiso, IN

Education

M.S., Biomedical Engineering September 2016

Northwestern University McCormick School of Engineering, Evanston, IL

Co-advisors: Igal Szleifer, Ph.D., and Yasin Dhaher, Ph.D.

B.S., Mechanical Engineering, Music Minor May 2013

Valparaiso University College of Engineering, Valparaiso, IN

Cumulative GPA: 3.9/4.0

Presentations

Posters

- Musculoskeletal Biology & Bioengineering Gordon Research Conference (August 6-12, 2016)
- Poster presentations at Movement and Rehabilitation Sciences Training Day (August 26, 2016 and August 21, 2015)
- Poster presentation at Northwestern University Computational Research Day (April 18, 2017)
- Poster presentation at the Northwestern University Bioprofessionals Current Research and Future Careers Symposium (August 21, 2017)

Podium presentations

- World Congress of Biomechanics (July 8-12, 2018)
- Symposium on Sex Inclusion in Biomedical Research (January 25, 2018)

Publications

- **Powell, B.,** Szleifer, I., & Dhaher, Y. Y. (2018). In silico study of principal sex hormone effects on post-injury synovial inflammatory response. PloS one, 13(12), e0209582.
- **Powell, B. S.,** Dhaher, Y. Y., & Szleifer, I. G. (2015). Review of the Multiscale Effects of Female Sex Hormones on Matrix Metalloproteinase– Mediated Collagen Degradation. Critical Reviews™ in Biomedical Engineering, 43(5-6).
- Caldwell, M., Casey, E., **Powell, B.,** & Shultz, S. "Hormones." *Sex Differences in Sports Medicine*. Ed. Ellen Casey. Springer Publishing Company, 2016. Print.

- **Powell, B.**, Malaspina, D., Dhaher, Y., and Szleifer, I. “Effect of collagenase to gelatinase ratio on collagen fibril degradation and mechanics: a combined Monte Carlo-Molecular Dynamics study.” Manuscript in preparation.